NASA CR-134856

DEVELOPMENT OF A HIGH POWER 12 GHZ PPM FOCUSED TRAVELING WAVE TUBE

By

Richard Lewis

LITTON INDUSTRIES

Electron Tube Division

Prepared For

NATIONAL AERONAUTICS AND SPACE ADMINISTRATION

NASA Lewis Research Center

Contract NAS3-14391

1. Report No.	2. Government Accession No.	3. Recipient's Catalog No.

4. Title and Subtitle	5. Report Date
Development of a High Power 12 GHz PPM Focused Traveling Wave Tube	May 1975
	6. Performing Organization Code
7. Author(s)	8. Performing Organization Report No.
R. Lewis	
	10. Work Unit No.
9. Performing Organization Name and Address LITTON SYSTEMS, INC. dba Litton Industries Electron Tube Division 960 Industrial Road San Carlos, California 94070	11. Contract or Grant No. NAS3-14391
	13. Type of Report and Period Covered Final Report
12. Sponsoring Agency Name and Address National Aeronautics and Space Administration Washington, D. C. 20546	14. Sponsoring Agency Code

15. Supplementary Notes

Project Manager, D. Connolly, Spacecraft Technology Division, NASA Lewis Research Center, Cleveland, Ohio.

16. Abstract

An analytical and experimental program to demonstrate the technical feasibility of a high efficiency coupled cavity traveling wave tube with periodic permanent magnetic focusing operating at 12.06 GHz, with 1 to 2 Kilowatts CW power is described. Such a tube would ultimately be used for broadcasting power transmission from a satellite.

The electron gun was designed to be demountable with a replaceable cathode, and the tube to be operable in a bakeable vacuum chamber with its collector replaced by a collector designed by NASA-LeRC. Therefore, the high efficiency design was concerned with the slow wave structure only, utilizing velocity resynchronization.

A special adapter was designed which incorporated an electromagnet refocusing section and a collector baseplate to facilitate testing the NASA-LeRC collector.

CW output power of 1000 watts yielding 21.5% electronic efficiency was demonstrated, with a minimum output power of 525 Watts across the specified 160 MHz bandwidth.

The program extended from July 1971 through December 1973.

17. Key Words (Suggested by Author(s))	18. Distribution Statement
Coupled Cavity Traveling Wave Tube Periodic Permanent Magnetic Focusing Replaceable Cathode Velocity Resynchronization Electromagnet Refocusing.	Unclassified - Unlimited

19. Security Classif. (of this report)	20. Security Classif. (of this page)	21. No. of Pages	22. Price*
Unclassified.	Unclassified	79	

* For sale by the National Technical Information Service, Springfield, Virginia 22151

FOREWORD

The work described herein was performed by Litton Industries, Electron Tube Division under NASA Contract NAS3-14391 with Dr. Otto Sauseng as principal investigator, followed by Mr. Richard Lewis. Dr. D. Connolly, Spacecraft Technology Division, NASA - Lewis Research Center, was Project Manager.

ABSTRACT

An analytical and experimental program to demonstrate the technical feasibility of a high efficiency coupled cavity traveling wave tube with periodic permanent magnetic focusing operating at 12.06 GHz with 1 to 2 kilowatts CW power is described. Such a tube would ultimately be used for broadcasting power transmission from a satellite.

The electron gun was designed to be demountable with a replaceable cathode, and the tube to be operable in a bakeable vacuum chamber with its collector replaced by a collector designed by NASA-LeRC. Therefore the high efficiency design was concerned with the slow wave structure only, utilizing velocity resynchronization.

A special adapter was designed which incorporated an electromagnet refocusing section and a collector baseplate to facilitate testing of various NASA-LeRC collector designs. CW output power of 1000 Watts yielding 21.5% electronic efficiency was demonstrated, with a minimum output power of 525 Watts across the specified 160 MHz bandwidth.

The program extended from July 1971 through December 1973.

TABLE OF CONTENTS

TABLE OF CONTENTS (continued) Page

LIST OF ILLUSTRATIONS

LIST OF ILLUSTRATIONS

(cont'd)

LIST OF ILLUSTRATIONS
(cont'd)

LIST OF TABLES

DEVELOPMENT OF A HIGH POWER 12 GHZ PPM FOCUSED TRAVELING WAVE TUBE

By: Richard Lewis
Litton Industries
San Carlos, California

1.0 SUMMARY

The program objective was to demonstrate the technical feasibility of a 1 to 2 kW, high efficiency, PPM focused, 12 GHz coupled cavity traveling wave tube. The design was to include a demountable electron gun with a replaceable cathode and a removable collector allowing the tube to be used as a test vehicle for evaluation of advanced NASA multistage collector designs, operating in a special bakeable vacuum chamber. Therefore the high efficiency design addressed the interaction circuit only using velocity resynchronization, and a simple one depressable stage collector was incorporated in the design.

Initially the design was directed at the 2 kW power level which required the use of alternate thick and thin pole pieces in the integrated RF circuit-beam focusing structure. The thick pole pieces were iron with copper cladding to provide the magnetic and thermal paths, and the alternate pole pieces of copper were reduced in thickness to provide an increased RF cavity height for higher interaction impedance and efficiency. However, early circuit investigations revealed unexpectedly high circuit losses associated with a slow wave structure whose cold bandwidth was chosen to fit the relatively narrow operating bandwidth requirement of 160 MHz, and was believed to be attributed to the thick-thin pole piece geometry.

This resulted in a complete redesign of the RF circuit-beam focusing structure, with uniform intermediate thickness pole pieces throughout. However, the reduction in available magnetic field (due to saturation effects in the reduced thickness magnetic pole pieces) redirected the design to the 1.25 kW power level.

The circuit losses proved to still be excessive and were then attributed to the coupling slot configuration, and a rectangular shaped slot design developed. It was found that the circuit losses were substantially lowered when the slot width (coupling) was increased above a certain critical value. This produced a wider cold bandwidth than desired and required operation at a lower phase angle for high efficiency.

1.0 SUMMARY (continued)

An experimental tube was built using the initial high loss circuit design without velocity resynchronization to confirm various novel assembly techniques which were developed and to evaluate the cooling and focusing design. The maximum collector transmission that could be achieved was 70% and was attributed to mechanical misalignments of the RF circuit-focusing structure, requiring improved assembly techniques. Saturated output power of approximately only 200 Watts throughout the 160 MHz frequency band was measured due to the very high RF losses characteristic of this design. The tube was delivered for the purpose of test equipment evaluation.

Development tube #1 was built using improved assembly techniques and the new low loss circuit design with a two step velocity taper. Collector transmission of 98% without RF was obtained and CW output power of 1000 watts was measured, yielding 21.5% electronic efficiency. The tube was used to successfully demonstrate the feasibility of the cathode replacement scheme, with the tube being let down to air, the cathode being replaced, and the tube reprocessed and retested. The thermal design capability proved to be more than adequate under normal operating conditions, however during subsequent testing at a different beam voltage the critical focusing conditions became apparent and excessive body current interception caused destruction of the tube.

Development tube #2 consisted of a modified velocity taper design with construction only partially completed at the end of the program.

Additional efforts consisted of the design and construction of two large collector baseplate-solenoid refocusing section assemblies to facilitate the testing of multistage collectors, two conflat flanges with waveguide window feedthroughs to allow testing within the special vacuum chamber, and nine replacement cathode assemblies.

It is concluded, based on the low measured efficiency of Development Tube #1, that the circuit design is not yet optimized with respect to bandwidth and loss. New studies indicate that an improved circuit design can be achieved with a modified coupling slot design, providing reduced cold bandwidth and allowing operation at a higher phase angle with improved efficiency.

2.0 INTRODUCTION

The program described in this report is part of an extensive effort directed by NASA Lewis Research Center to develop satellite communications systems powerful enough to broadcast directly to individual end receivers rather than to ground based distribution systems. These efforts were initiated with detailed studies on several types of power amplifiers for such a system, one of which was an "Analytical Study Program to Develop the Theoretical Design of Traveling Wave Tubes" by NASA Contract NAS3-9719.[1] An outgrowth of this study was a development program and feasibility evaluation for a high efficiency solenoid focused 12.2 GHz, 4 kW CW coupled cavity traveling wave tube (Contract NAS3-13728).[2]

The objective of this program was to demonstrate the technical feasibility of a 1 to 2 kW high efficiency coupled cavity traveling wave tube with periodic permanent magnet focusing operating at 12.06 GHz. The electron gun was to be demountable with a replaceable cathode, and the collector was to be removable such that the tube could be used as a test vehicle for evaluation of multistage collector designs at NASA Lewis Research Center.

The program consisted of the development of a RF circuit design based on RF cold tests and computer analysis, the development of a electron gun design based on computer prediction and experimental verification in an electrostatic beam analyzer, and the development of a beam focusing design based on computer prediction and experimental verification through magnetic field measurements. Two tubes were built and evaluated and a third tube was partially completed. Associated hardware was also designed and fabricated consisting of nine replacement cathode assemblies, two collector baseplates with solenoid refocusing sections, and two conflat flanges with waveguide window feedthroughs.

3.0 DESIGN APPROACH

The design approach was guided by the high average output power requirement with reliable operation and long life potential. The coupled cavity circuit was judged to be the only type capable of providing this high power level as a result of its superior thermal properties. A velocity taper was chosen for efficiency enhancement rather than a voltage jump for reasons of reliability. Brillouin flow beam focusing with low cathode loading was used, consistent with long life design.

3.1 SUMMARY OF SPECIFICATIONS

A summary of TWT specifications is given in Table 3.1. Originally the program was directed at the 2 kW power level, however was modified in June 1972 to the 1.25 kW level due to magnetic and thermal limitations revealed at that time.

3.2 TUBE DESIGN

The required performance of the tube represented significant advancements in the state of the art, especially with respect to efficiency and average power capability. Advanced methods of efficiency enhancement and thermal design were therefore incorporated.

Efficiency enhancement was accomplished with velocity resynchronization between slow wave structure and beam velocity using a velocity taper near the output of the circuit. The tube was designed to permit experimental evaluation of advanced multistage collector depression schemes for further efficiency enhancement.

For this purpose provisions were made to replace the conventional depressed collector by a variety of multistage collectors and include a refocusing section between output coupler and first collector stage. A liquid cooled coupled cavity slow wave structure was chosen as the one with the best thermal capability among available circuits. This type of structure can conveniently be combined with an integrated periodic permanent magnet (PPM) focusing configuration, such that portions of the circuit structure (cavity walls and ferrules) are simultaneously used as pole pieces for the focusing configuration. These parts are therefore made of vacuum iron (rather than copper) and the thermal capability of such a tube is significantly lower than that of an all-copper tube with solenoid focusing.

TABLE 3.1

SUMMARY OF TWT SPECIFICATIONS

Frequency:	12.06 GHz
Bandwidth:	160 MHz
Electronic Efficiency:	35% minimum.
Power:	1.0 kW CW minimum
Gain:	40-45 dB
Focusing:	PPM
RF Beam Transmission:	95% minimum
Water Cooling	
Operable in vacuum chamber	
Replaceable Cathode	
Removable Collector	

This is partly because the thermal conductivity of iron is substantially lower than that of copper, and in addition the focusing quality of a PPM tube is generally lower than that of the same size solenoid focused tube. Power losses due to beam interception have therefore to be expected to be higher. The power handling capability of such a conventional PPM focused tube was considered marginal for the specified power level. Special advanced thermal design features were therefore incorporated into the tube. These included a thick copper cladding of the magnetic pole pieces to nearly double their thermal conductance. In addition the tube used a double period magnetic focusing system in which the internal pole pieces consist of magnetic ferrules with copper (rather than iron) webs to further improve their thermal conductance. The focusing system incorporated Platinum Cobalt magnets which exhibit high magnetic performance with exceptional uniformity in characteristics. These magnets were subsequently replaced by similar Samarium Cobalt magnets.

In addition the tube incorporated several unique features designed to allow use of the tube as a test vehicle for experimental evaluation of a variety of multistage collector configurations inside a large bakeable vacuum chamber. These features included:

1. A demountable gun assembly such that the cathode assembly could be removed and conveniently replaced by a self-aligning new cathode assembly.

   Cathode replacement was expected to be required at the initiation of a new multistage collector experiment.

2. The tube used a conventional (depressible) collector that could be replaced by a special collector plate with a removable vacuum envelope. The collector plate was designed for the assembly of a variety of multistage collector configurations and included a number of high voltage vacuum feedthrough leads. The collector plate also incorporated a solenoid driven refocusing section located between output coupler and first collector stage.

The tubes were therefore initially tested and evaluated at Litton before they were to be used as test vehicles for multistage collector experiments in the special vacuum test chamber.

3.2 TUBE DESIGN (continued)

These multistage collector experiments require therefore that the conventional collector be removed and be replaced by the collector plate with refocusing. When the assembly of a selected multistage collector configuration is completed the removable collector vacuum envelope is replaced and the tube is mounted inside the vacuum chamber for reprocessing (bakeout) in vacuum. The vacuum chamber has special provisions to remove the collector envelope when good vacuum is obtained in the chamber. The vacuum chamber provides liquid cooling for the tube during bakeout so that the magnets remain cool and operative.

4.0 CIRCUIT DESIGN AND VELOCITY RESYNCHRONIZATION

The coupled cavity type circuit was judged to be the only slow wave structure capable of fulfilling the high RF output power requirement utilizing PPM focusing. The high RF interaction efficiency demand required that some form of velocity resynchronization be used, and a two step velocity taper was considered to be the most suitable choice.

4.1 BANDWIDTH AND LOSS CONSIDERATIONS

In order to avoid excessive efficiency reduction circuit loss must be considered. As shown in Figure 1 circuit efficiency is reduced by approximately 17% for each 0.1 dB of RF loss per cavity in the low loss range. Loss varies inversely with circuit cold bandwidth as shown in Figure 2 such that a wide cold bandwidth circuit yields low circuit loss. However, such a wide cold bandwidth circuit produces a reduced interaction impedance as shown in Figure 3, which in turn provides for weak RF circuit-beam wave interaction causing reduced efficiency. Consequently a compromise must be made between cold bandwidth and low loss which produces maximum RF output power.

4.2 BASIC CIRCUIT DESIGN

A. Initial Design (2 kW)

In order to fulfill the high efficiency requirement the initial circuit investigated employed a unique scheme for increased interaction impedance. Due to the feasibility of double period PPM focusing in the design, alternate non-magnetic pole pieces (copper with magnetic ferrules) were reduced in thickness to effect an increased cavity height which provides higher interaction impedance. The dispersion diagram of the circuit appeared to exhibit a small stopband at its center when viewed by conventional resonant measuring techniques. This was attributed to the non-periodicity of the circuit due to the alternate variation of cavity web thickness and was eliminated by displacing the coupling slot in the thin pole pieces farther from the cavity center to equalize the electrical length from the center of each cavity to the next. The circuit had a cold bandwidth of 1350 MHz, (8.4 times the hot bandwidth) however exhibited losses nearly an order of magnitude greater than predicted by conventional circuit loss theory for this bandwidth. It was believed that these excessively high losses were possibly attributed to cut-off frequency effects of the thicker (magnetic) pole piece coupling

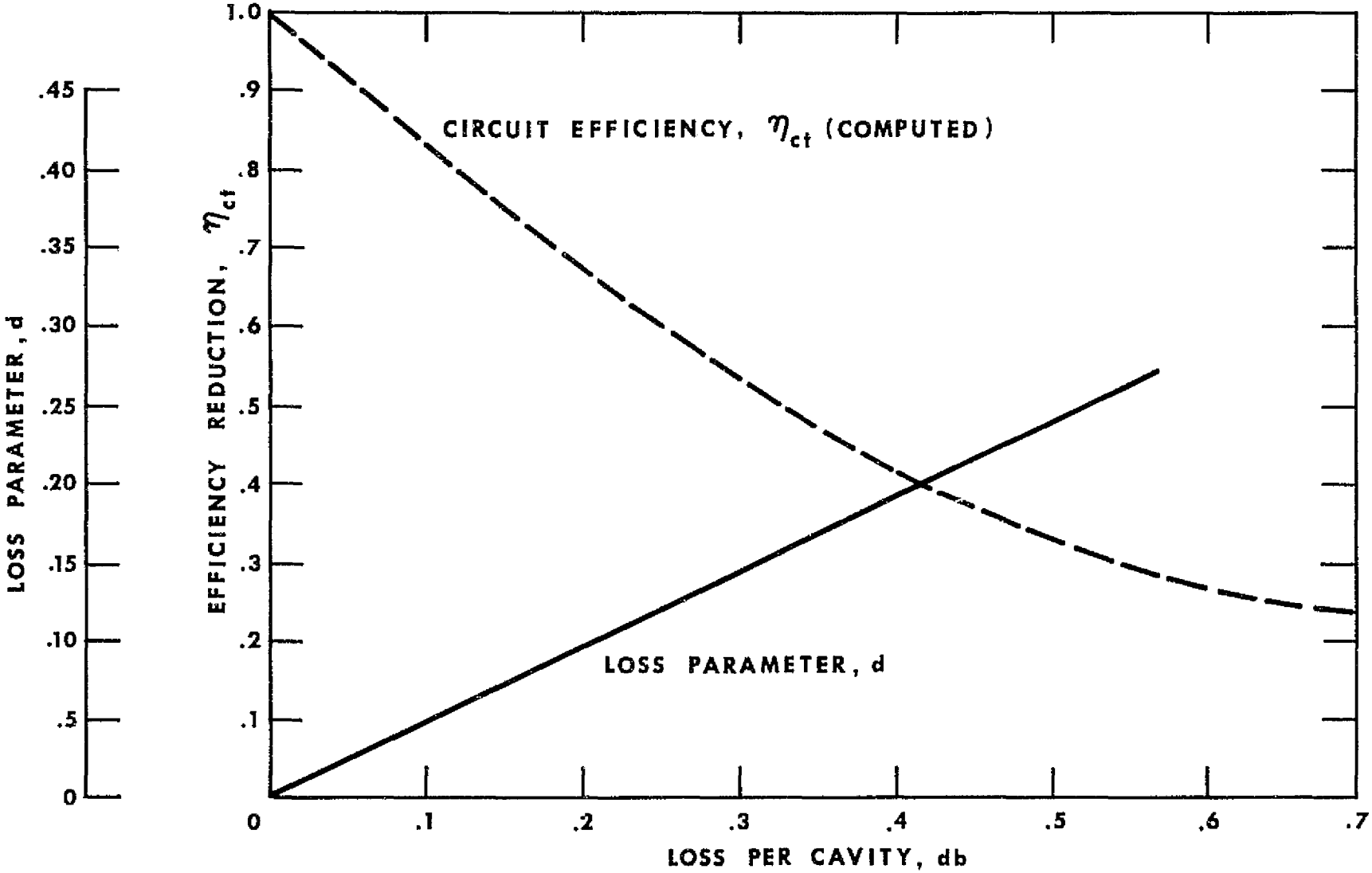

FIGURE 1 - PREDICTED EFFICIENCY REDUCTION WITH CIRCUIT LOSS

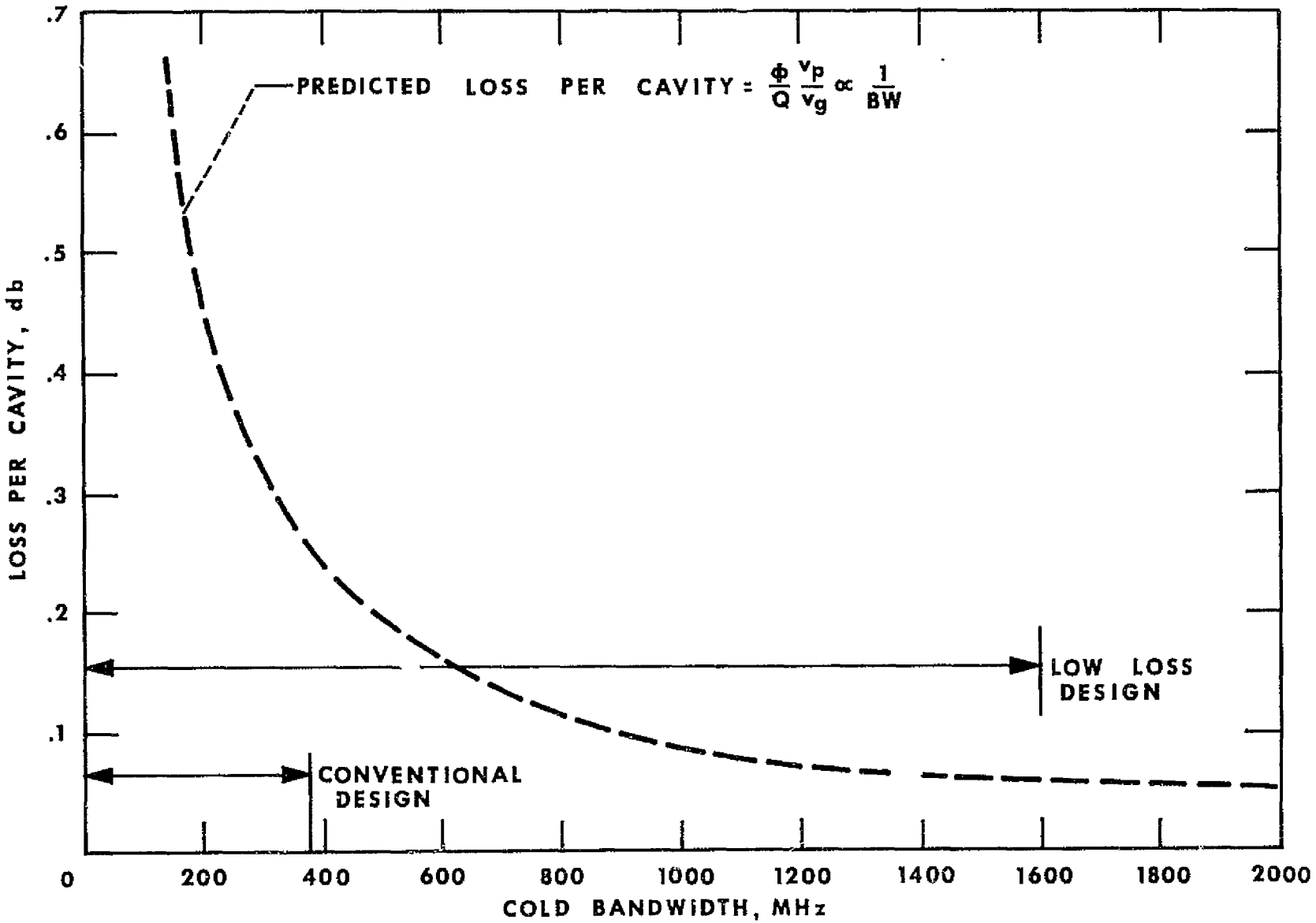

FIGURE 2 - EFFECT OF COLD BANDWIDTH ON CIRCUIT LOSSES

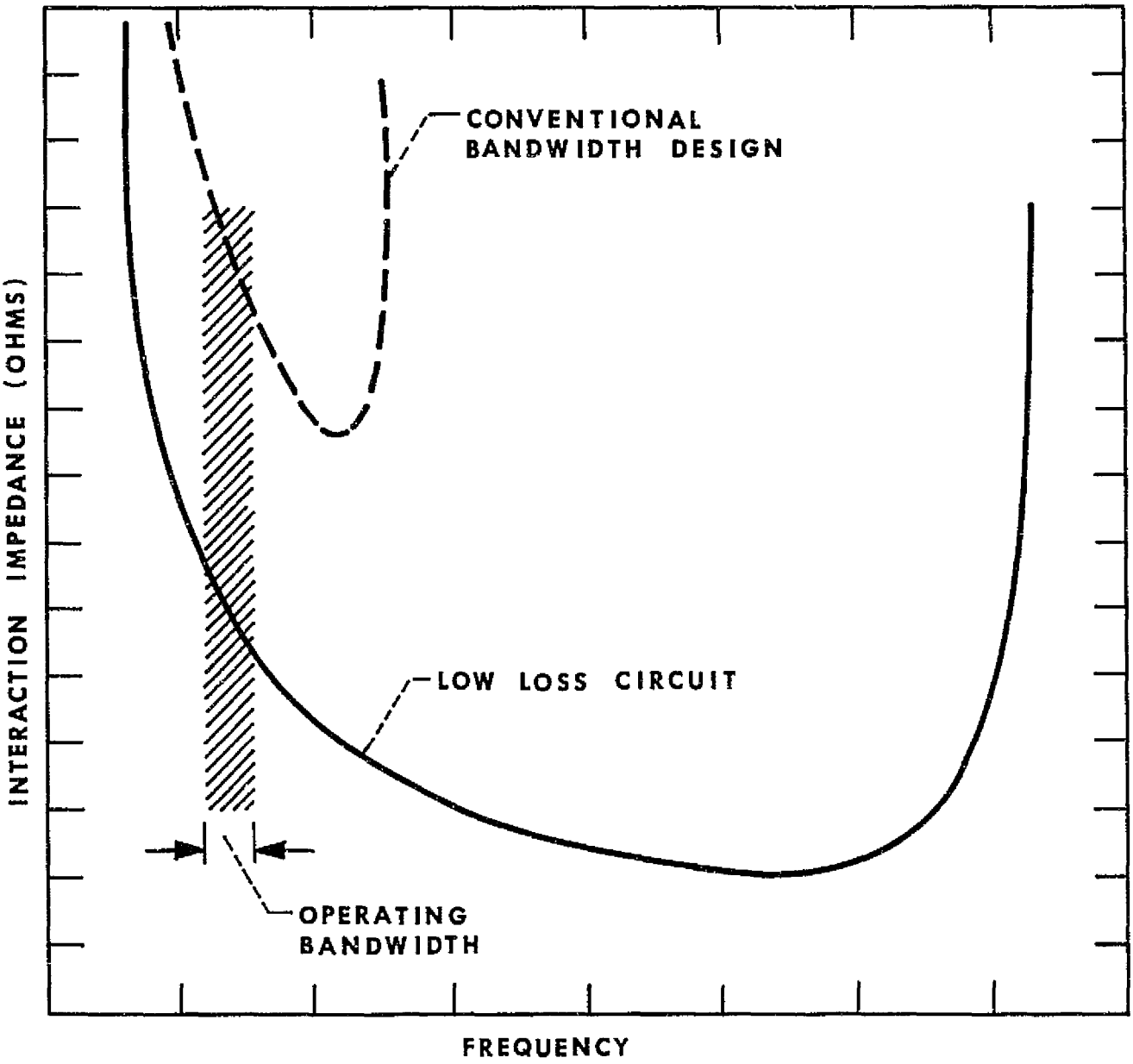

FIGURE 3 - INTERACTION IMPEDANCE FOR COUPLED CAVITY CIRCUITS

4.0 CIRCUIT DESIGN AND VELOCITY RESYNCHRONIZATION

4.2 BASIC CIRCUIT DESIGN

A. Initial Design (2 kW) (continued)

slots. The slot, when considered as a short waveguide section would be subject to lower cut-off frequency effects below which very high reactive losses would result. The lower cut-off frequency of such a waveguide would be 17.6 GHz. A circuit consisting of uniform reduced thickness pole pieces did not appear to suffer these high losses and it was concluded that a high efficiency design with PPM focusing at this power level was not feasible.

At that time construction of the Experimental Tube was nearly complete utilizing the high loss circuit design without a velocity taper. It was although, considered useful to complete the tube to allow evaluation of new assembly techniques, focusing, RF bandwidth, higher mode stability, and thermal design, while gain and efficiency results would be of little significance.

B. Modified Design (1.25 kW)

Due to the high RF losses associated with the thick pole piece circuit, a reduction in pole piece thickness appeared feasible to fulfill the high efficiency requirement. This however caused a reduction in the available magnetic field due to saturation effects in the pole pieces, requiring that the design be redirected to the 1.25 kW power level.

The loss versus bandwidth relationship was once again investigated through RF cold tests and still found to increase more rapidly with decreasing bandwidth than predicted by theory, however was considerably lower than the thicker pole piece design for a given bandwidth. A cold bandwidth of 1580 MHz, as shown in Figure 4, was required to reduce the loss to an acceptable level of approximately 0.1 dB per cavity. The passband is also shown shifted down 190 MHz in frequency as expected to result from beam space charge loading.

This larger than desired cold bandwidth (9.88 times the hot bandwidth rather than 4 or 5) required operation at a very low phase angle in order to attain a high interaction impedance, as shown in Figure 5.

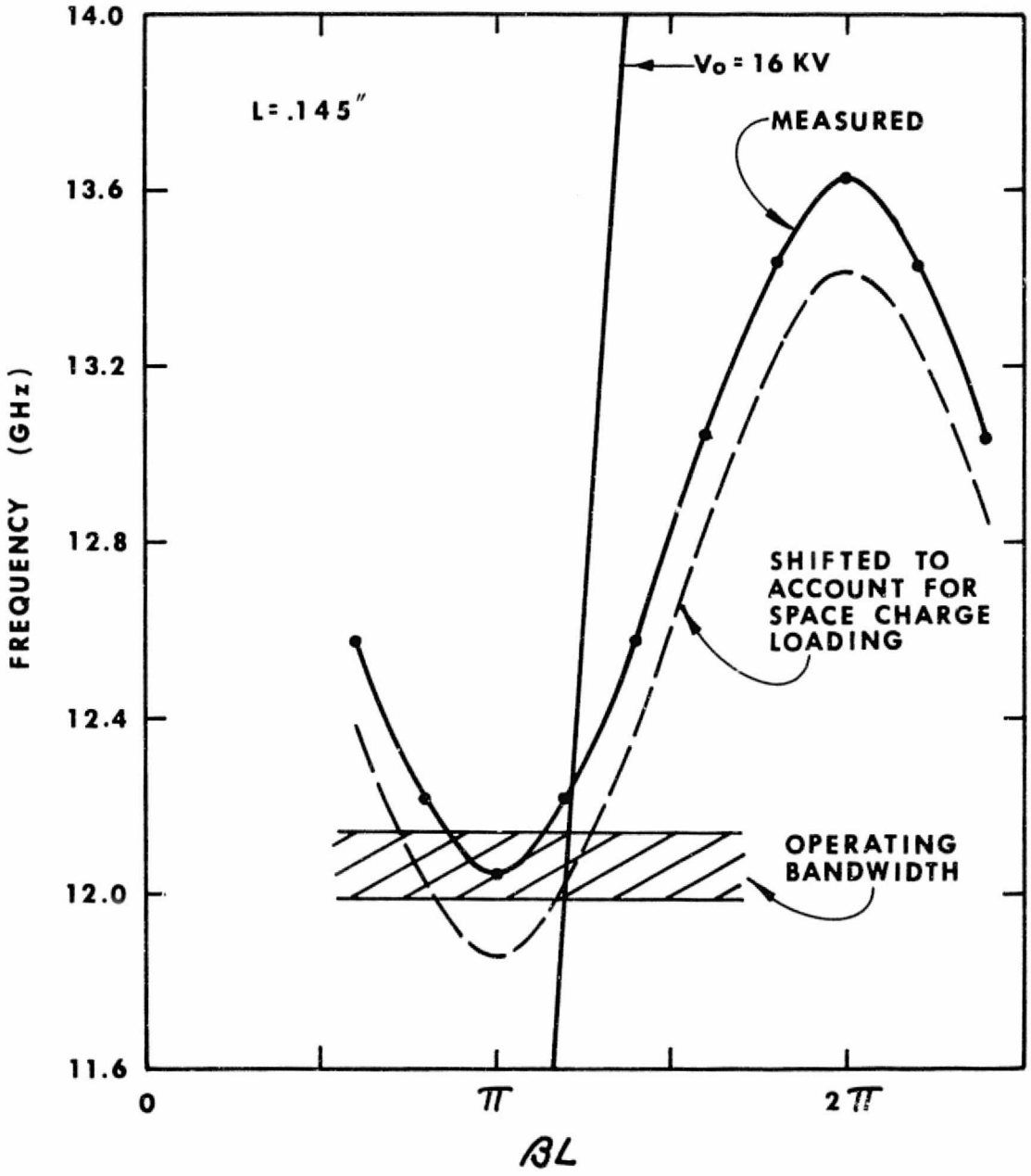

FIGURE 4 ω-β DIAGRAM OF STANDARD CIRCUIT

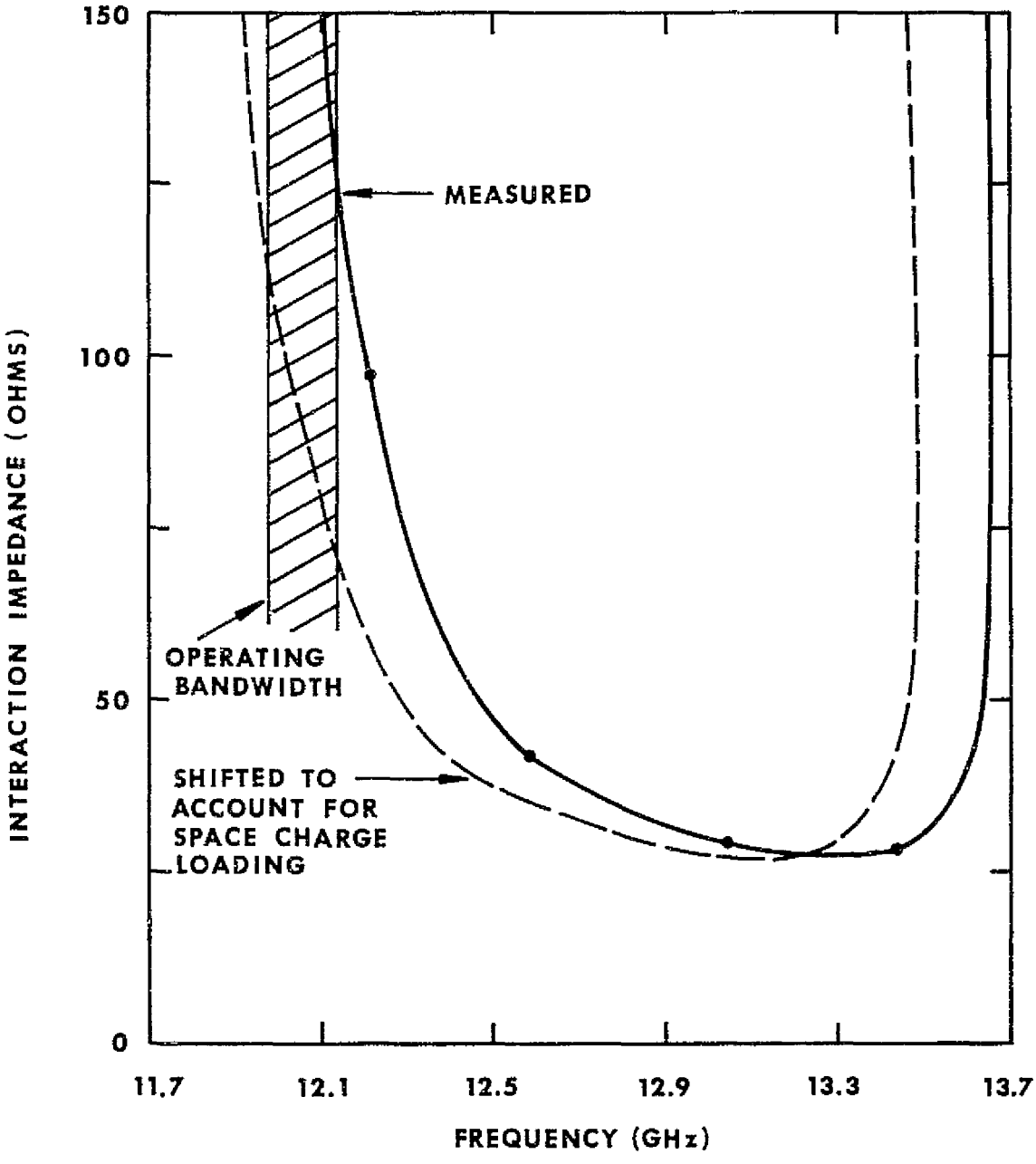

FIGURE 5 - INTERACTION IMPEDANCE OF STANDARD CIRCUIT

4.0 CIRCUIT DESIGN AND VELOCITY RESYNCHRONIZATION

4.2 BASIC CIRCUIT DESIGN

B. Modified Design (1.25 kW) (continued)

The cold passband actually had a lower cut-off frequency above the prescribed operating band, requiring that the space charge loading effect be accounted for in order that the operating tube high efficiency region be properly located in frequency. The impedance varied from 113 ohms at the low frequency band edge to 70 ohms at the high band edge. The circuit phase velocity variation is shown in Figure 6, also showing intersection with a 16 kV operating voltage line. The upper end of the operating bandwidth is shown to be overvoltaged at 16 kV, providing a more favorable synchronism relationship to compensate for the reduced interaction impedance. The lower end of the operating bandwidth is shown to be undervoltaged at 16 kV, an undesirable synchronism condition. However efficient interaction in this range would result from its increased interaction impedance. In this manner the circuit interaction impedance variation and phase velocity variation were made to compensate for one another to produce a desirable electronic efficiency variation across the operating bandwidth for inclusion of a velocity taper. Figure 7 shows the calculated small signal circuit parameters QC, b, and C for the basic circuit operating at 16 kV. QC, the space charge parameter which should be minimized for high efficiency, is seen to vary from .085 to .12, consistent with that demand. The synchronism parameter b is seen to vary from -0.65 to +0.65 having been adjusted to compensate for the impedance variation. Pierce's gain parameter C which should be maximized for optimum efficiency is shown to vary from .077 to .064 across the operating bandwidth.

Predicted basic circuit efficiency based on these parameters is included in the next section covering velocity taper design.

Figure 8 gives the major dimensions of the final basic circuit design. The three resonant loss cavities shown are covered in detail in Section 4.4 covering tube stabilization.

The cavity period was determined by the design operating voltage which was in turn determined by the available magnetic field. In general, Pierce's gain parameter C, to which circuit efficiency is proportional, increases as the voltage is reduced at con-

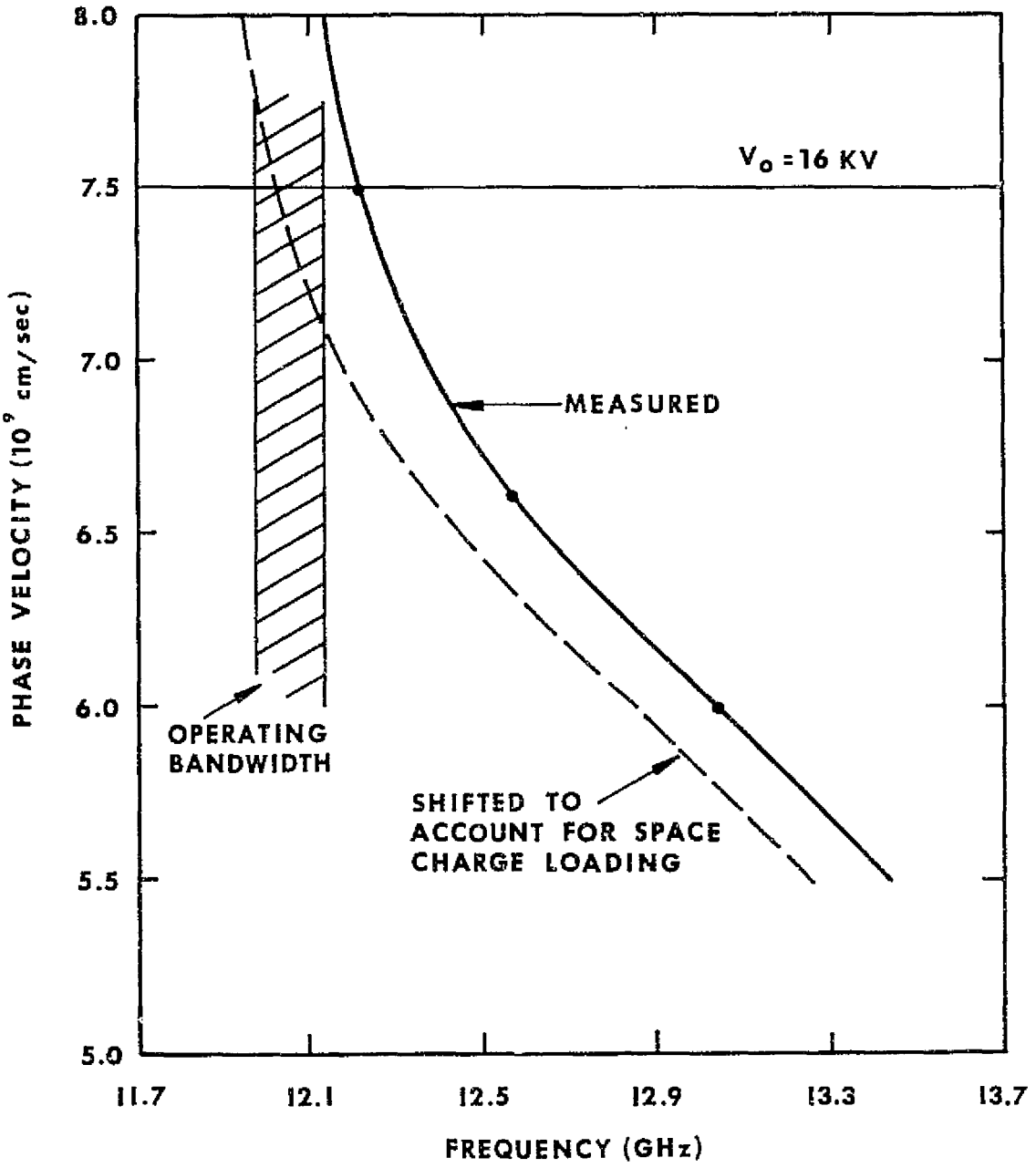

FIGURE 6 - PHASE VELOCITY OF STANDARD CIRCUIT

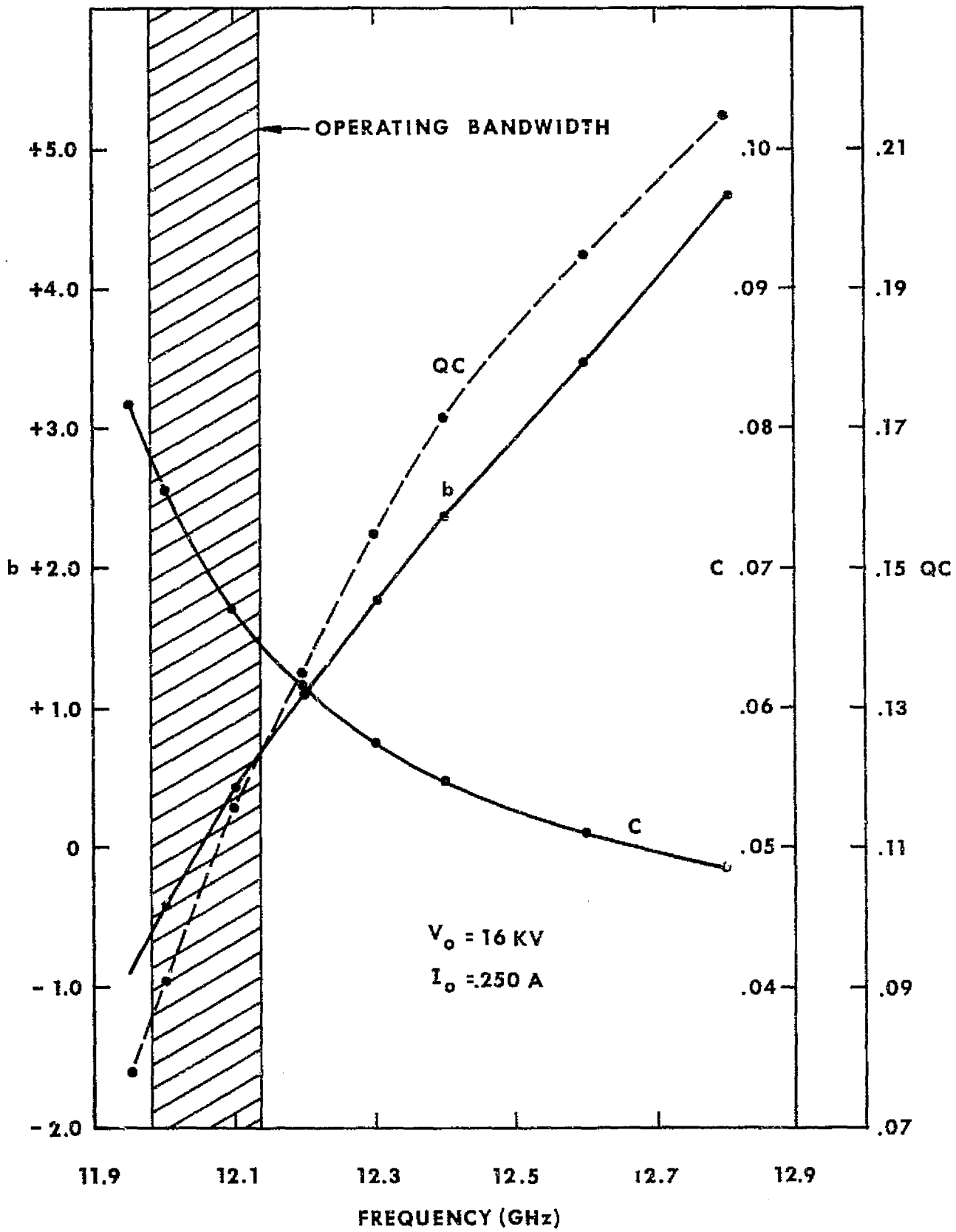

FIGURE 7 - SMALL SIGNAL CIRCUIT PARAMETERS — CALCULATED

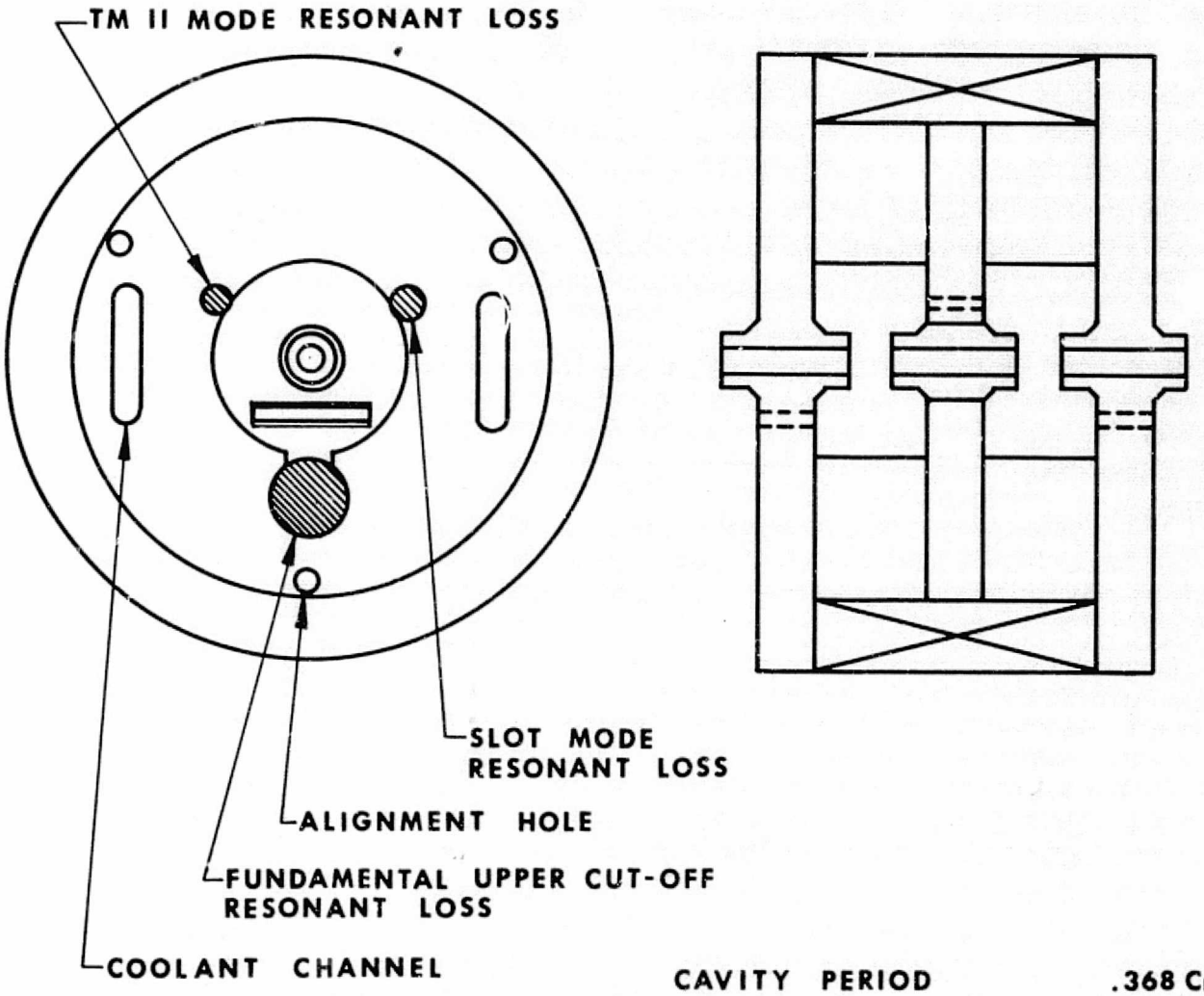

CAVITY PERIOD	.368 Cm
CAVITY HEIGHT	.241 Cm
WEB THICKNESS	.127 Cm
CAVITY DIAMETER	1.372 Cm
BEAM HOLE	.168 Cm
FERRULE DIAMETER	.345 Cm
FERRULE LENGTH	.076 Cm
GAP	.089 Cm
COUPLING HOLE HEIGHT	.102 Cm
COUPLING HOLE WIDTH	.864 Cm

FIGURE 8 - COUPLED CAVITY CONFIGURATION

4.0 CIRCUIT DESIGN AND VELOCITY RESYNCHRONIZATION

4.2 BASIC CIRCUIT DESIGN

B. Modified Design (1.25 kW) (continued)

stant beam power. However the available magnetic field placed a lower limit of 15 to 16 kV at which good focusing could be maintained.

The web thickness was determined by magnetic and thermal requirements, and the loss considerations discussed previously.

The gap was chosen to provide a gap to period ratio of 0.24, consistent with favorable interaction, and in turn determined the cavity diameter required for proper frequency passband location. The coupling hole dimensions were determined empirically to yield the bandwidth-loss relationship also discussed previously, with the narrow height (.102cm.) producing considerably lower loss than larger heights at constant bandwidths.

The beam hole size was chosen to yield a circuit radial propagation constant (γr_a) of 0.84 midband consistent with high efficiency design, with focusing design preventing any further reduction. The ferrule diameter was minimized, still allowing sufficient thermal and magnetic capability.

Figure 9 shows the uniform circuit cavity configuration of the Development Tube. Three gain sections 12 cavities, 14 cavities, and 13 cavities respectively were considered necessary to meet the specified gain requirement with stable operation. The predicted small signal gain based upon measured parameters for this configuration is shown in Figure 10, varying from 55 dB to 45 dB across the specified operating band.

4.3 VELOCITY TAPER DESIGN

Velocity resynchronization schemes have been found to be more effective when the resynchronization is provided in steps rather than in a continuous fashion. This assures that the beam bunch is moved most rapidly from the neutral phase (saturation) into the favorable phase position for energy extraction. In a coupled cavity velocity taper resynchronization is accomplished by a reduction in the cavity period, however a large abrupt change produces a intolerable mismatch requiring that several transition

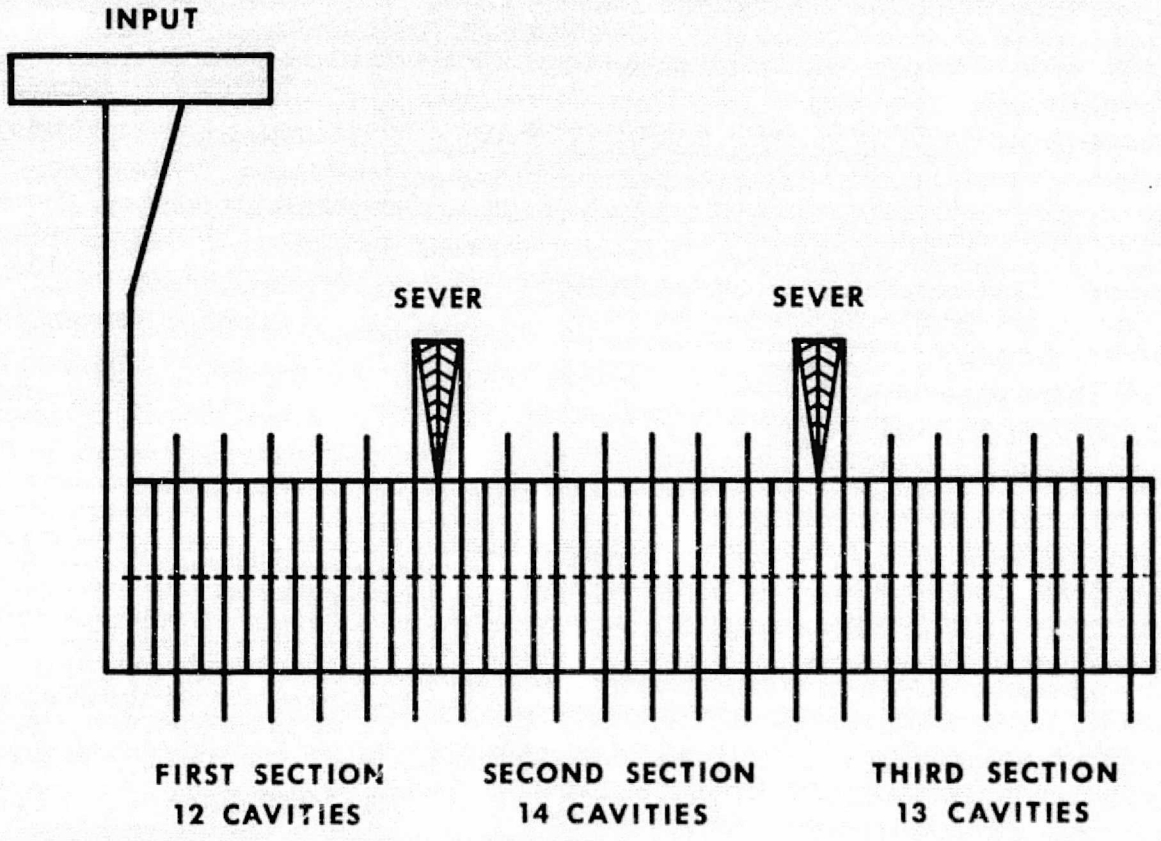

FIGURE 9 - UNIFORM CIRCUIT CAVITY CONFIGURATION

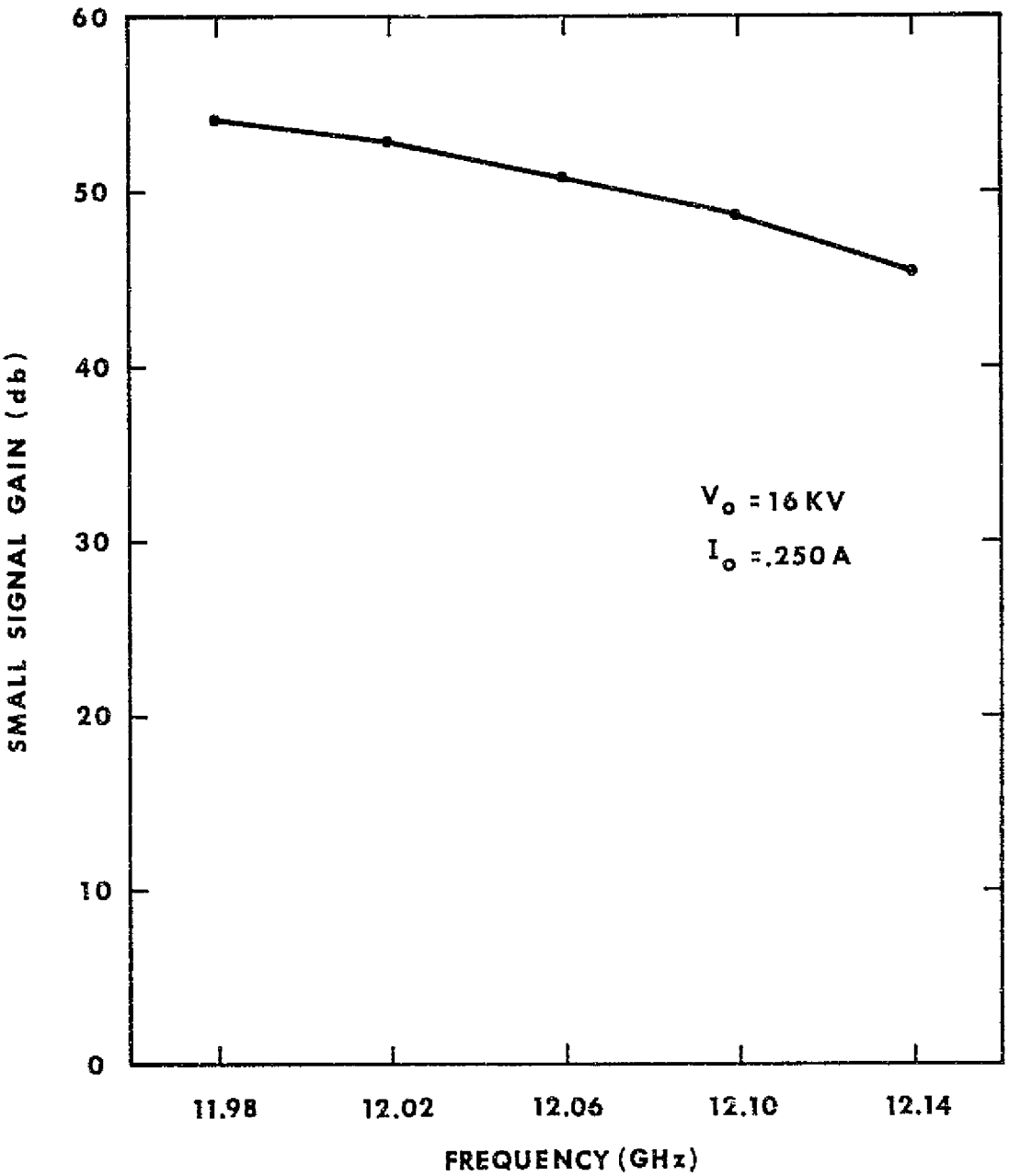

FIGURE 10 - PREDICTED SMALL SIGNAL GAIN

4.3 VELOCITY TAPER DESIGN (continued)

cavities precede the step. The reduction in cavity period is accomplished by reducing the cavity height since the pole piece thickness has already been minimized. RF loss varies inversely with cavity height, and a period reduction level is reached where the loss cancels any additional energy extracted from the beam, placing an upper limit on attainable efficiency through this means. For X-Band the optimum number of steps is about two, with the terminal velocity reduced to approximately 70% of the initial phase velocity. The length of these steps is determined by the requirement that optimum beam bunching is provided at the beginning of the following taper step.

Cold test measurements were performed on various reduced period circuit sections to yield accurate interaction impedance values for large signal computer analysis. The frequency passband of each section was carefully aligned with the basic circuit passband such that the phase velocity reduction was directly proportional to the period reduction.

The original velocity taper design consisted of two steps preceded by transitions, with the terminal step velocity equal to 69% of the initial phase velocity. The estimated circuit losses of 400 watts were however determined to be unacceptable.

The design was therefore modified to reduce the circuit losses with as little efficiency degradation as possible. This was accomplished with a shorter more gradual taper with a short terminal step velocity equal to 77% of the initial phase velocity. Its circuit losses were estimated to be only 200 watts while its predicted efficiency was only slightly less than for the original design.

Figure 11 shows the velocity taper cavity configuration consisting of 11 cavities excluding the output coupler and the corresponding normalized velocity profile.

Figure 12 shows the measured interaction impedance variation acorss the operating bandwidth of the standard (uniform) circuit and the intermediate and terminal velocity steps of the taper design.

Figure 13 shows the phase velocity variation across the operating bandwidth of the standard (uniform) circuit and the intermediate and terminal velocity steps of the taper design along with various constant voltage lines.

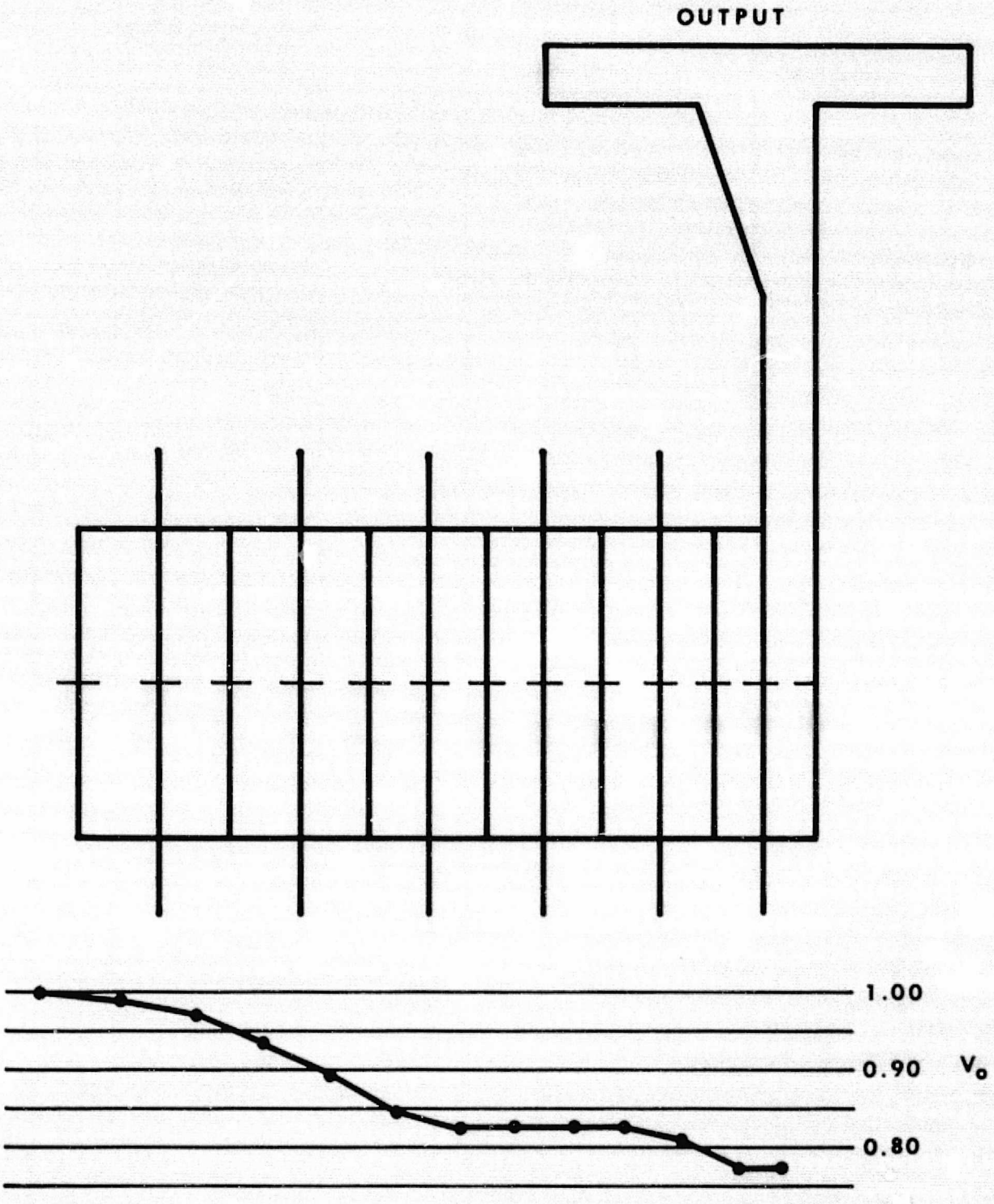

FIGURE 11 VELOCITY TAPER CAVITY CONFIGURATION

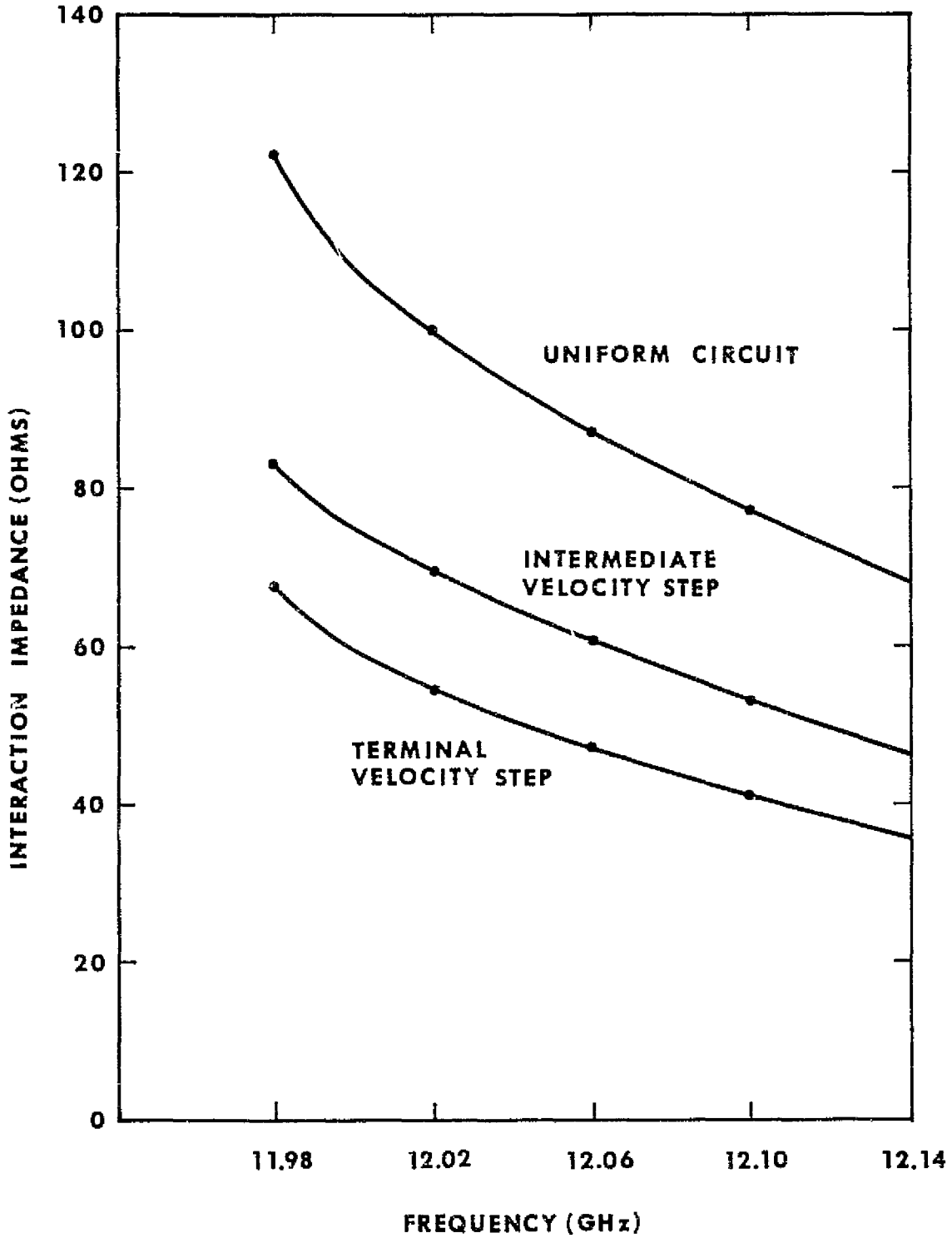

FIGURE 12 - INTERACTION IMPEDANCE OF STANDARD CIRCUIT AND VELOCITY TAPER STEPS (Measured)

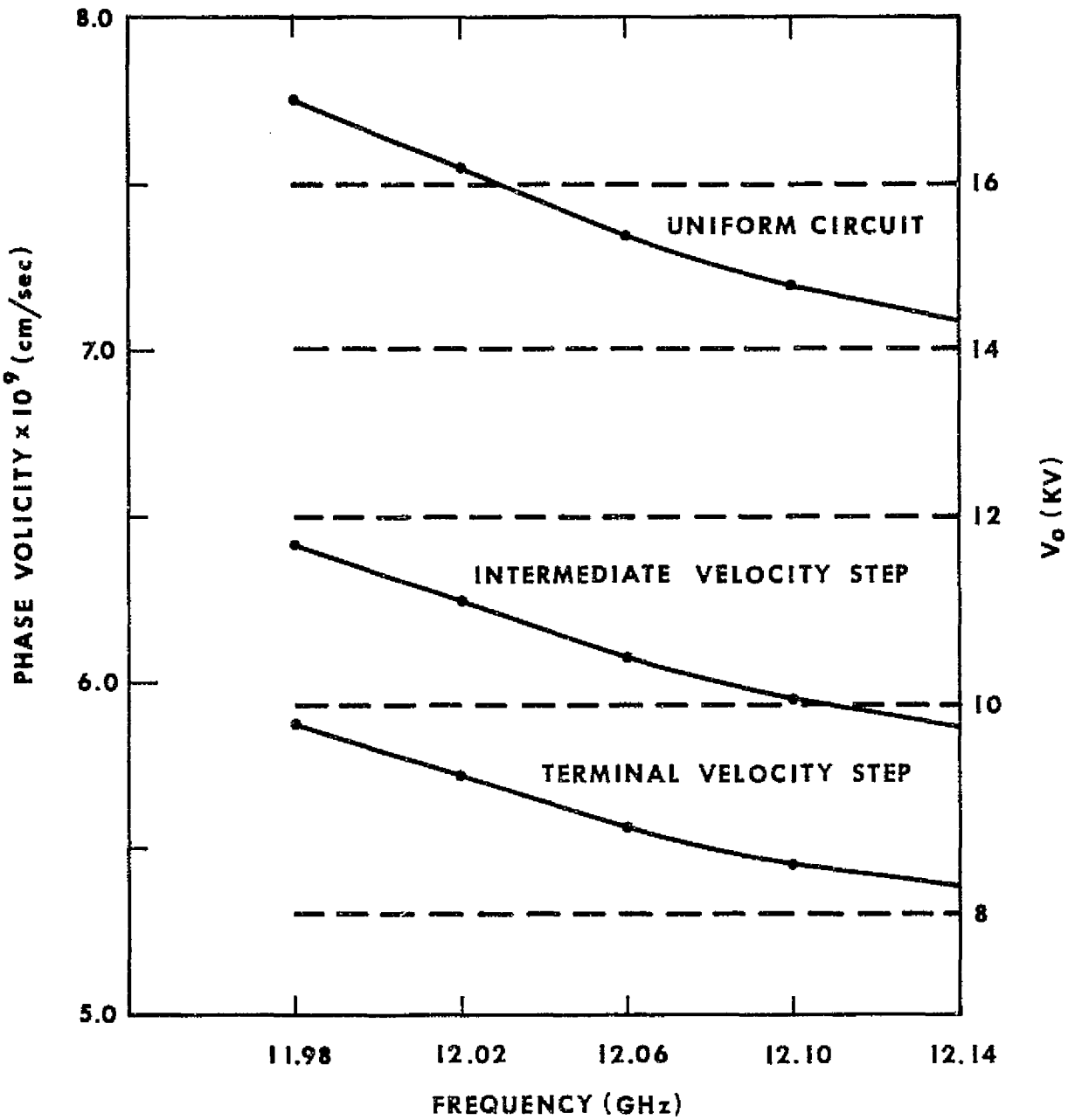

FIGURE 13 - PHASE VELOCITY OF STANDARD CIRCUIT AND VELOCITY TAPER STEPS

4.0 CIRCUIT DESIGN AND VELOCITY RESYNCHRONIZATION

4.3 VELOCITY TAPER DESIGN (continued)

Figure 14 shows the large signal computer prediction of efficiency across the operating bandwidth for the standard circuit with and without a velocity taper. The taper is most effective at the low end of the operating band where the standard circuit efficiency is low due to undervoltaged operation; whereas only a moderate improvement is seen at the upper band edge.

4.4 TUBE STABILIZATION

Coupled cavity tubes are subject to the following types of instabilities:

1. Regenerative oscillations in the operating frequency band.

2. Oscillations at the cut-off frequencies of the operating mode.

3. Oscillations in higher order modes, particularly at their cut-off frequencies.

A. Regenerative Oscillations

Regenerative oscillations can occur within the operating bandwidth when the gain is excessive. In this case, internal feedback occurs from the output of a cavity section to its input due to mismatches, causing oscillations at selected frequencies.

In high gain tubes these oscillations are generally eliminated by separating the slow-wave structure into several terminated gain sections. The coupling between gain sections is accomplished with the modulated electron beam and stability is assured when the gain in each of the sections is less than a critical value, depending on the quality of the termination matches.

A measurement fixture, as shown in Figure 15, was built to allow the evaluation of insertion loss and reflection coefficient of terminations of various lengths. Insufficient loss would appear as a degradation of the impedance match of the termination when inserted in a shorted waveguide as in actual operation and was consequently of concern.

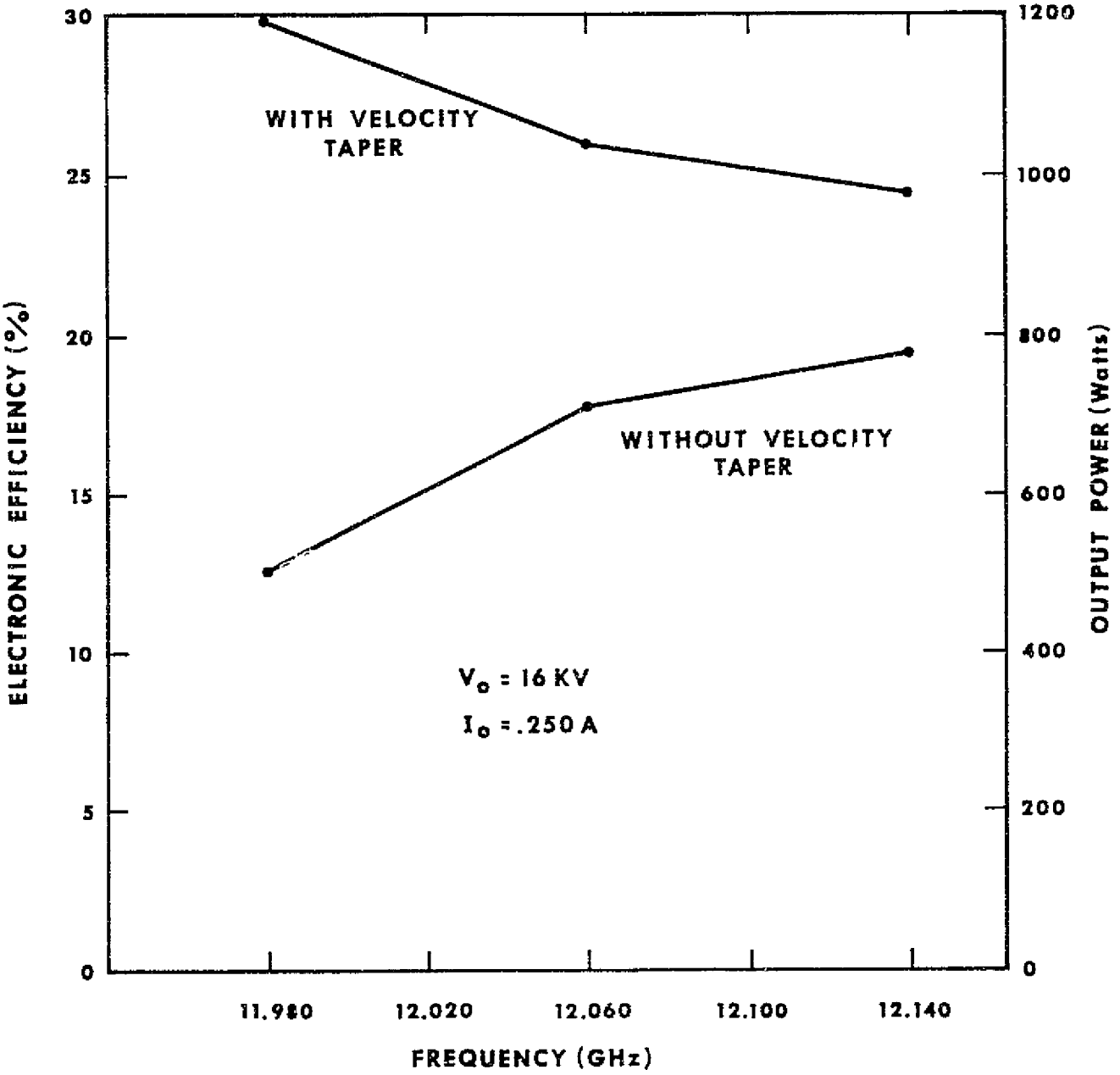

FIGURE 14 - PREDICTED ELECTRONIC EFFICIENCY OF CIRCUIT WITH AND WITHOUT VELOCITY TAPER (Computed)

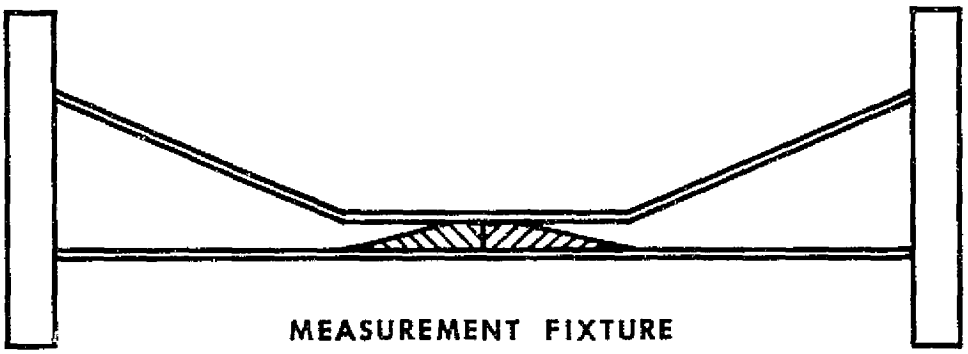

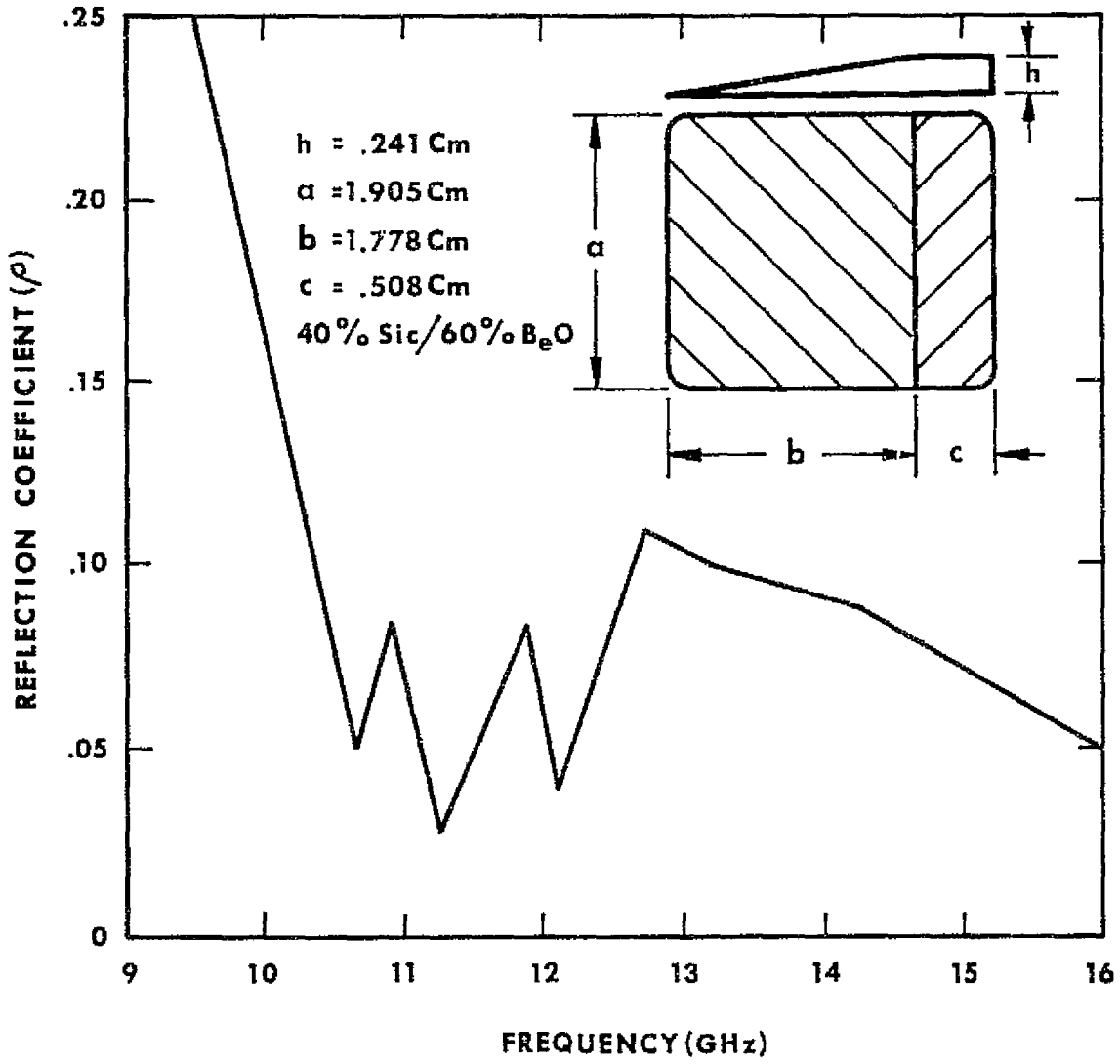

FIGURE 15 – CIRCUIT TERMINATION SCHEMATIC AND REFLECTION COEFFICIENT (Measured)

4.0 CIRCUIT DESIGN AND VELOCITY RESYNCHRONIZATION

4.4 TUBE STABILIZATION

A. Regenerative Oscillations (continued)

The design given in Figure 15 with its resultant reflection coefficient required separation of the slow wave structure into three gain sections to assure stable operation.

The terminations were not brazed to the copper circuit body because of the relatively low power dissipation requirement.

B. Cut-off Frequency Oscillations

The upper cut-off frequency of the operating mode represents generally the strongest instability region due to the impedance becoming infinite at that frequency. These oscillations may occur without drive or they may be produced only with drive at relatively large signal levels (drive-induced oscillations). In this case the average beam velocity is reduced due to energy extraction at large signal levels and then becomes better synchronized with the cut-off frequency range leading to oscillations.

Such oscillations were eliminated with a tuned loss resonator in each cavity, as shown in Figure 8. The resonator consisted of a cylindrical cavity filled with lossy dielectric material which was slightly coupled to the main cavity. Its diameter was chosen to cause it to resonate in the region of the operating mode upper cut-off frequency, introducing high losses to dampen oscillation growth. The cavities were stagger tuned over a 500 MHz range by variable "dimpling" of the flat surface of the dielectric material to blanket the entire high impedance range with high loss.

The lower cut-off frequency, as a result of the high circuit dispersion, was synchronous at 22 kV and not considered a potential instability at the operating voltage of 16 kV. Consequently no oscillation supression schemes were employed in that range.

C. Higher Order Mode Oscillations

The coupled cavity structure is a filter-type circuit and thus is capable of propagating a number of higher order modes.

4.0 CIRCUIT DESIGN AND VELOCITY RESYNCHRONIZATION

4.4 TUBE STABILIZATION

C. Higher Order Mode Oscillations (continued)

Figure 16 shows the slot mode and TM_{11} mode coupled cavity circuit. These modes may also oscillate if the beam velocity is synchronized near any of their cut-off frequencies.

The instabilities of such higher modes are weak, because their interaction fields are generally much smaller than those of the fundamental (TM_{01}) mode. These modes were eliminated with a tuned loss resonator for each mode in each cavity also, as shown in Figure 8. Their diameter was also chosen to cause them to resonate in the region of synchronism with the operating voltage.

The resonant frequency of such resonators is independent of height, allowing their use throughout the velocity taper where cavity heights were reduced.

The composition of the lossy dielectric material affects the cavity Q such that the lower the percentage of silicon carbide the higher the Q, and the greater the loss at resonance. The fundamental upper cut-off resonator material was chosen to provide high loss over a narrow frequency range to avoid introducing loss within the operating bandwidth, and the material for the higher modes was chosen for broad coverage to provide supression over a greater portion of their bandwidth.

The coupling width and major cavity reentrancy were determined empirically to produce the desired magnitude of loss with minimum mismatch.

Table 4.1 summarizes the resonant loss stabiliation design.

4.5 ASSOCIATED MICROWAVE COMPONENTS

A. Waveguide Window

A poker chip type window was developed empirically based on similar existing X-Band window designs. High purity alumina was chosen because of its very low RF loss and superior brazing strength. A schematic of the window design and its performance is shown in Figure 17.

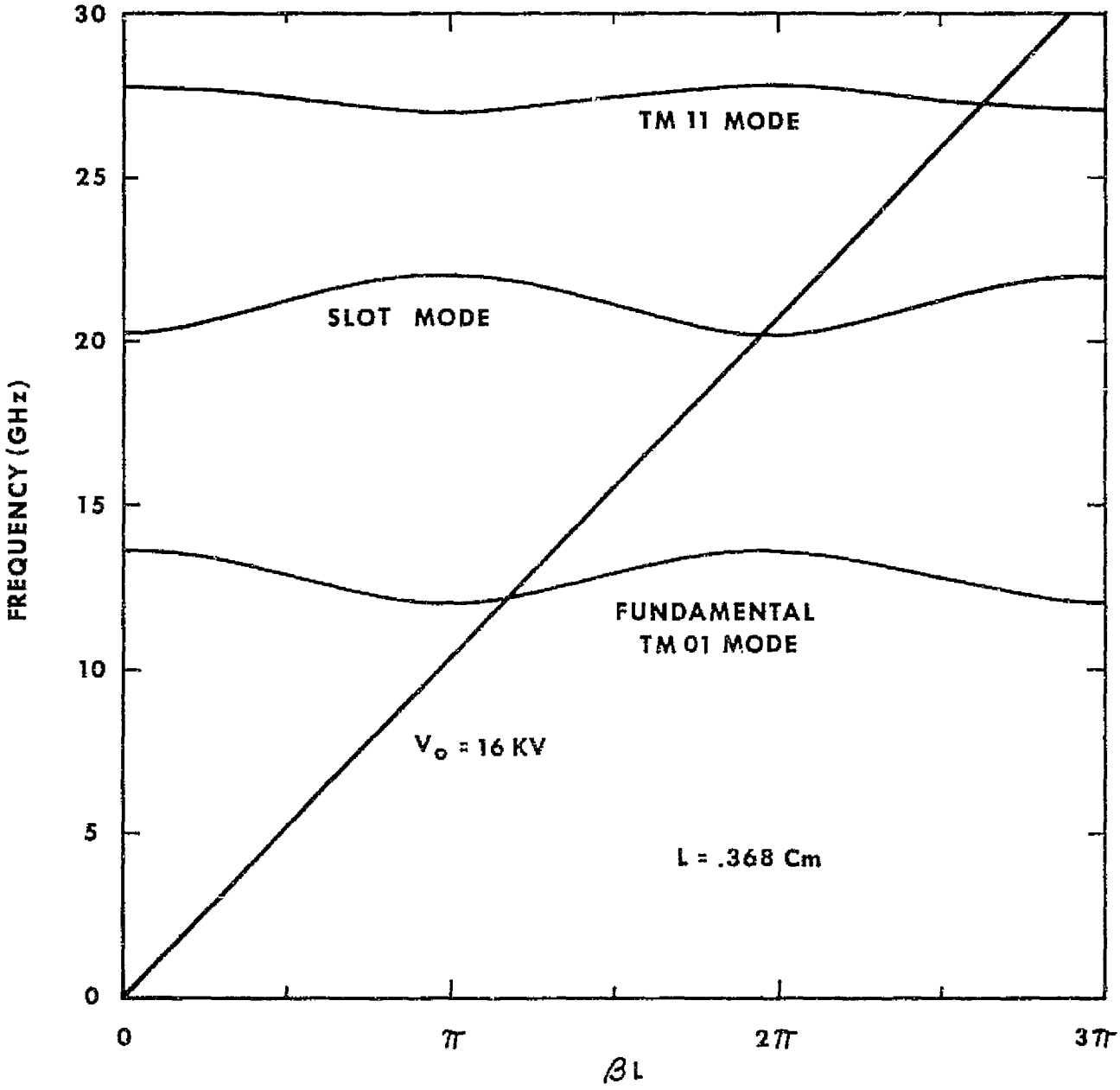

FIGURE 16 - STANDARD CIRCUIT MODES OF PROPOGATION

TABLE 4.1

SUMMARY OF RESONANT LOSS STABILIZATION DESIGN

Instability Region (mode)	Resonator Diameter (cm.)	Resonator Composition %SiC/% MgO	Coupling Width (cm.)	Major Cavity Reentrancy (cm.)	Loss Bandwidth (MHz)
Fundamental (upper cut-off)	.538	1 / 99	.310	0	500
Slot	.284	3 / 97	.267	.051	2000
TM_{11}	.216	3 / 97	.188	.036	≈3000

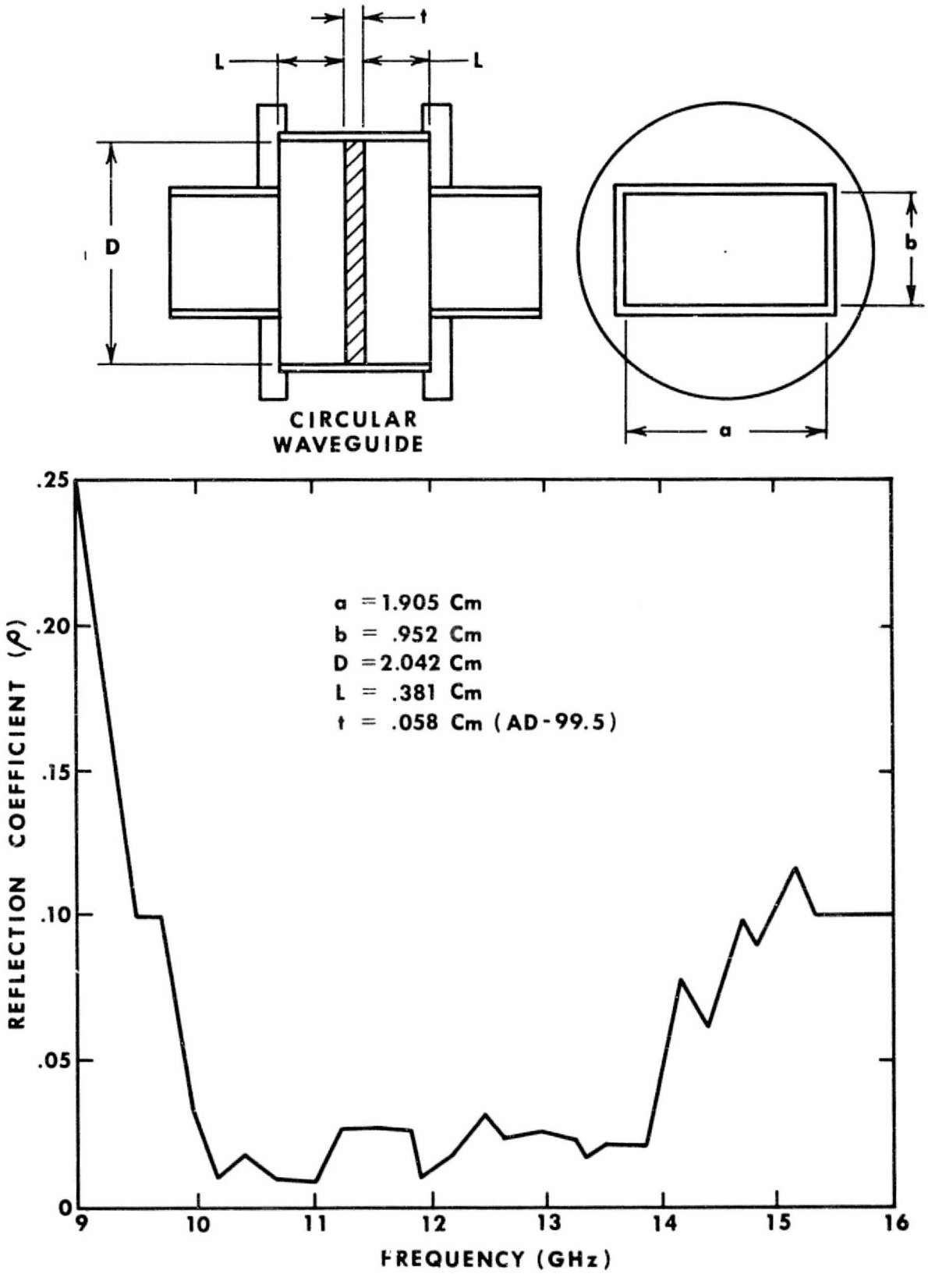

FIGURE 17 - WAVEGUIDE WINDOW SCHEMATIC AND REFLECTION COEFFICIENT (MEASURED)

4.0 CIRCUIT DESIGN AND VELOCITY RESYNCHRONIZATION

4.5 ASSOCIATED MICROWAVE COMPONENTS

A. Waveguide Window (continued)

The voltage reflection coefficient is found to be 2% or less throughout the 10 GHz to 14 GHz range. A ghost mode was identified at 16.3 GHz and was, therefore, of no concern since the circuit was not capable of propagation at that frequency.

An alternate design (D=2.228cm.) was evaluated, however exhibited impedance match degradation above 13 GHz.

B. Waveguide Step Transformer

A four step waveguide transformer was designed to provide a impedance match between the standard input and output waveguide heights and the reduced height waveguides of the couplers. The design was based on quarter wavelength transformer theory[3] and included step susceptance corrections. A Litton computer program was used which allows specification of bandwidth and number of steps. Step dimensions and resultant VSWR are then given. The design and performance of the transformer is shown in Figure 18.

C. Vacuum Tank Feedthroughs

To facilitate testing of the tube within the NASA vacuum chamber two conflat flanges with waveguide window feedthroughs were required. The window design used was identical to the design developed for the tube windows. Figure 19 is a photograph of the assembly.

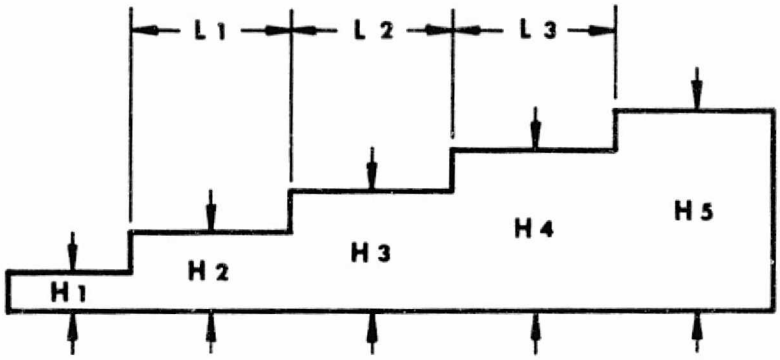

L 1 = .734 Cm H 1 = .241 Cm H4 = .782 Cm
L 2 = .706 Cm H 2 = .295 Cm H5 = .952 Cm
L 3 = .767 Cm H 3 = .480 Cm

WAVEGUIDE WIDTH =1.905 Cm

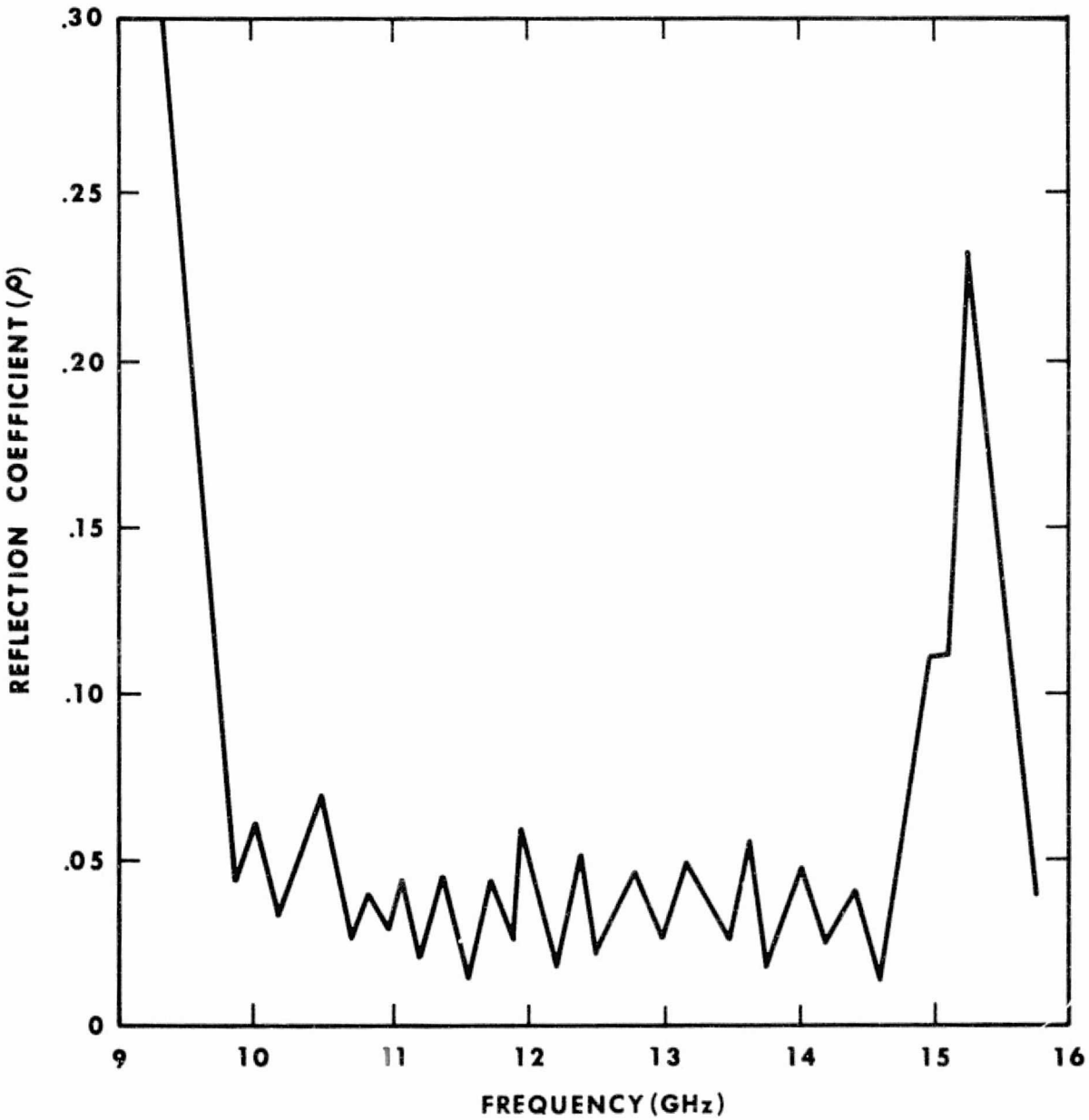

FIGURE 18 - WAVEGUIDE STEP TRANSFORMER SCHEMATIC AND REFLECTION COEFFICIENT (Measured back to back)

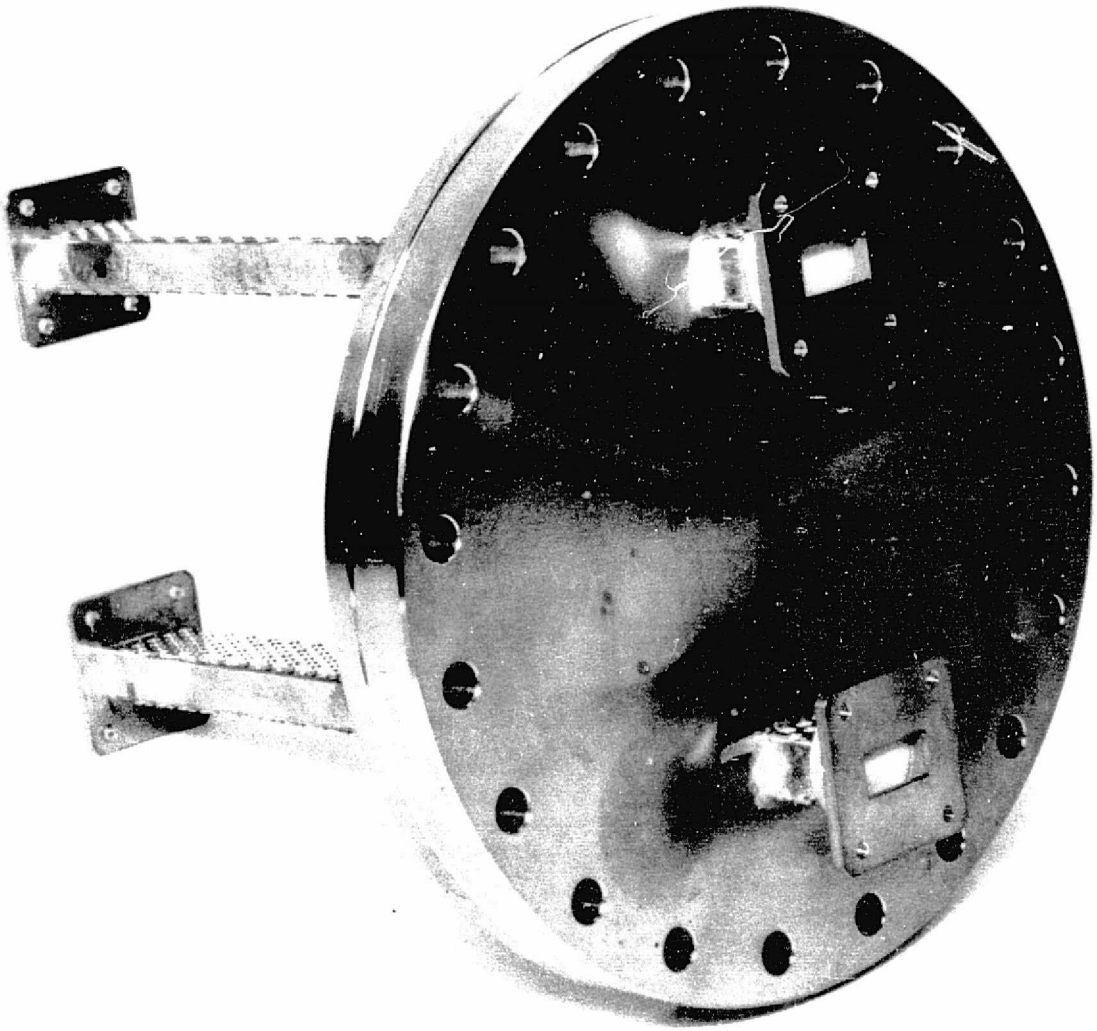

FIGURE 19 - CONFLAT FLANGE WITH WAVEGUIDE WINDOWS

5.0 GUN AND FOCUSING DESIGN

A. Gun Design

The gun design was based on well known methods for Pierce type guns[4], using the Litton gun trajectory analysis computer program. Because of the low gun perveance, a high area convergence design with good beam laminarity was possible. The high area convergence allowed for relatively low cathode current density, permitting low cathode operating temperature and long life capability.

A tungsten matrix cathode was chosen because of its suitability for operation in the NASA vacuum chamber, since it is very rugged and can be easily reactivated after exposure to air.

The maximum field gradient was maintained below 40 kV/cm. to avoid voltage breakdown problems.

The design included an insulated anode (modulation anode) to allow evaluation of tube performance at various beam currents at constant circuit potential. The design provided for the anode to produce the desired perveance when operating at a slightly elevated voltage (a few hundred volts with respect to circuit potential), creating an ion trap to prevent positive ion bombardment of the cathode surface.

1. Initial Design

The initial design was directed at the 2 kW operation level with a design objective of 0.2 micro-perveance and an area convergence of approximately 50. The cathode diameter was .711 cm., yielding a cathode current density of 1 amp/cm^2. The trajectory analysis computer program predicted a minimum beam size of .074 cm., located 1.092 cm. from the anode face. The computer analysis however did not take thermal velocity effects into account and consequently a larger beam size was expected.

The computer analysis was also performed at a beam potential of 15 kV, at which measurement in the electrostatic gun analyzer was not desirable due to the possibility of damage to the aperture at that high a potential. Measurements were generally limited to 10 kV beam potential at very low duty cycle.

Extrapolation of beam size, based on previous experimental data and analysis, was therefore necessary to compare measured results with computer predictions.

5.0 GUN AND FOCUSING DESIGN

A. Gun Design

1. Initial Design (continued)

The perveance was measured at 5 kV to be 0.238 microperveance, slightly higher than the design objective. No anode interception current was detected. Beam profiles were measured in .254 cm. increments along the axis at the 5 kV potential and were found to be well defined at their edges and showed fairly uniform current density distributions in their cross sections, indicating a high degree of laminarity.

The performance was also evaluated at .118 microperveance by depressing the anode voltage 2.1 kV. These profiles showed that the beam perveance could be varied over a large range without affecting the quality of the beam. The gap between anode and tube body was .432 cm. in order to minimize its lens effect at reduced perveance operation.

The measured minimum beam size containing 95% of the total current at 5 kV was .160 cm. at 0.238 microperveance and .155 cm. at .118 microperveance, showing a very small variation with change in perveance. The measured beam minimum location showed excellent agreement with the computer prediction, and was found to be independent of perveance. The beam size for 15 kV operation was extrapolated to be .112 cm., giving a beam (95% of total current) to tunnel diameter ratio of 0.67 and an area convergence of 40.

This design was used on the Experimental Tube.

2. Modified Design

The program redirection to be 1.25 kW operation level required a modification of the initial gun design from 0.2 microperveance to 0.13 microperveance, since the change was to be effected by a reduction in current at constant beam voltage.

The cathode and anode geometry were not modified, thereby reducing the cathode current density to 600 mA/cm^2, however the spacing between them was increased to cause the reduction in perveance. The focus electrode geometry was then modified based upon computer trajectory analysis. The mechanical configuration was not altered to allow the cathode replacement scheme to remain the same.

5.0 GUN AND FOCUSING DESIGN

A. Gun Design

2. Modified Design (continued)

The design achieved a microperveance of 0.125 with a extrapolated minimum beam diameter containing 95 percent of the total current of .084 cm. at 15 kV, corresponding to a beam to tunnel diameter ratio of 0.5.

Although this design appeared feasible for use in the Development Tube, focusing data obtained on the Experimental Tube indicated that a somewhat smaller beam size appearance preferable for good focusing.

The design was therefore modified by a small change in the focus electrode geometry to produce a somewhat smaller beam size. Figure 20 is the trajectory analysis prediction at 15 kV for this design, showing a minimum beam size of .084 cm. located approximately .762 cm. from the anode face.

Figure 21 shows the measured current density profiles at five varying axial locations for this design at 10 kV. Analysis of these profiles produced the data shown in Figure 22, wherein beam contours containing various percentages of total beam current are shown. The beam diameter containing 95 percent of the total current is .079 cm. at its minimum, located .635 cm. from the anode face. A single profile measurement at this location at 15 kV revealed a beam diameter of .057 cm. containing 95 percent of the total current and a diameter of .089 cm. containing 99 percent of the total current. This design yielded a beam (99% of total current) to tunnel diameter ratio of 0.53 and was used in the Development Tube.

B. Focusing Design

1. PPM Structure Design

The PPM focusing design was considered very critical due to the unusually high average power requirement for the relatively high frequency of operation. Efficient beam wave-circuit interaction at 12 GHz is accomplished by compressing the beam to a comparitively small diameter, producing high beam space charge density and thus requiring high focusing peak fields.

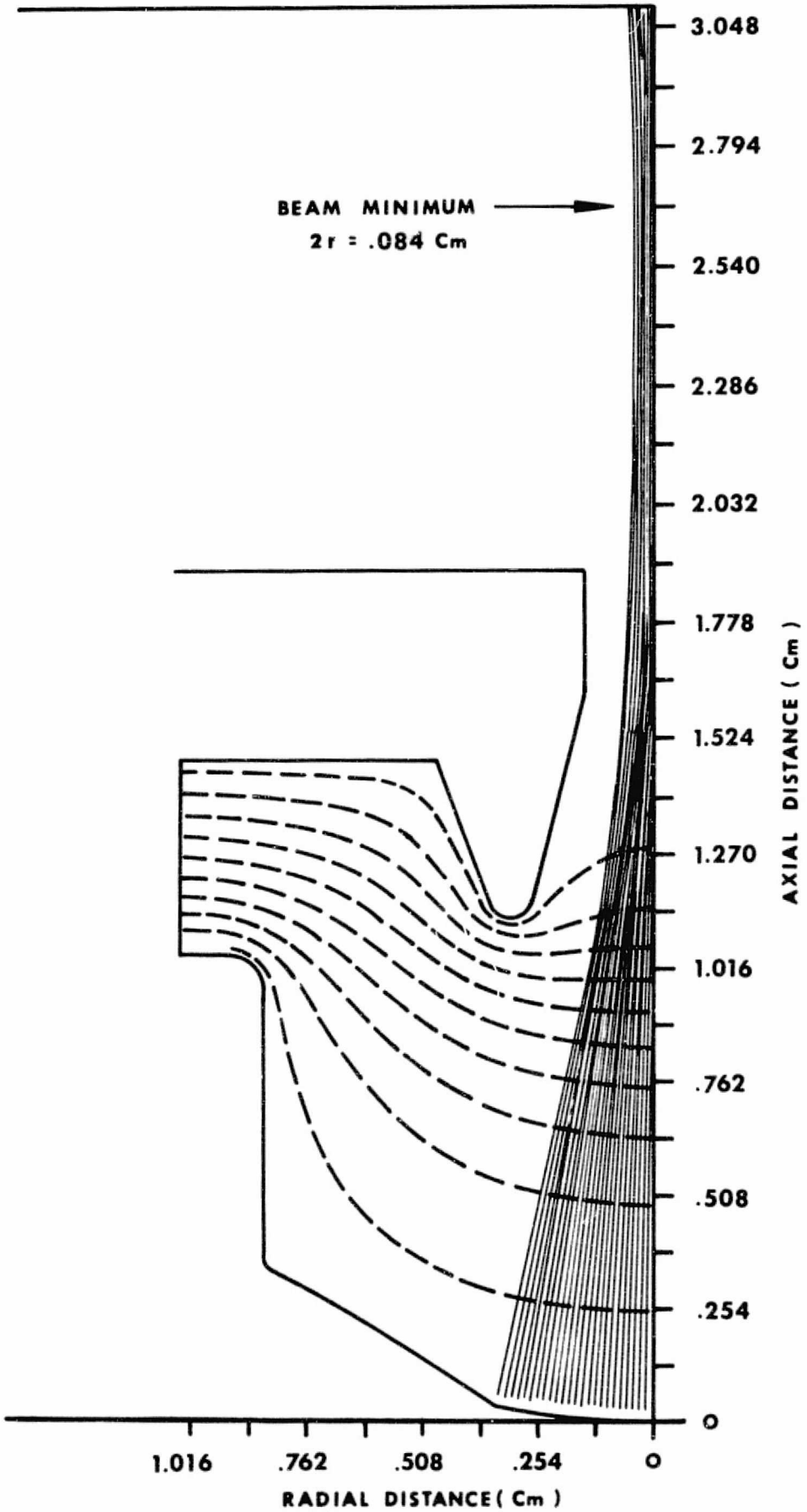

FIGURE 20 – GUN TRAJECTORY ANALYSIS (Computed)

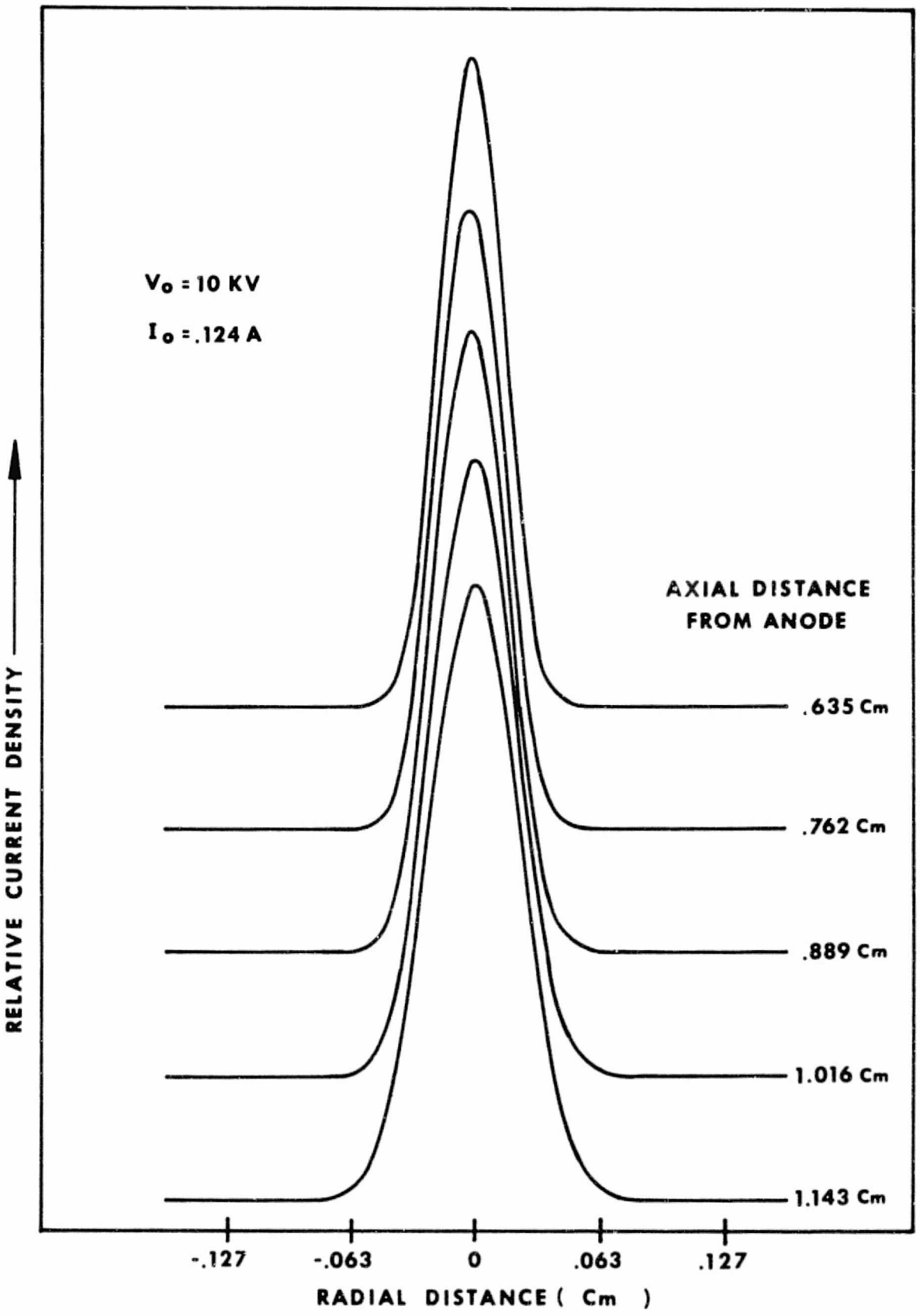

FIGURE 21 – BEAM CROSS SECTION CURRENT DENSITY AT VARYING AXIAL LOCATION (Measured)

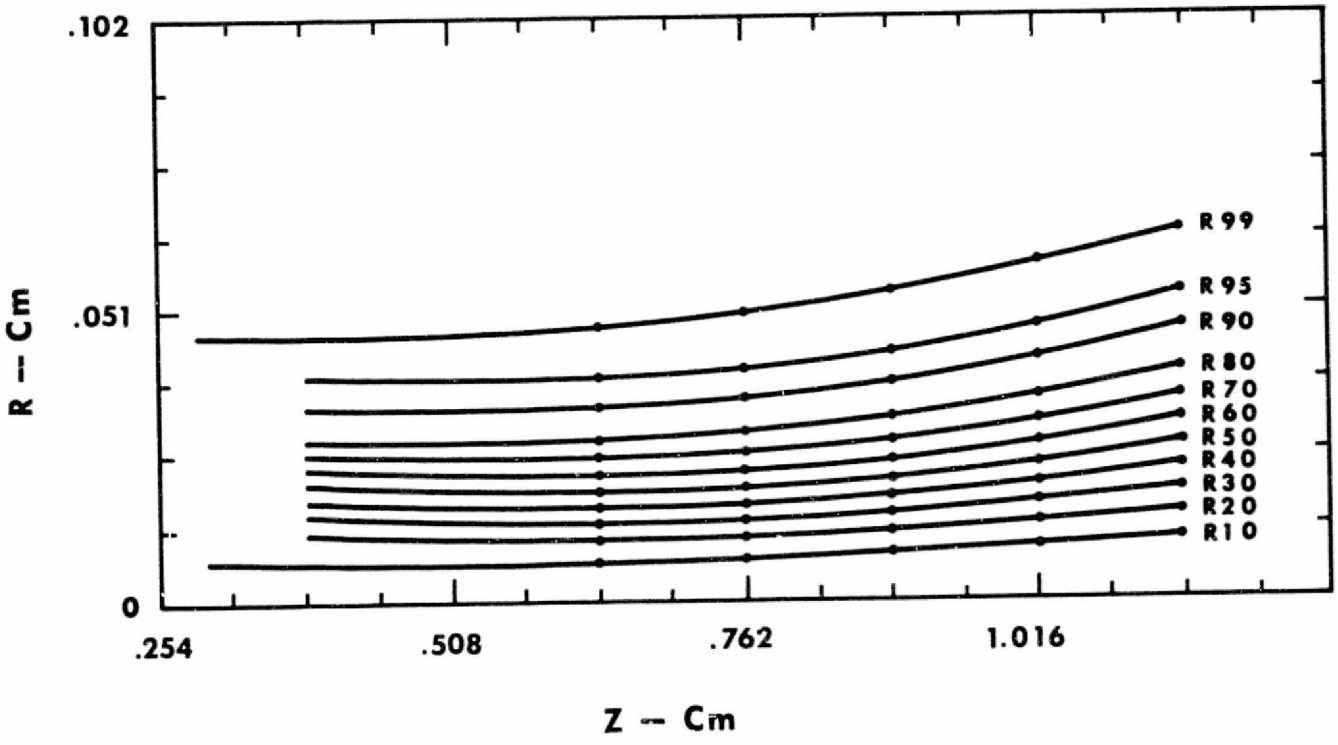

FIGURE 22 - BEAM CONTOURS CONTAINING VARIOUS PERCENTAGES OF TOTAL CURRENT

5.0 GUN AND FOCUSING DESIGN

B. Focusing Design

1. PPM Structure Design (continued)

The calculated Brillouin field for the initial design, with a beam to tunnel diameter ratio of 0.6 at 0.2 microperveance and 16 kV operating voltage is 930 gauss. This relates to a peak field requirement of approximately 2600 gauss to achieve good focusing with the high efficiency design.

Platinum Cobalt was initially chosen as the magnetic material because of its high coercive force and suitability for operation in the NASA vacuum chamber. The material is a solid metal (rather than a sintered powder) and was believed not to exhibit outgassing problems. Consequently this material was used on the Experimental Tube.

However due to the extremely high cost of Platinum Cobalt it seemed appropriate to evaluate the outgassing characteristics of Samarium Cobalt (made by sintering of fine powder) as compared to Platinum Cobalt.

Sample magnets were cleaned and sealed into a stainless steel chamber connected to a 1 l/sec vac-ion pump. The test chamber with its pump was sealed on to a high vacuum exhaust system and baked at 100° - 125°C for twelve hours. The test chamber was then sealed off and operated with its appendage pump. A four hour bakeout was performed at 100° - 105°C to simulate operation in the NASA vacuum chamber. A final test was made by letting the test chamber stand for five days without pumping in order to determine if residual outgassing of the various materials was a problem.

The results of the tests are given below:

TABLE 5.1

MAGNET OUTGASSING CHARACTERISTICS

Material	Vendor	Bakeout Pressure (Torr) Max.	Bakeout Pressure (Torr) Final	Sealed Off Pressure @ 105°C
PtCo	Hamilton	1×10^{-6}	5×10^{-8}	8×10^{-8}
SmCo	Raytheon	5×10^{-7}	4×10^{-8}	4×10^{-8}
SmCo	G.E.	4×10^{-6}	2×10^{-7}	9×10^{-8}

5.0 GUN AND FOCUSING DESIGN

B. Focusing Design

1. PPM Structure Design (continued)

There was no residual outgassing detected from any of these materials after a five day period without pumping.

It was therefore concluded that both materials were acceptable for operation in the NASA vacuum chamber and SmCo was substituted because of its lower cost in the Development Tube.

Since SmCo has a higher coercive force it was possible to use the same magnet design with SmCo as for PtCo by reducing the magnetization of the magnets slightly to the desired value.

In order to provide the required axial peak magnetic field double period focusing with intermediate magnetic ferrules was utilized.

Double period focusing provides a higher axial magnetic field than is possible with single period focusing due to the larger amount of magnetic material between the pole pieces.

The design analysis of the PPM configuration was performed on the Litton PPM computer program based on rotational symmetry.[5] This program calculates the leakage flux in detail, so that the axial field can be determined as a function of the configuration, the magnet material, and the inner and outer radius (R4 and R5) of the magnet material. In addition, the flux density at various locations in the pole piece is calculated.

In the initial 2 kW level design at the chosen pole piece thickness, the maximum calculated flux density was 18,000 Gauss, exceeding the capability of vacuum iron (15,000 Gauss). Increasing the pole piece thickness would have significantly reduced the available magnet thickness and lowered the peak field even further, as well as reduced the interaction impedance. Consequently Permendur was chosen as the pole piece material in the Experimental Tube due to its higher maximum flux density (18,000 to 20,000 Gauss).

However the program redirection to the 1.25 kW level lowered the peak field requirements substantially, rendering vacuum iron magnetically capable. This material was then substituted in the Development Tube because of its easier machinability and processing.

5.0 GUN AND FOCUSING DESIGN

B. Focusing Design

1. PPM Structure Design (continued)

It was then found necessary to incrementally increase the magnet and pole piece outer radii in the velocity taper region in order to compensate for the field reduction associated with the incremental reduction in magnet thickness. The terminal magnet radius in the velocity taper region was enlarged by .292 cm. to effect this compensation.

The stability factor $\frac{\lambda p}{T}$ was equal to 6.1 in the uniform circuit sections, increasing to 8.1 in the velocity taper, consistent with good RF focusing requirements.

Figure 23 gives the details of the magnetic focusing design for the uniform circuit of the Development Tube.

Figure 24 shows the resultant measured axial magnetic field distribution of the Development Tube.

2. Beam Launching Design

The Litton trajectory computer program was used to optimize the beam entrance conditions into the magnetic focusing field. The axial location of the gun was varied with respect to the magnetic field as well as the magnitude of the first field peak to determine the optimum launching conditions. This is achieved when the beam ripple is minimized. The optimized result of the 0.125 microperveance gun used on the Developmental Tube is shown in Figure 25, with the electrostatic beam minimum position located where the magnitude of the first magnetic peak has decayed to zero (.508 cm. axial distance). The trajectory plot shows the outermost electron to be well contained within the beam hole radius, indicating excellent dc focusing. 98% dc transmission was achieved on the Development Tube and 91.4% at saturation.

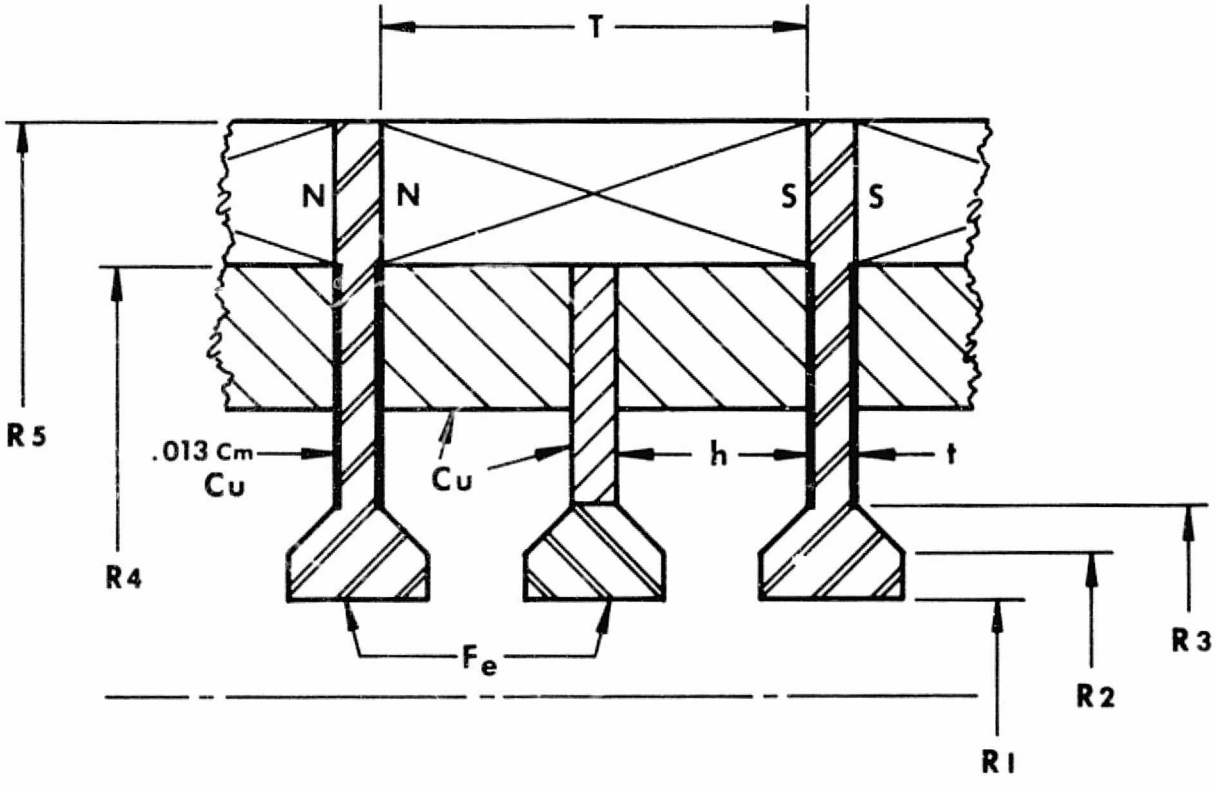

T =.610 Cm (uniform circuit)
t =.127 Cm
h=.241 Cm (uniform circuit)

R1 = .084 Cm
R2 = .160 Cm
R3 = .198 Cm
R4 = 1.651 Cm
R5 = 1.994 Cm (uniform circuit)

FIGURE 23 — SCHEMATIC OF DOUBLE PERIOD MAGNETIC FOCUSING

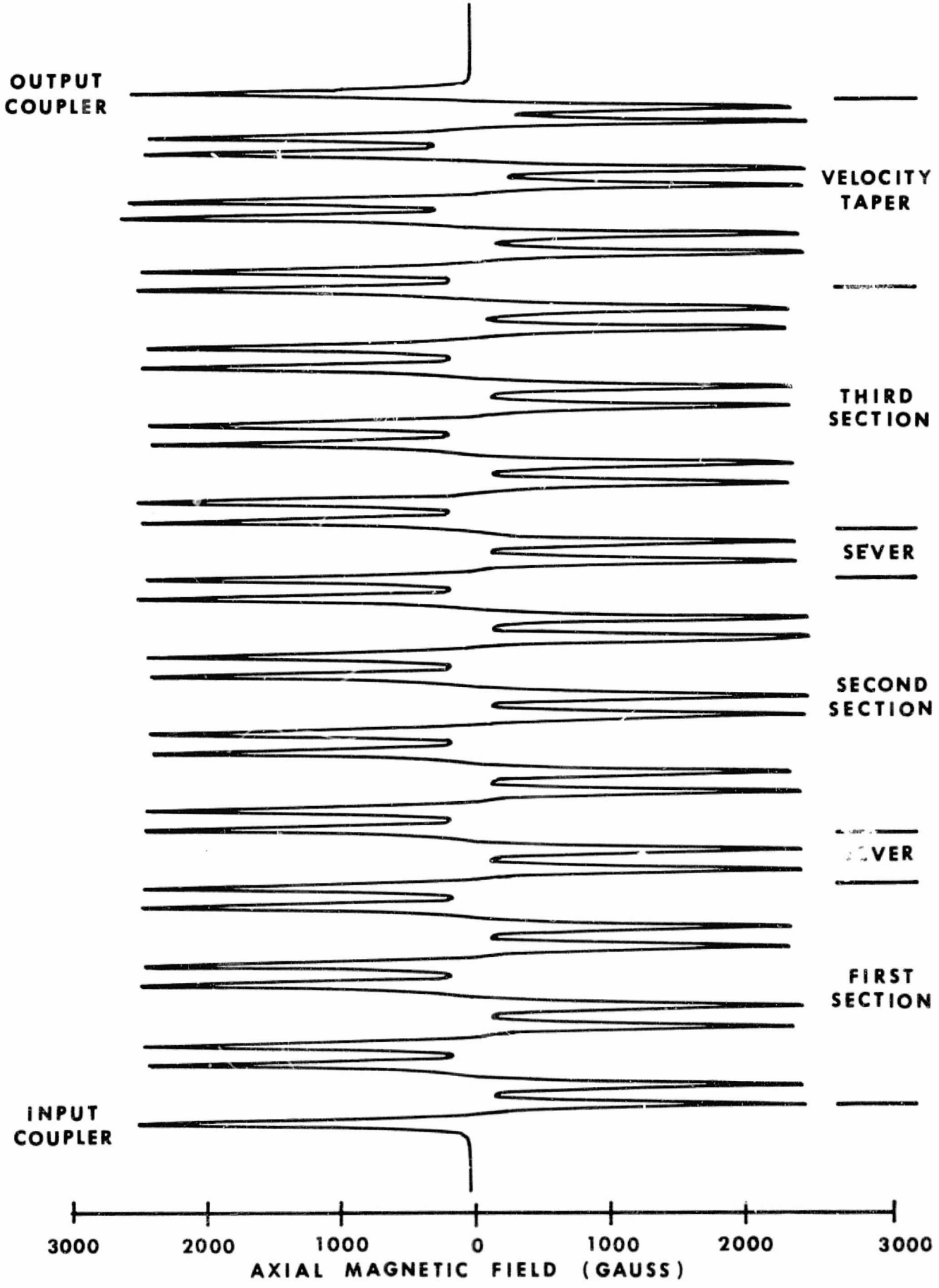

FIGURE 24 - AXIAL MAGNETIC FIELD DISTRIBUTION (MEASURED)

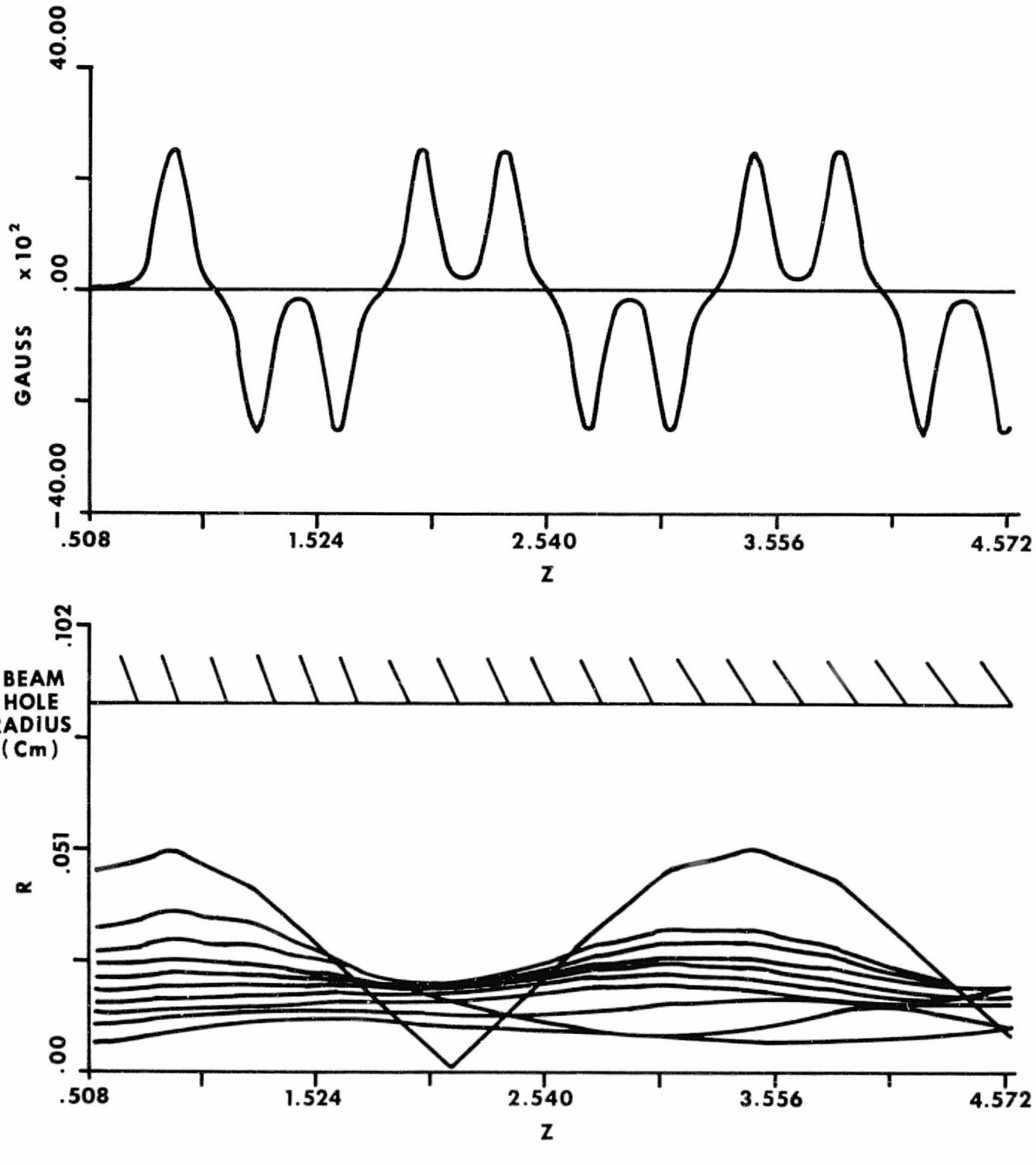

FIGURE 25 - BEAM LAUNCHING CONDITIONS INTO MAGNETIC FOCUSING FIELD

6.0 REFOCUSING DESIGN

A refocusing section design was included as part of the collector baseplate assembly to be used in conjunction with the Development Tube as a test vehicle for the evaluation of NASA designed multistage collectors. In order for the multistage collector to yield maximum energy recovery the spent beam must be reconditioned before entrance into the collector. This is accomplished in the refocusing section by means of a specified magnetic field distribution. This distribution allows the spent beam to first expand and thereby reduce its space charge forces, after which it is refocused to cause the electron trajectories to become more parallel for more effective velocity sorting in the collector.

The proposed refocusing field configuration with solenoids and permanent magnets in shown in Figure 26. Early investigations revealed that permanent magnet refocusing was feasible only if a field reversal between the tapered field region and the uniform field region was permittable. The desired field shape without a field reversal can be generated with permanent magnets, however excessive magnetic leakage fields are then induced outside the refocusing region in the PPM stack and collector.

The refocusing field pattern was specified by Dr. H. Kosmahl of NASA as follows:

a) The magnitude of the first magnetic peak was chosen to be the root mean square of the periodic field.

b) The length of the taper field was chosen to be equal to two cyclotron wavelengths of the spent beam with respect to the average magnetic focusing field.

c) The uniform field was chosen to be a factor of 2.5 smaller than the first magnetic peak to allow the beam size to increase by the same factor.

d) The length of the uniform field was chosen to be equal to 0.46 cyclotron wavelengths of the spent beam in the uniform drift region.

Figure 27 shows the closest refocusing field configuration achieved with permanent magnets (Samarium Cobalt) with and without a pole piece located at the transition. No leakage field was induced in the PPM stack yet some was present in the collector region slightly in excess of the maximum specified value. This however could be reduced with additional shielding if necessary.

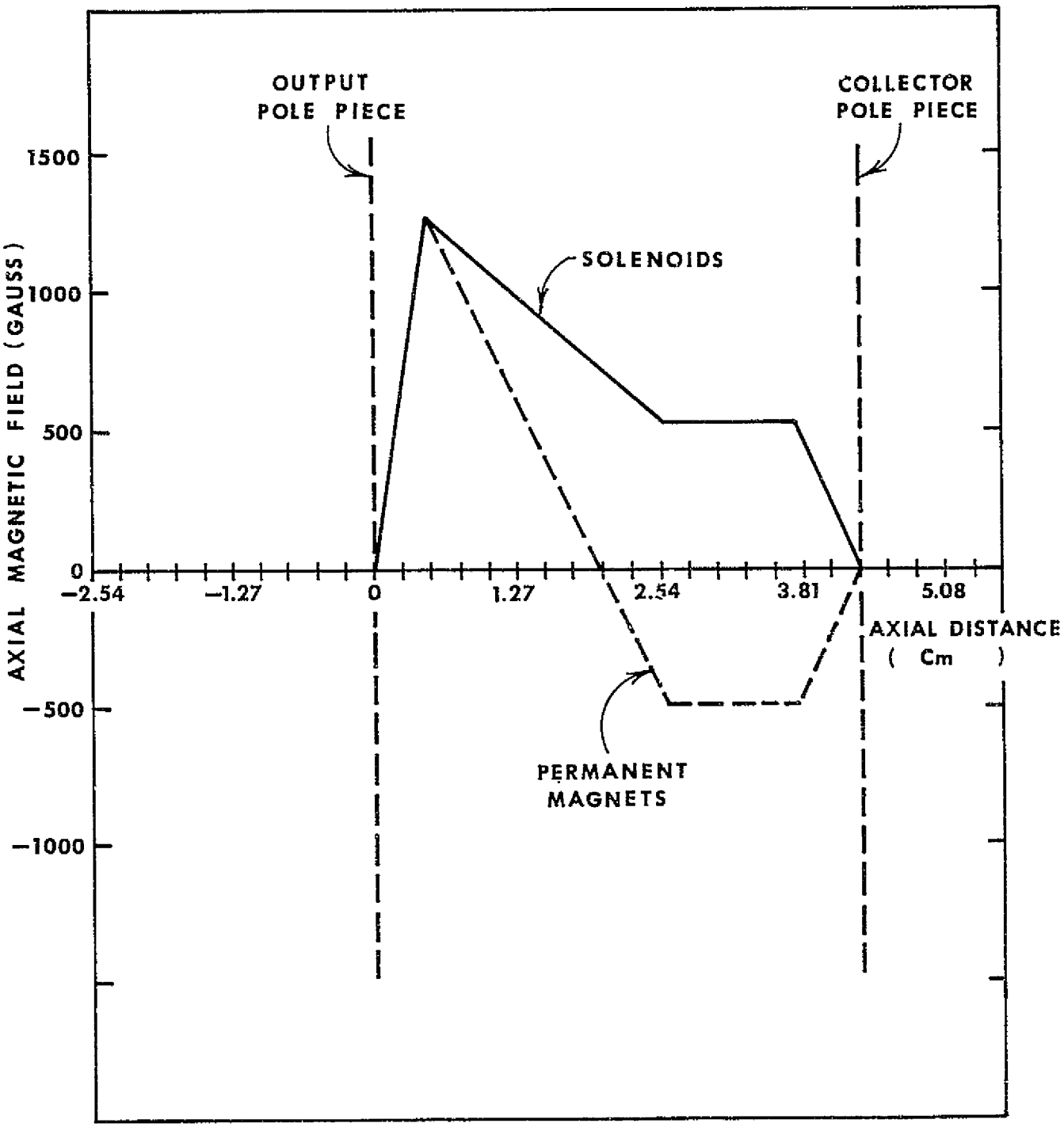

FIGURE 26 - PROPOSED REFOCUSING FIELD CONFIGURATION WITH SOLENOIDS AND PERMANENT MAGNETS

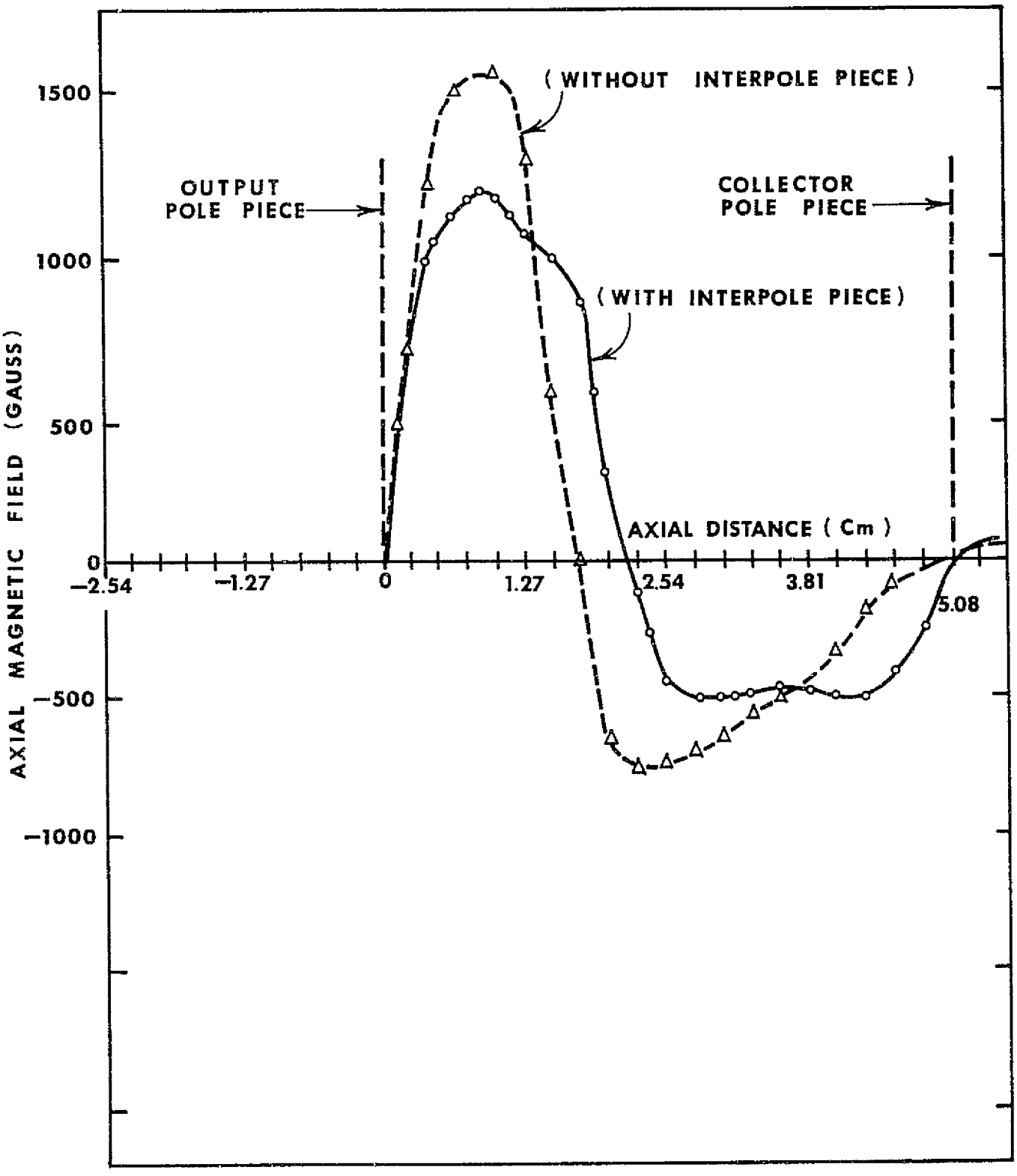

FIGURE 27 - REFOCUSING FIELD CONFIGURATION WITH PERMANENT MAGNETS (MEASURED)

6.0 REFOCUSING DESIGN (continued)

A solenoid refocusing design was undertaken in parallel with the permanent magnet design. A two section coil tester was constructed and evaluated with the two coils in series and anti-series. The latter type of operation produces a field reversal between the tapered field and the uniform field and was intended to simulate a permanent magnet design. Magnetic field shaping was found to be flexible by variation of the currents in either of the two coil sections, including the field reversal configuration.

Figure 28 shows the closest field configuration achieved with the solenoids operated in series. Figure 29 shows the closest field configuration achieved with the two solenoids operated in anti-series to produce the field reversal pattern.

The refocusing section of the collector baseplate assemblies was constructed of this design to allow experimental optimization of the multistage collector performance. Power consumption to produce the given field shapes was in the 85 to 100 Watt range for series operation and in the 105 to 130 Watt range for anti-series operation.

Details of the mechanical design of the solenoid refocusing assembly are given in Section 7.4.

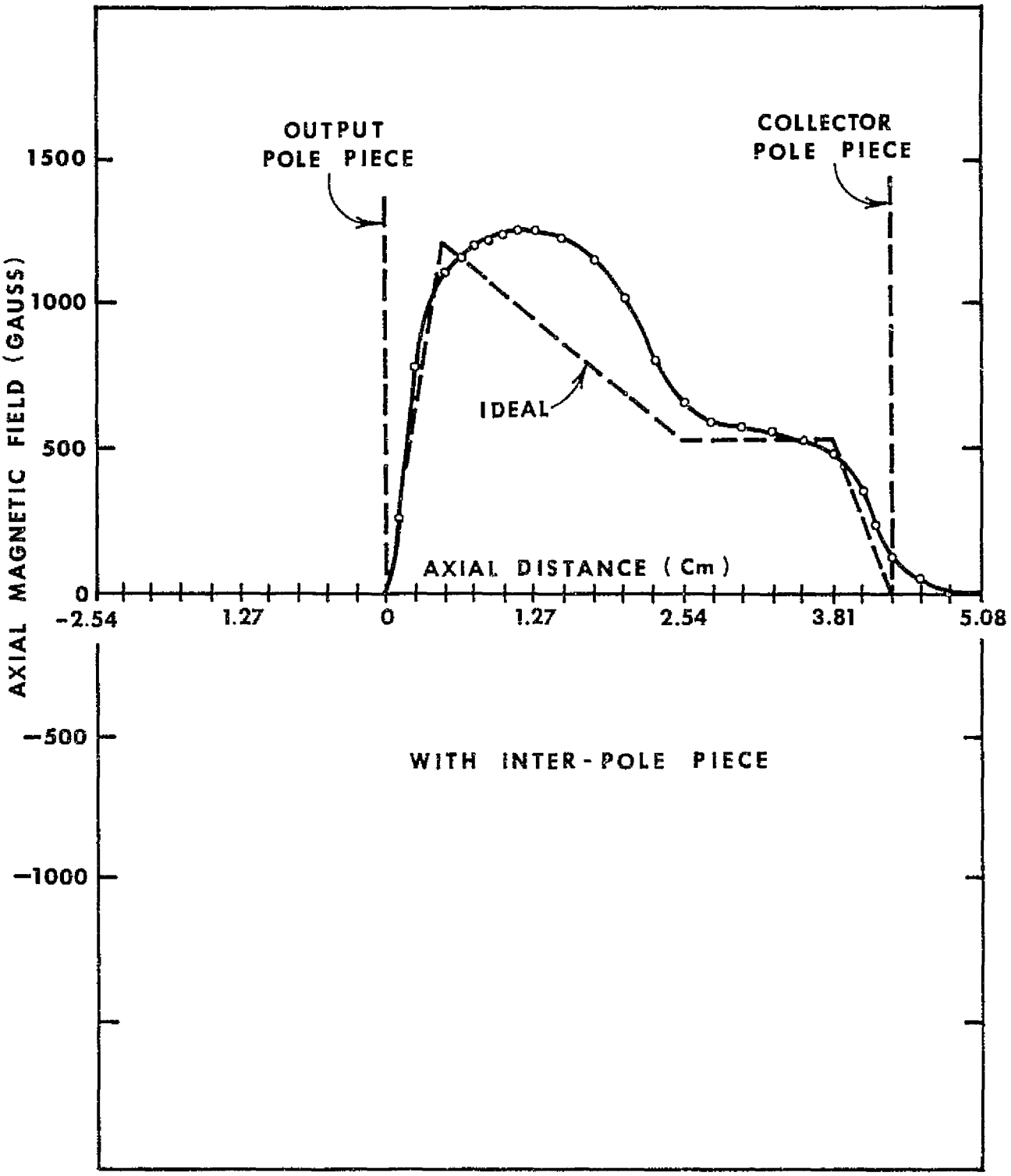

FIGURE 28 - REFOCUSING FIELD CONFIGURATION WITH SOLENOIDS (MEASURED)

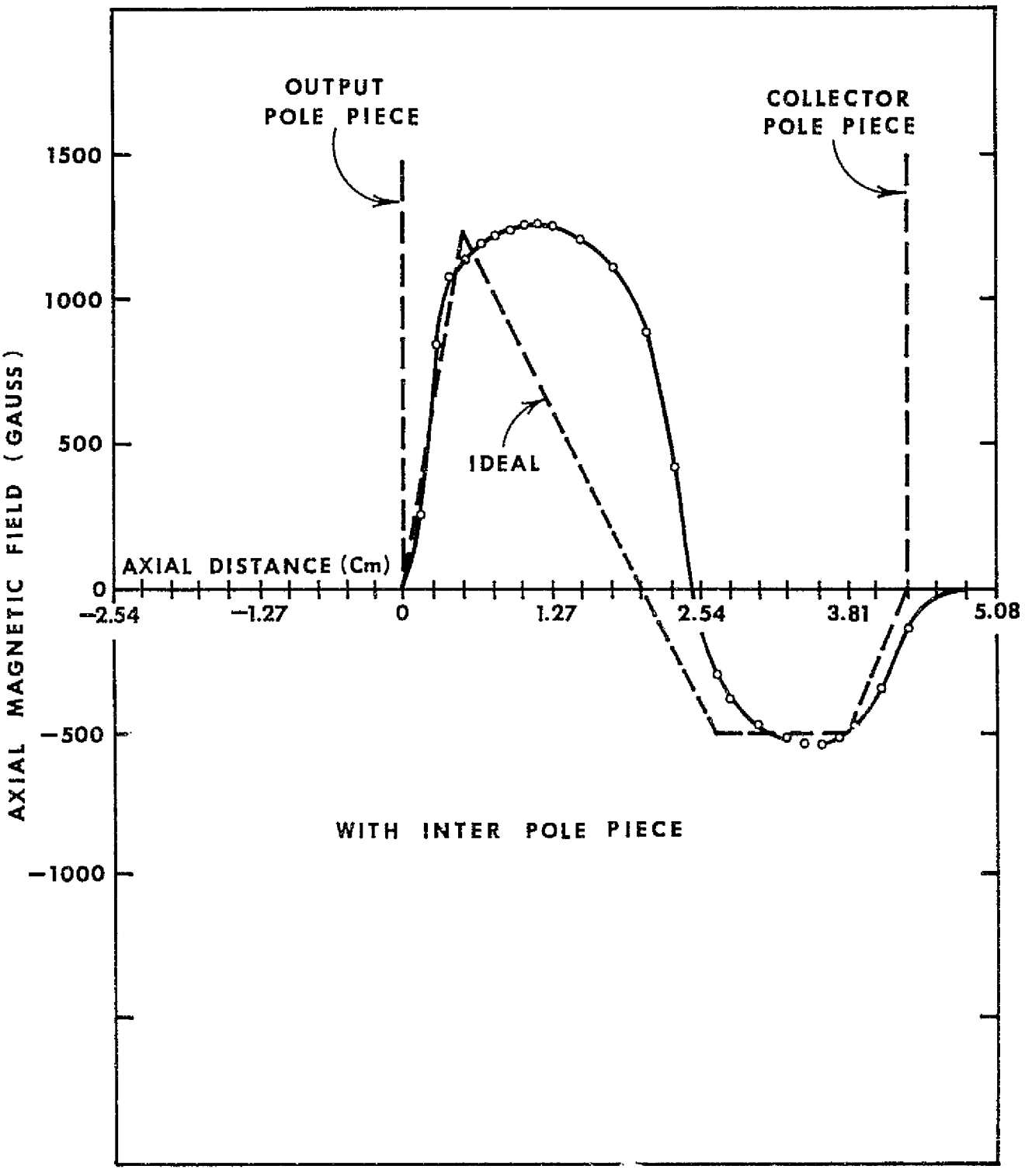

FIGURE 29 - REFOCUSING FIELD CONFIGURATION WITH SOLENOIDS WITH FIELD REVERSAL (MEASURED)

7.0 MECHANICAL DESIGN

7.1 THERMAL CIRCUIT ANALYSIS

Beam current interception at the ferrule tip is the most important heat source to be considered, imposing a limitation on the power handling capability of the circuit. The circuit pole pieces must be thermally capable of transferruing this heat to the coolant fluid region while maintaining a temperature differential within acceptable limits. The coolant fluid was channeled through the cavity spacers and pole pieces as shown in Figure 8. Assuming that the fluid temperature could reach 100°C (T_o) and that the cavity wall would be maintained at this temperature, a 200°C maximum temperature differential was considered permissible, allowing a ferrule temperature of 300°C (T_i). This provided a safety margin of approximately two against Curie point destruction.

The circuit thermal schematic is shown in Figure 30. Copper cladding (t_2) of the iron pole pieces was necessary to keep the temperature gradient within the permissible limit, almost doubling the thermal capability of an all iron pole piece.

The design was based on the specified minimum RF collector transmission of 95%, corresponding to 200 Watts of interception power. Actually this value would be considerably less since generally intercepted electrons have lost some of their energy to the RF wave, however 200 Watts was used in the analysis. It was then assumed that the interception would be evenly distributed over at least 4 cavities, or a maximum of 50 Watts per cavity. The analysis is performed for the copper-iron pole piece only since the alternate all copper pole pieces exhibit far superior thermal capability. The thermal conductance of the pole piece from the ferrule tip to the cavity wall including the coupling slot effect is given by:

$$G_T = \frac{2\pi}{\left[\frac{1}{(t_1k_1 + 2t_2k_2)}\right]\left[\frac{360}{360-2\arctan w/2X}\right]\ln\frac{2r_3}{r_1+r_2} + \frac{(4f+t_1+2t_2)^2}{16k_1(2f+t_1+2t_2)^2(r_2-r_1)^2}}$$

where t_1 = .1016 cm.

t_2 = .0127 cm.

k_1 = thermal conductivity of iron (200°C) = .64 $\frac{\text{watts}}{\text{cm°C}}$

k_2 = thermal conductivity of copper (200°C) = 3.6 $\frac{\text{watts}}{\text{cm°C}}$

w = coupling slot width = .340" = .8636 cm.

X = coupling slot center to circuit center = .3708 cm.

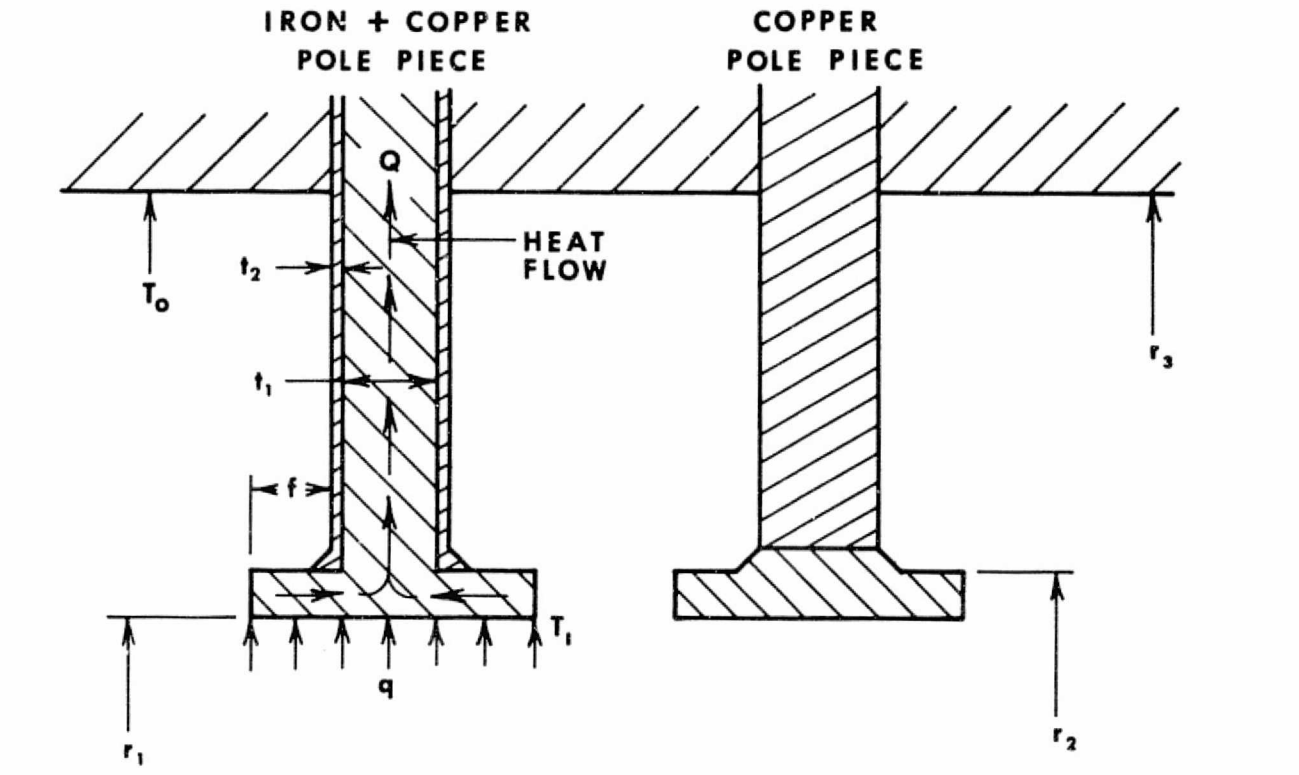

FIGURE 30 - THERMAL SCHEMATIC OF
COUPLED CAVITY CIRCUIT

7.0 MECHANICAL DESIGN

7.1 THERMAL CIRCUIT ANALYSIS (continued)

r_1 = .0838 cm.
r_2 = .1727 cm.
r_3 = .6858 cm.
f = .0762 cm.

yielding a pole piece thermal conductance of 0.25 Watts/°C.

This allowed for 50 Watts of interception power per cavity for a 300°C ferrule temperature.

7.2 CIRCUIT ASSEMBLY

The mechanical circuit assembly with cooling of the Development Tube is shown in Figure 31, consisting of input and output waveguide assemblies, input and output cooling lines, three gain sections with a velocity taper at the end of the last section, and two sever assemblies.

The individual gain sections were pre-brazed using three point alignment as shown in Figure 8, as were the sever assemblies. The input and output waveguide assemblies were assembled using conventional construction techniques, and an appendage pump was provided for at the input waveguide. The individual assemblies were then interconnected in a final circuit body braze.

Beam hole alignment by means of a mandrel was not possible due to its unusually small size and relied on the external three point alignment for concentricity.

The magnetic pole pieces of the Experimental Tube were made of Permendur because of its higher flux density. Considerable difficulty was encountered in developing a technique for the copper cladding of these pole pieces. Originally it was attempted to electroform the .0127 cm. copper to each side of the Permendur, however in a subsequent braze cycle the copper blistered and a vacuum tight bond could not be retained. This was believed to be due to cobalt bleeding from the Permendur at high temperature.

The final technique developed was to braze copper discs on both sides of the pole piece and machine these down to the desired thickness.

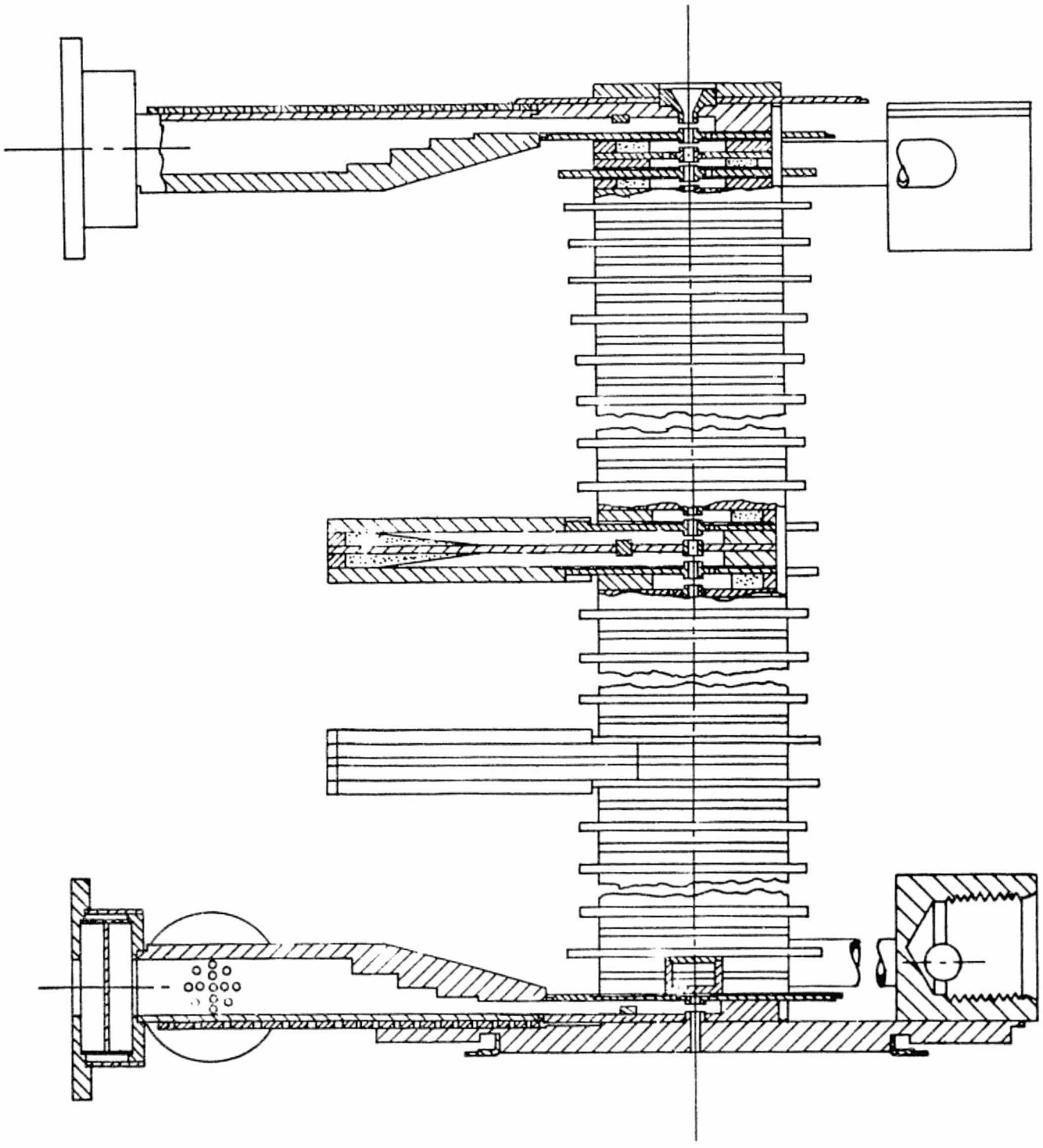

FIGURE 31 - MECHANICAL CIRCUIT ASSEMBLY WITH COOLING

7.0 MECHANICAL DESIGN (continued)

7.3 GUN WITH REPLACEABLE CATHODE

The electron gun assembly, shown in Figure 32, was designed to permit replacement of the cathode. The heater-cathode structure was designed to be self-aligning and self-positioning by means of precision machined surfaces. Its outside diameter was centerless ground to provide a high precision fit within the mating diameter. Contact is made at two axial locations to reduce the contact area between the parts and reduce the possibility of seizing or scoring. The cathode assembly support and the mating alignment cylinder were made of molybdenum to maintain the very close tolerances required during the temperature cycles encountered during bakeout and operation. The total indicated runout and axial location of a replacement cathode was designed to be within .0013 cm.

Nine replacement cathodes were delivered in evacuated containers to prevent damage or contamination.

7.4 COLLECTOR BASEPLATE WITH REFOCUSING SECTION

The collector baseplate assembly with refocusing section is shown in Figure 33. The large (50.8 cm. dia.) stainless steel baseplate included 31 feedthrough connectors to facilitate multistage collector evaluation. A circular cal rod heater was attached near the baseplate outer diameter to allow testing of a indium sealed "blow open" collector enclosure. The refocusing section consisted of two solenoid coils separated by .584 cm. with an intermediate pole piece. The coils were made of high purity anodized aluminum to eliminate the need for winding insulation between turns. The larger coil was designed to produce the high peak field, the separation to produce the transition field, and the small coil to produce the uniform field. The large coil consisted of 300 turns of .013 cm. thick by 1.905 cm. wide ribbon, and the small coil consisted of 104 turns of .015 cm. thick by 1.778 cm. wide ribbon. Both coils had an inner diameter of 1.156 cm.

Kapton H-film .013 cm. thick was used to insulate the edges of the coils from their pole pieces and the entire assembly was subjected to a 450°C bakeout with no apparent change in performance.

A photograph of the finished assembly is shown in Figure 34.

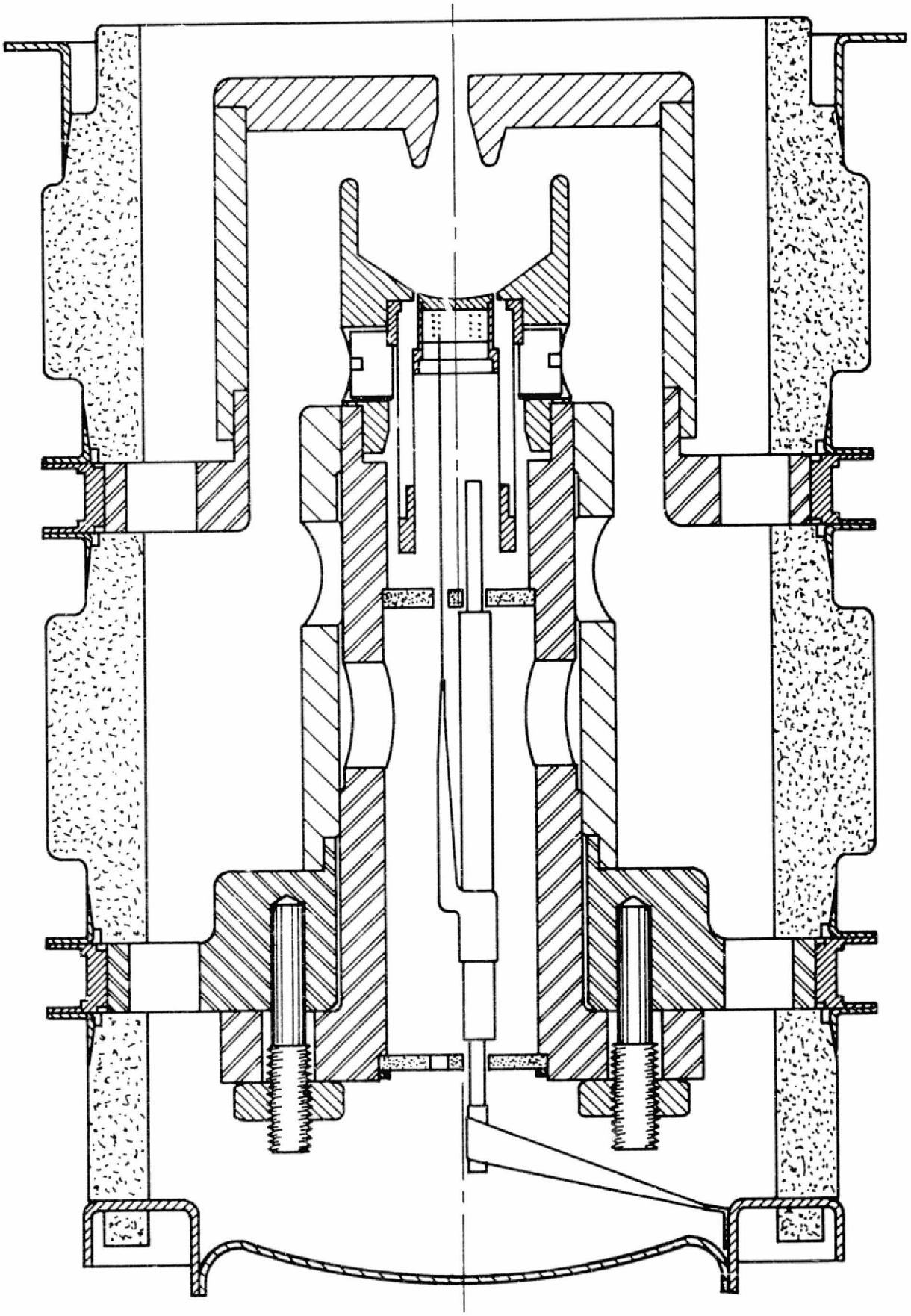

FIGURE 32 - REPLACEABLE GUN ASSEMBLY

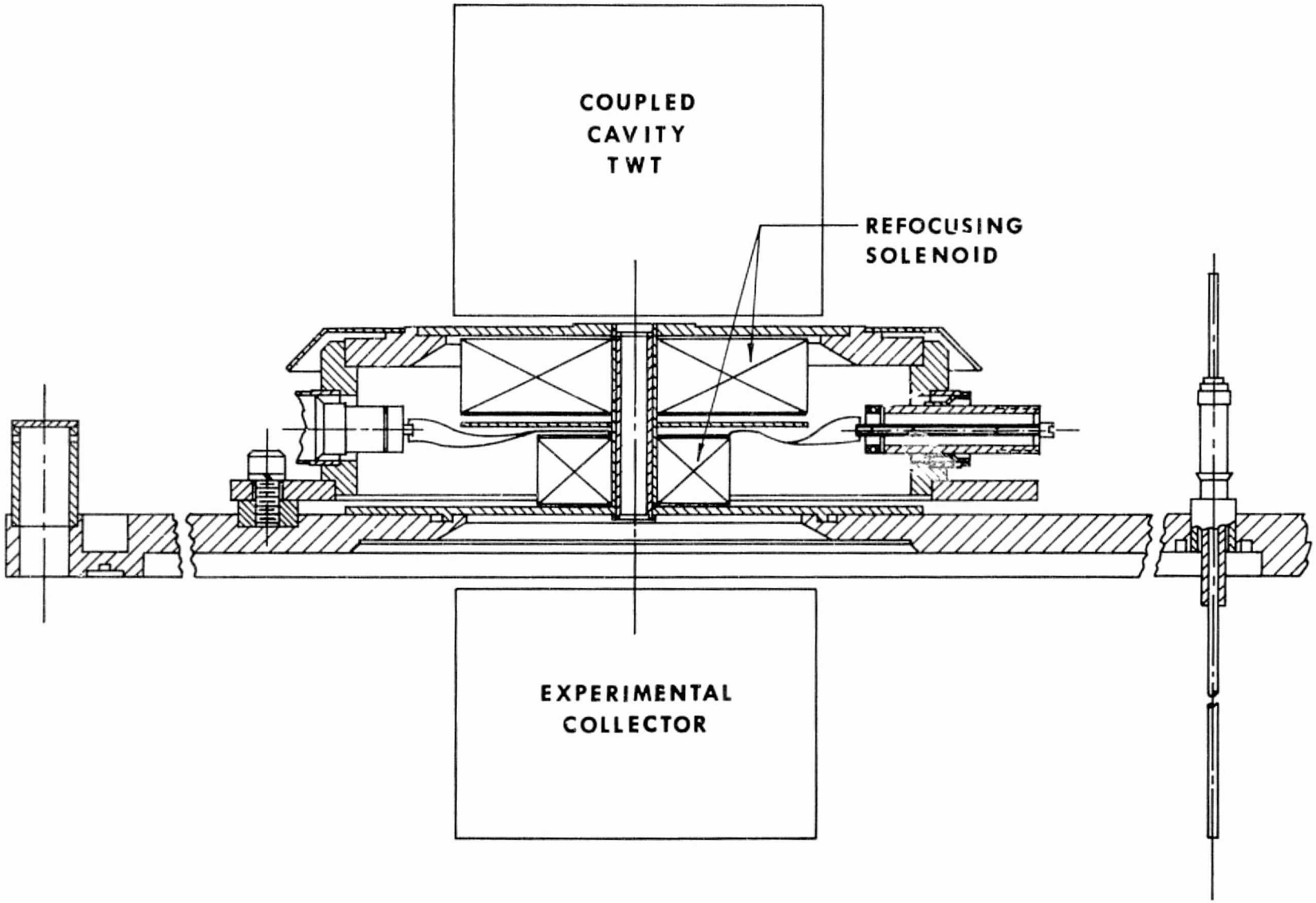

FIGURE 33 - COLLECTOR BASEPLATE ASSEMBLY WITH REFOCUSING SECTION

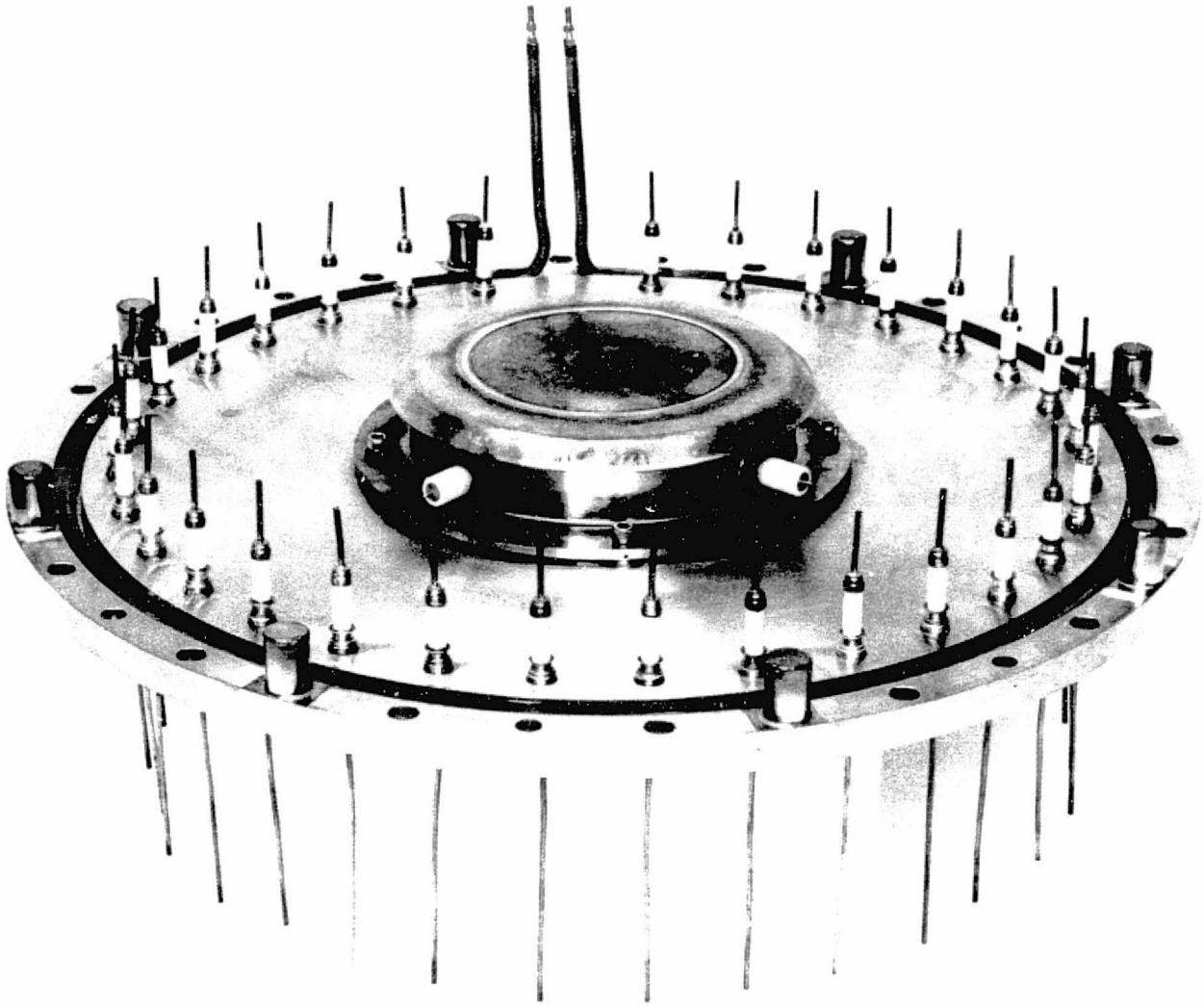

FIGURE 34 - COLLECTOR BASEPLATE WITH REFOCUSING ASSEMBLY

8.0 EXPERIMENTAL RESULTS AND DISCUSSION

An Experimental Tube and a Development Tube were designed, constructed and evaluated.

8.1 EXPERIMENTAL TUBE

The Experimental Tube utilized the high loss circuit design without a velocity taper in conjunction with the original high perveance gun design. It was constructed primarily for the purpose of evaluating and establishing suitable assembly techniques. Useful information could also be obtained relative to the focusing design, RF bandwidth, higher mode stability, and thermal design. RF gain and efficiency performance however would be of little significance.

Beam transmission into the collector was without RF about 70%, and at saturation about 60% of the cathode current. This was attributed to misalignments of the circuit and focusing structure during the brazing and final assembly operations. Because of this the tube was not considered a good test vehicle for evaluation of the replaceable gun feature.

Output power and gain data are shown in Figures 35 and 36. The tube operated at the design voltage of 15 kV, with an upper voltage limit of 16 kV. At higher voltages instabilities were observed. The operating bandwidth (11.99 GHz to 12.175 GHz) was slightly higher than the bandwidth objective (11.98 GHz to 12.14 GHz).

RF data were only taken at selective frequencies since the circuit match was very poor. At these frequencies the output power was about 200 Watts, with a saturation gain in the order of 30 dB. Small signal gain was nearly 40 dB.

Measurements were performed at 1% duty cycle without taper cooling. Due to the poor beam transmission higher duty testing was not attempted. The tube was then refocused for maximum DC beam transmission, achieving 76.5%, and delivered to NASA for use as a load for power supply testing.

8.2 DEVELOPMENT TUBE

The Development Tube consisted of the modified low loss circuit design with a short two step velocity taper, and the modified low perveance gun design for operation at the 1.25 kW level. A photograph of the tube is shown in Figure 37.

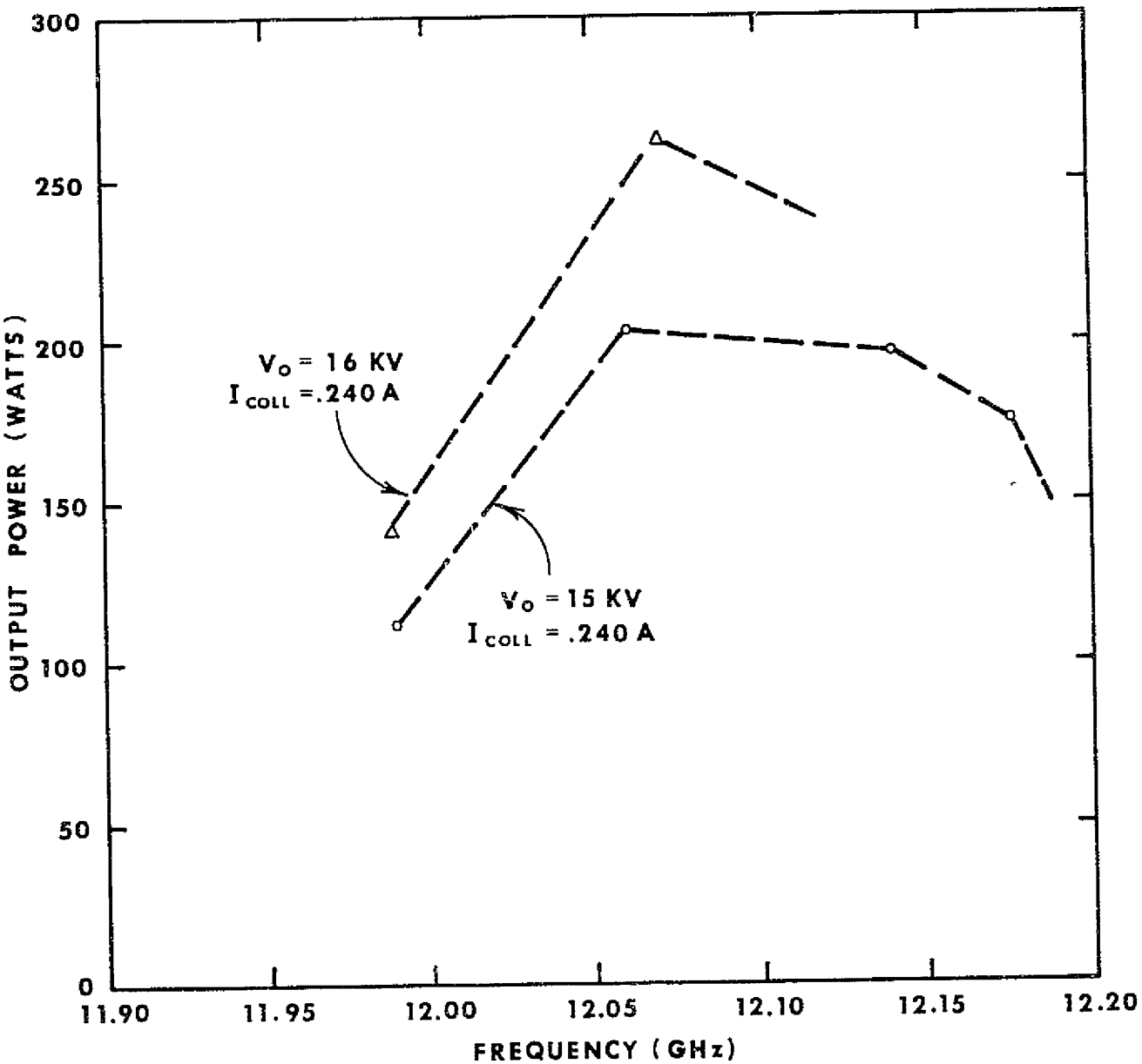

FIGURE 35 - OUTPUT POWER OF EXPERIMENTAL TUBE (MEASURED)

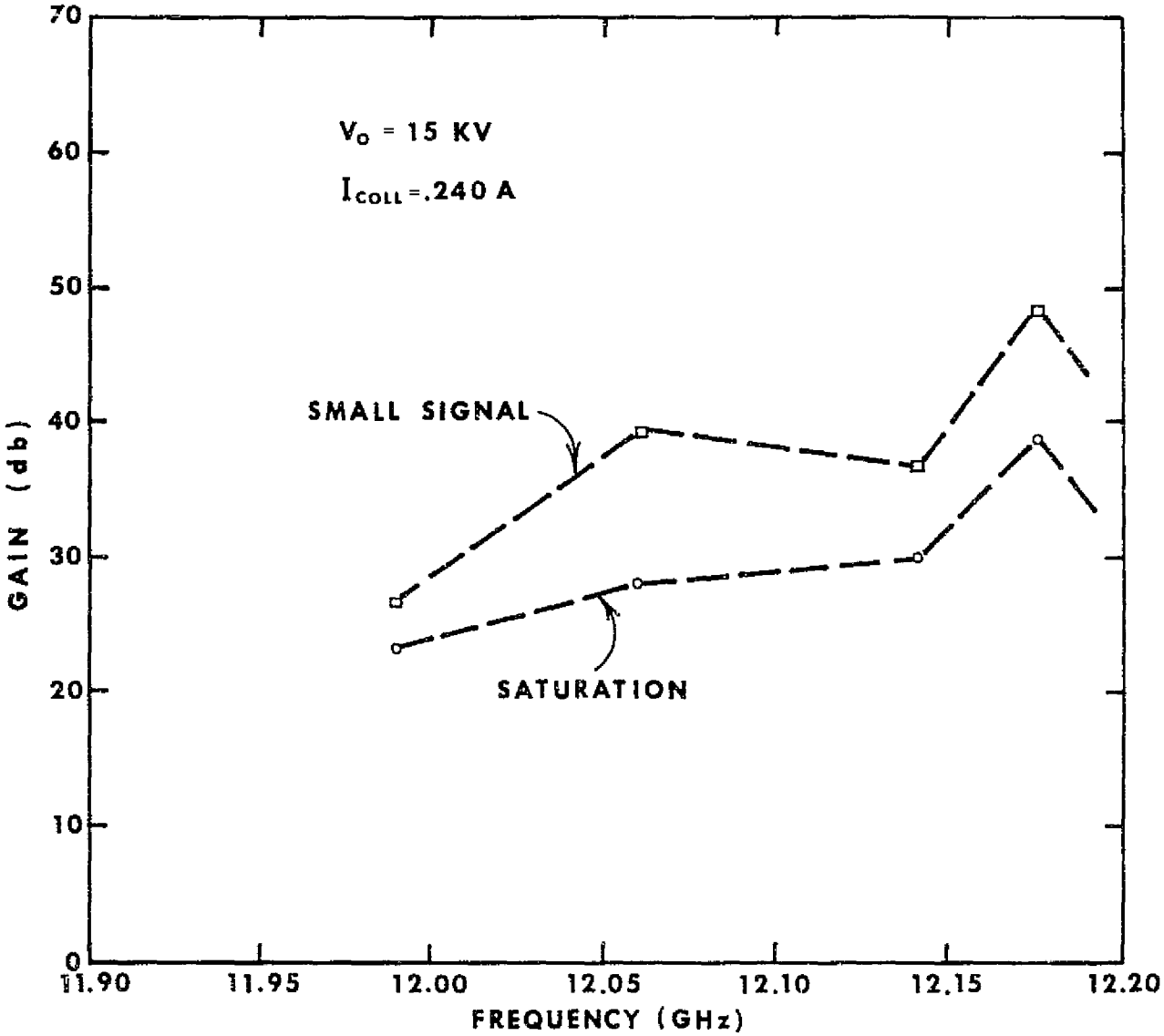

FIGURE 36 - GAIN OF EXPERIMENTAL TUBE (MEASURED)

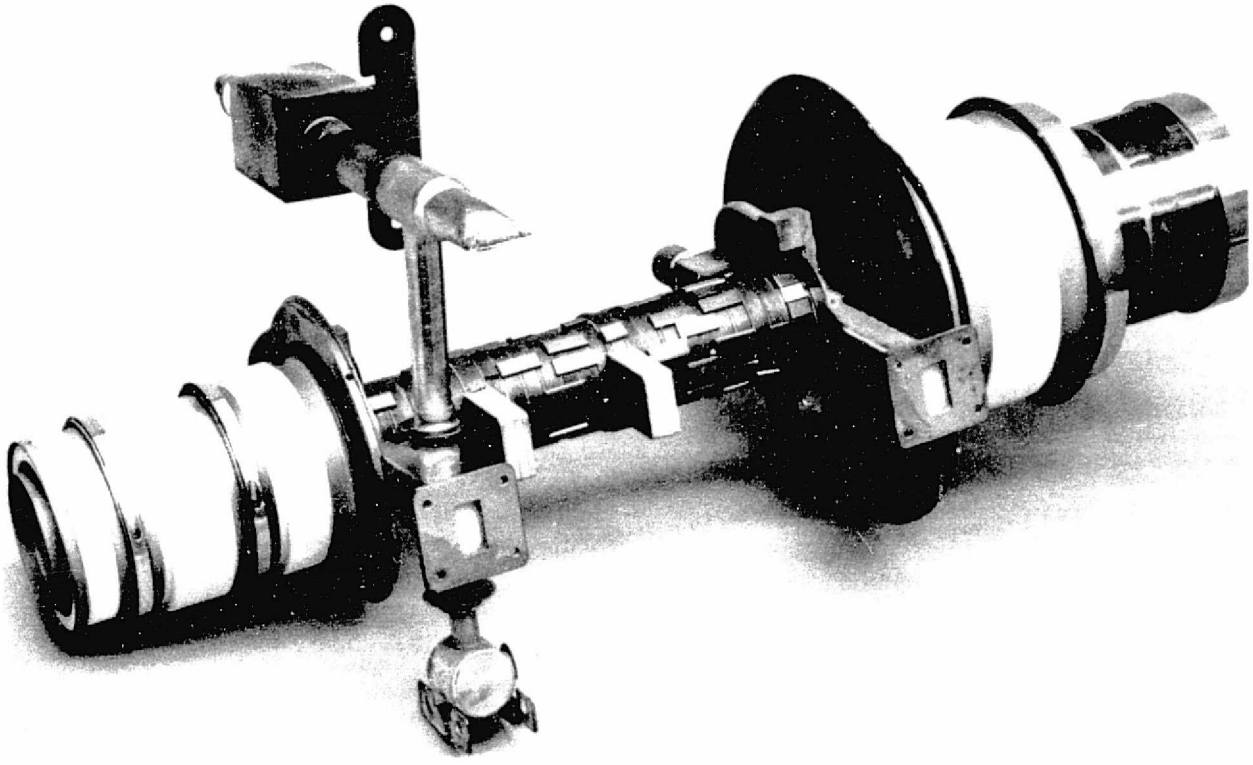

FIGURE 37 - DEVELOPMENT TUBE

8.0 EXPERIMENTAL RESULTS AND DISCUSSION

8.2 DEVELOPMENT TUBE (continued)

The tube was turned on at a 0.1% duty cycle and had 30% DC beam transmission. By the removal and adjustment of various shunts and with the aid of some samarium cobalt button type magnets, 70% beam transmission was achieved.

It was then observed that by placing various button magnets on the outside of the external gun shield (not shown in photograph) that further improvement could be made. An optimum DC beam transmission of 97.3% was achieved after very extensive efforts. Measurement of the transverse field at the cathode location revealed approximately 3 gauss, and the magnet requirement was attributed to a slight gun to circuit misalginment.

The duty cycle was then raised to 0.5% and RF measurements were taken. Figure 38 shows the small signal gain variation with frequency at various beam voltages, across essentially the entire band in which interaction occurred.

Small signal measurements above 17 kV were not possible because of lower cut-off oscillation above this voltage.

Figure 39 shows the saturated gain variation with frequency at various beam voltages across the operating band.

Figure 40 shows the saturated output power variation with frequency at various beam voltages across the operating band. The optimum power and gain region is shown to be well located in frequency. Since 16 kV was the optimum voltage more data points were taken at that voltage.

Figure 41 shows the drive characteristics at the lower, middle, and upper band frequencies at 16 kV.

The collector transmission while operating at the maximum power point (1005 watts) was 86.5%, far below the specified 95%. An effort was then made to improve this, resulting in 91.4%. Additionally the tube was completely stable at all voltages below 17.5 kV, at which an in band oscillation occurred with no RF drive.

The PPM stack was removed and subsequently put back on the tube to evaluate the degree of difficulty involved, under NASA observation. The tube was turned back on without duplicating the original magnet shunting arrangement and was readily reshunted to give approximately 98% collector transmission with no RF drive. However, it was believed that it would require a rather extensive effort to duplicate the focusing under saturated RF conditions after removal and subsequent reinsertion of the magnets.

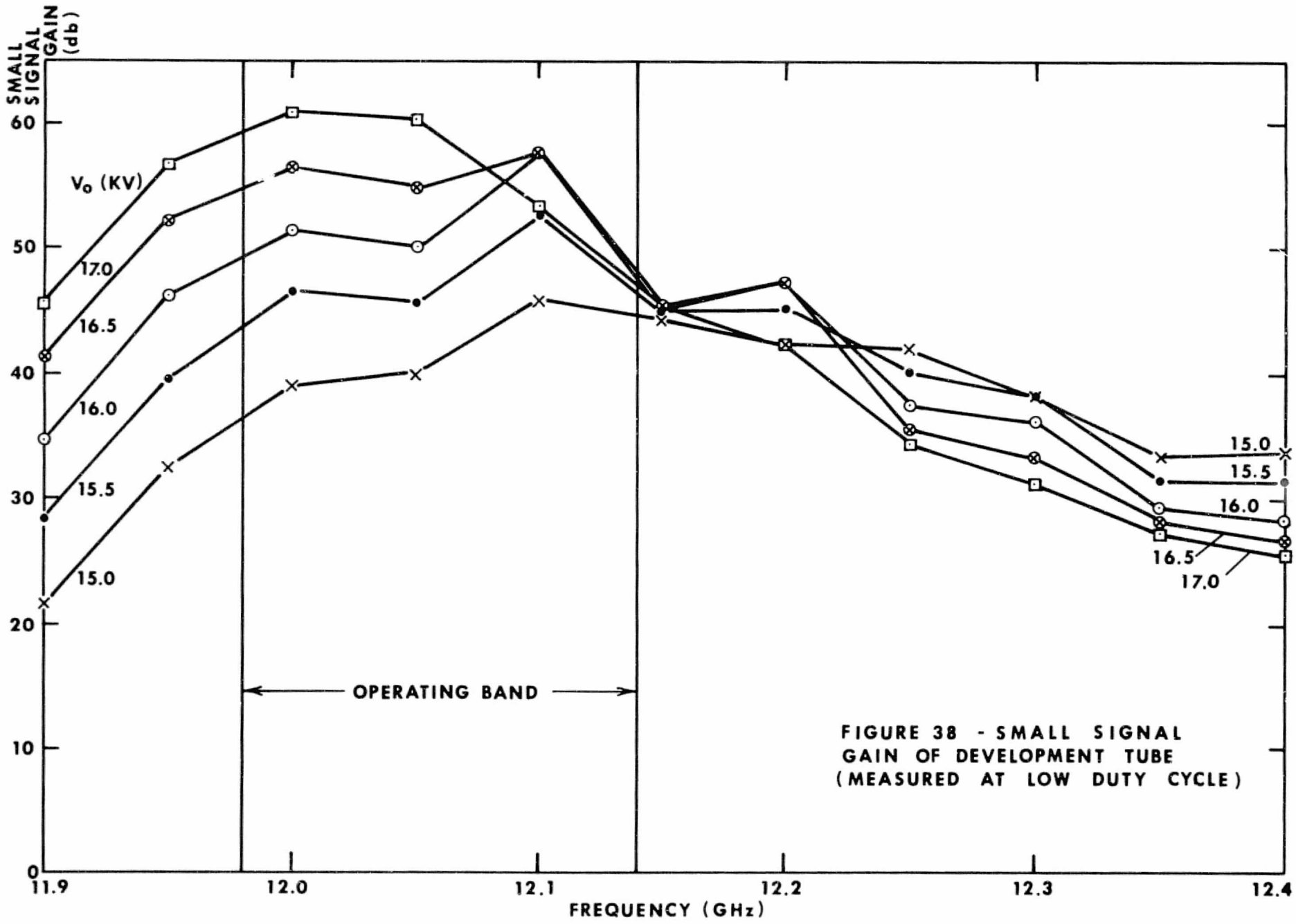

FIGURE 38 - SMALL SIGNAL GAIN OF DEVELOPMENT TUBE (MEASURED AT LOW DUTY CYCLE)

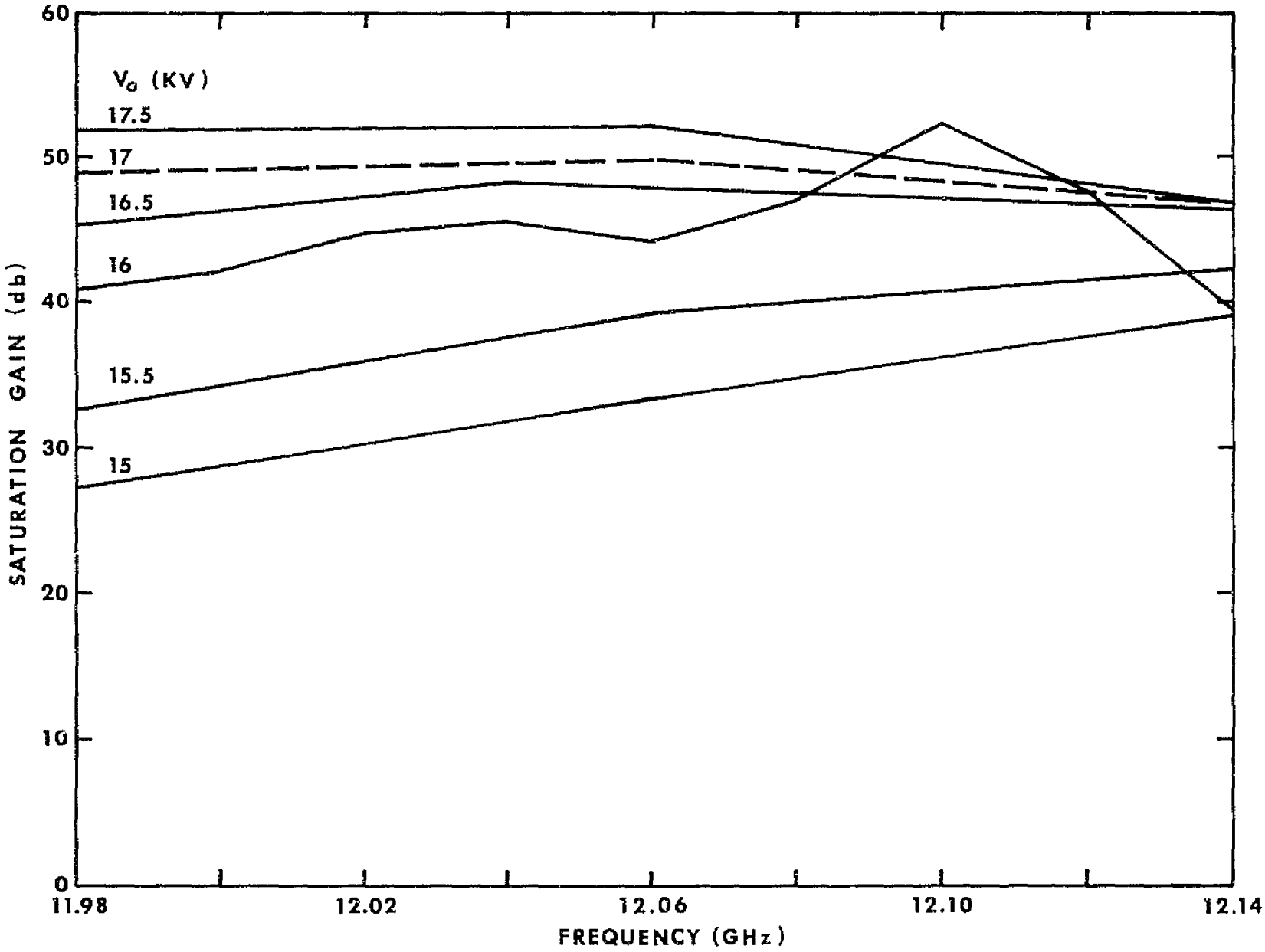

FIGURE 39 - SATURATION GAIN OF DEVELOPMENT TUBE (MEASURED AT LOW DUTY CYCLE)

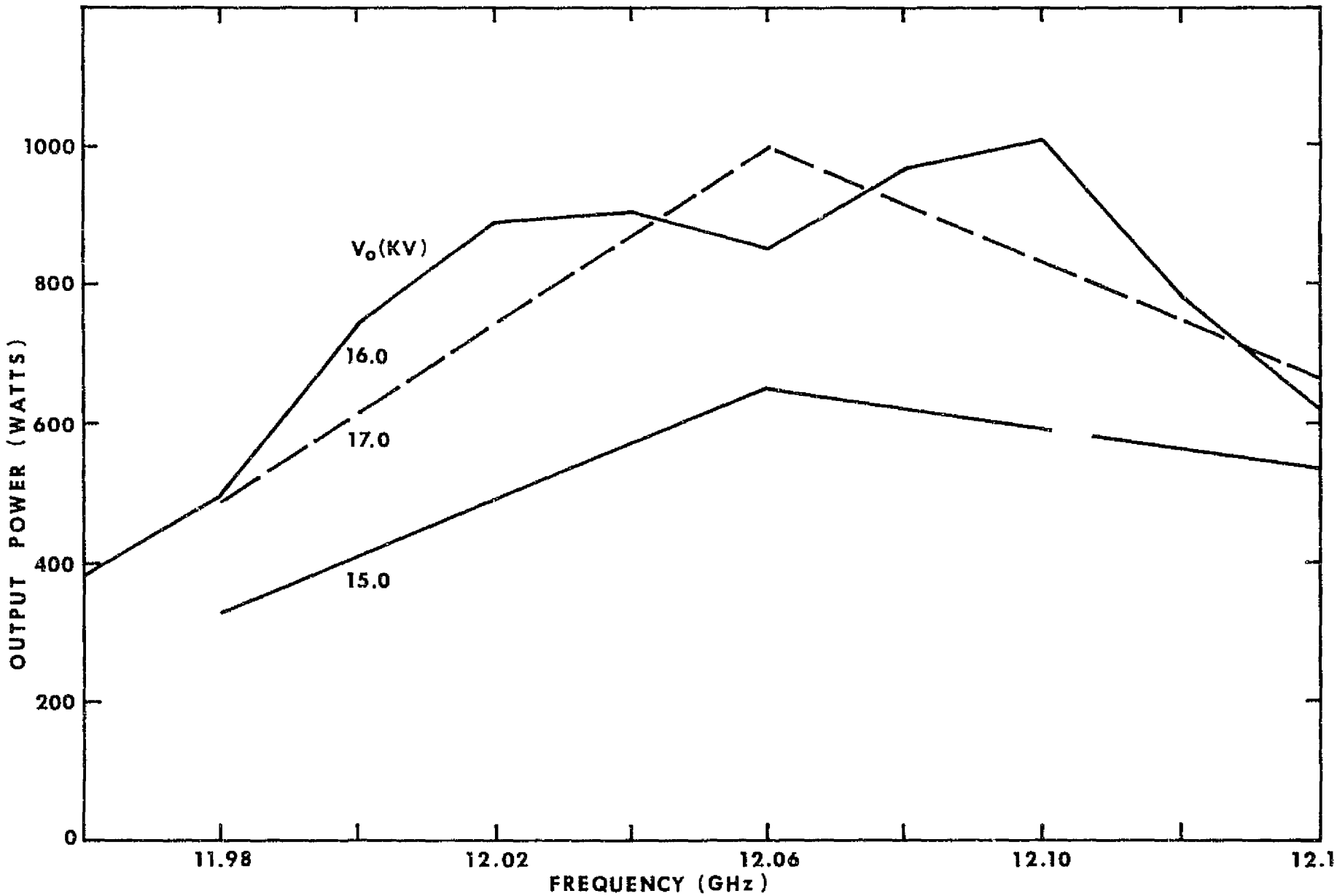

FIGURE 40 -OUTPUT POWER OF DEVELOPMENT TUBE (MEASURED AT LOW DUTY CYCLE)

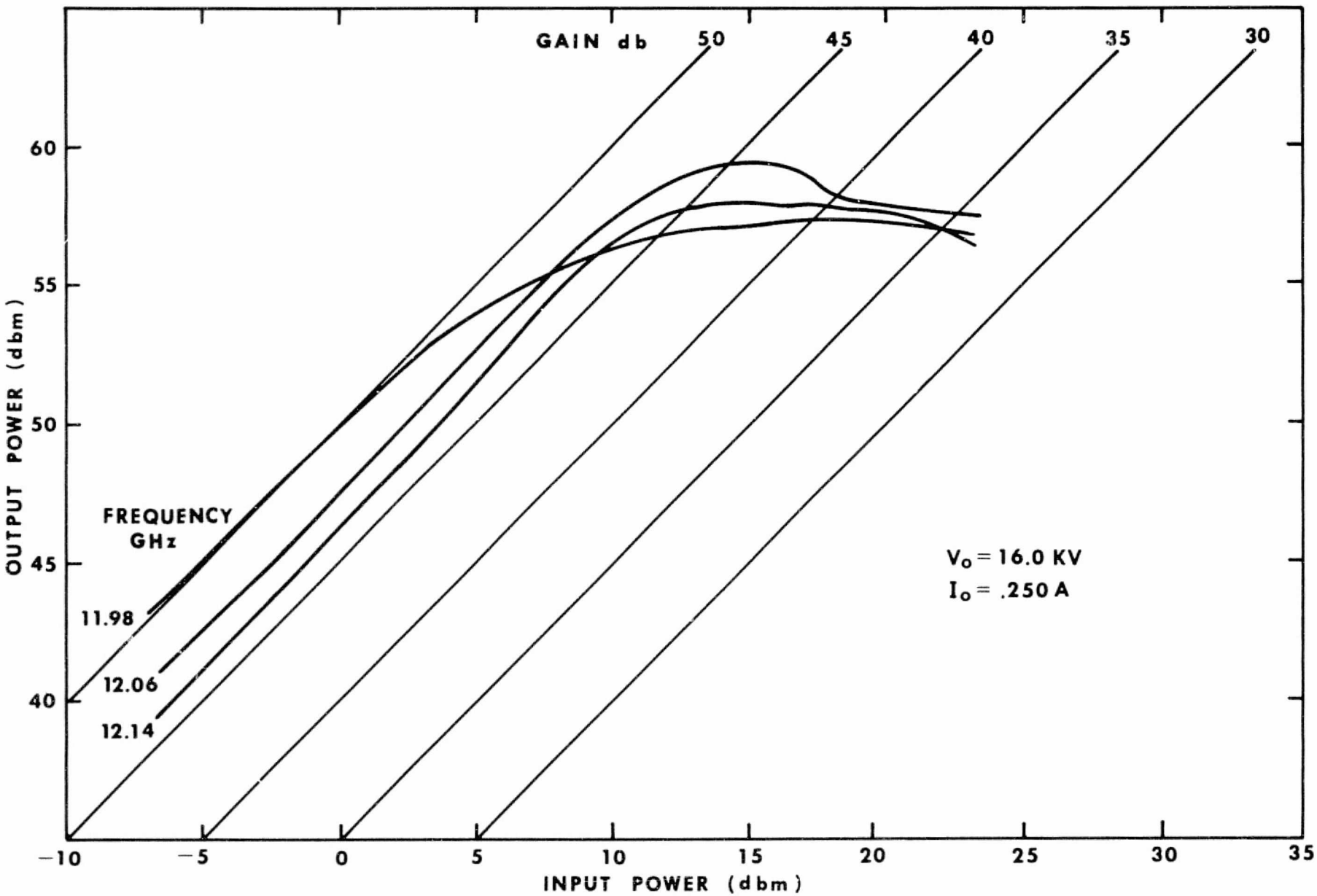

FIGURE 41 - DRIVE CHARACTERISTICS OF DEVELOPMENT TUBE (MEASURED AT LOW DUTY CYCLE)

8.0 EXPERIMENTAL RESULTS AND DISCUSSION

8.2 DEVELOPMENT TUBE (continued)

The tube was then let down to air and the cathode removed. It could be seen by eye that the gun was misaligned with the input pole piece, as suspected. The entire gun assembly was removed and rewelded to the pole piece using a mandrel to correct the misalignment. A new cathode was substituted and the tube was reprocessed.

The tube was then retested with the new cathode, turning on with approximately 50% DC collector transmission which was readily improved to 95% with the use of magnetic shunts. RF drive was then applied and the focusing was readjusted to give 88% collector transmission in the saturated RF output condition. The duty cycle was then increased gradually and the tube reached CW operation in a period of 2 hours with no indications of any large pressure increases. The circuit and collector were cooled in series with water (20°C inlet temperature) flowing at approximately 2 GPM, with the collector surface temperature stabilizing below 60°C. The CW input power consisted of 4 kW, with 900 Watts of RF output power, approximately 400 Watts of interception power being dissipated in the circuit, and approximately 2700 Watts being dissipated in the collector (undepressed). This confirmed that the cooling design was very adequate.

Swept CW RF data were then taken at 16 kV beam voltage and 0.250 amps beam current with the results shown in Figures 42 through 45. These data are considered to be more accurate than that taken previously under pulsed conditions. Figure 42 shows the small signal and saturation gain across the operating frequency band, with approximately 8 dB variation. Figure 43 shows RF output power at four different drive levels across the band. Figure 44 shows the electronic efficiency across the band with a maximum efficiency of 22.5%. Figure 45 is a derived plot of power compression curves at 40 MHz intervals across the band. No instabilities were detected at any time and the tube appeared to be completely oscillation free at the operating voltage and current.

Upon attempting to measure performance characteristics at a reduced beam voltage the focusing degraded sufficiently to melt a cavity ferrule in the circuit output section. Based on previous tests during which the focusing did not appear to be voltage sensitive, this was not expected and was not understood. This however prevented further RF testing and did not allow for collector depression evaluation.

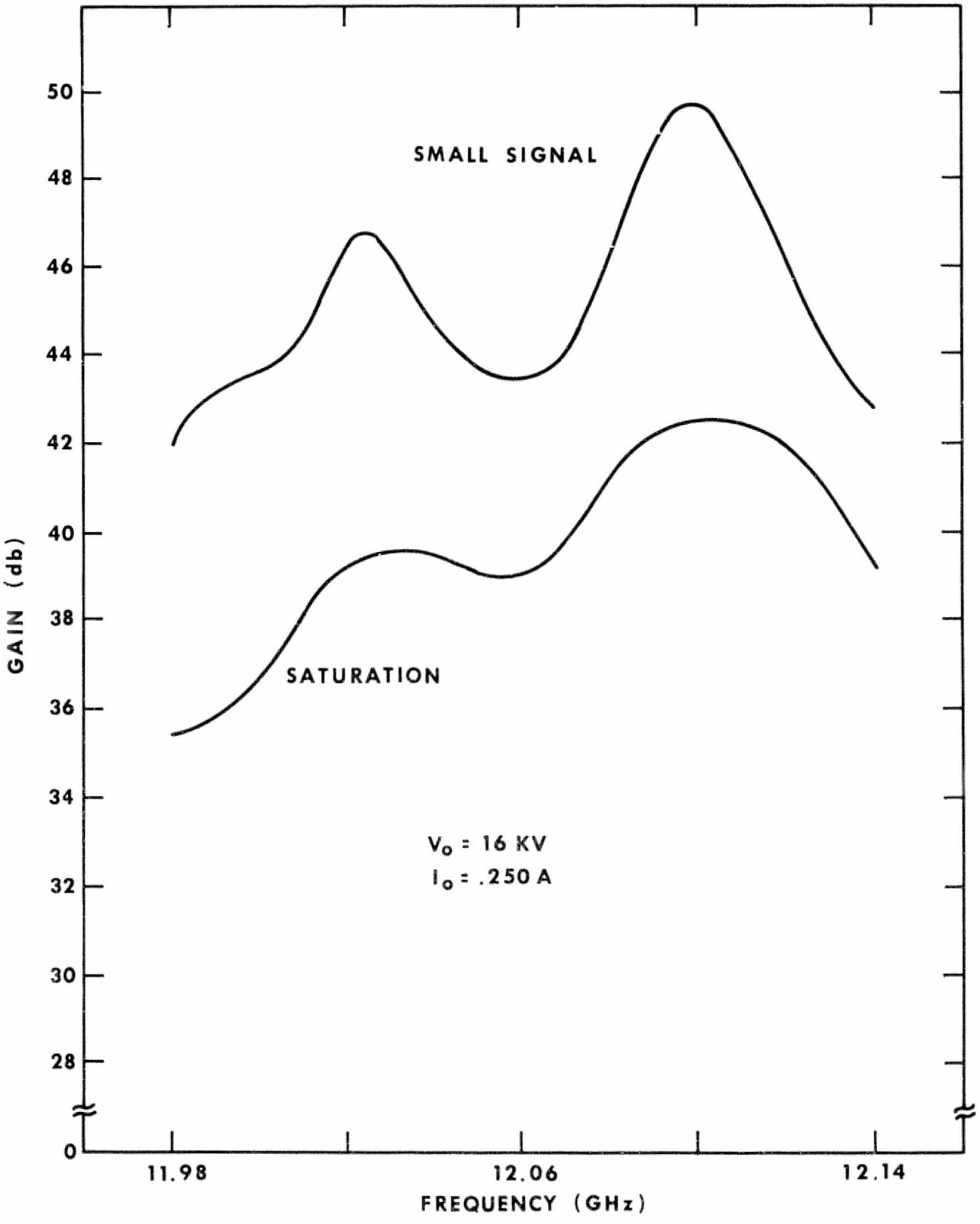

FIGURE 42 - GAIN OF DEVELOPMENT TUBE
(MEASURED AT CW OPERATION)

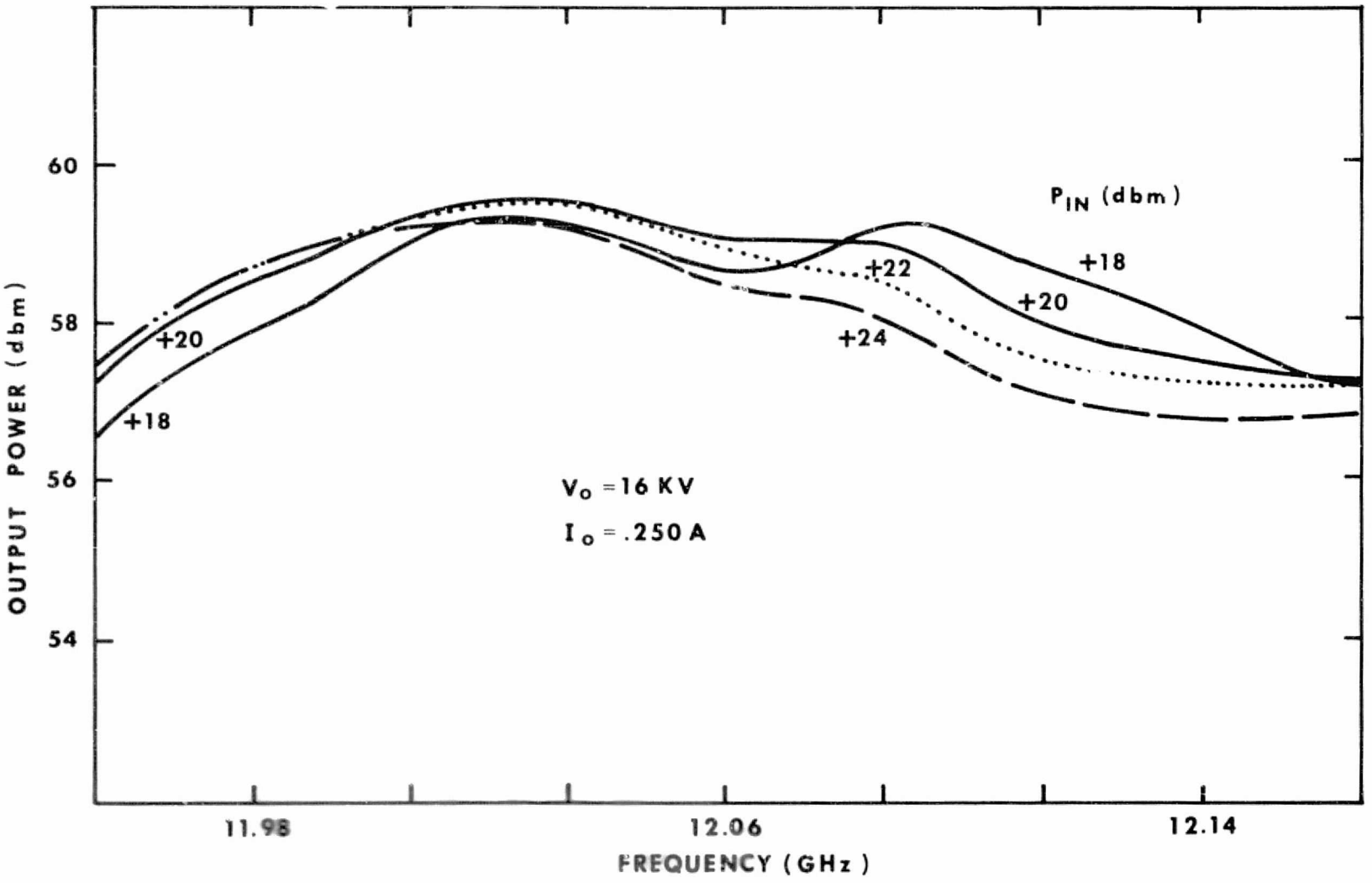

FIGURE 43 - OUTPUT POWER AT CONSTANT INPUT POWER LEVELS OF DEVELOPMENT TUBE (MEASURED AT CW OPERATION)

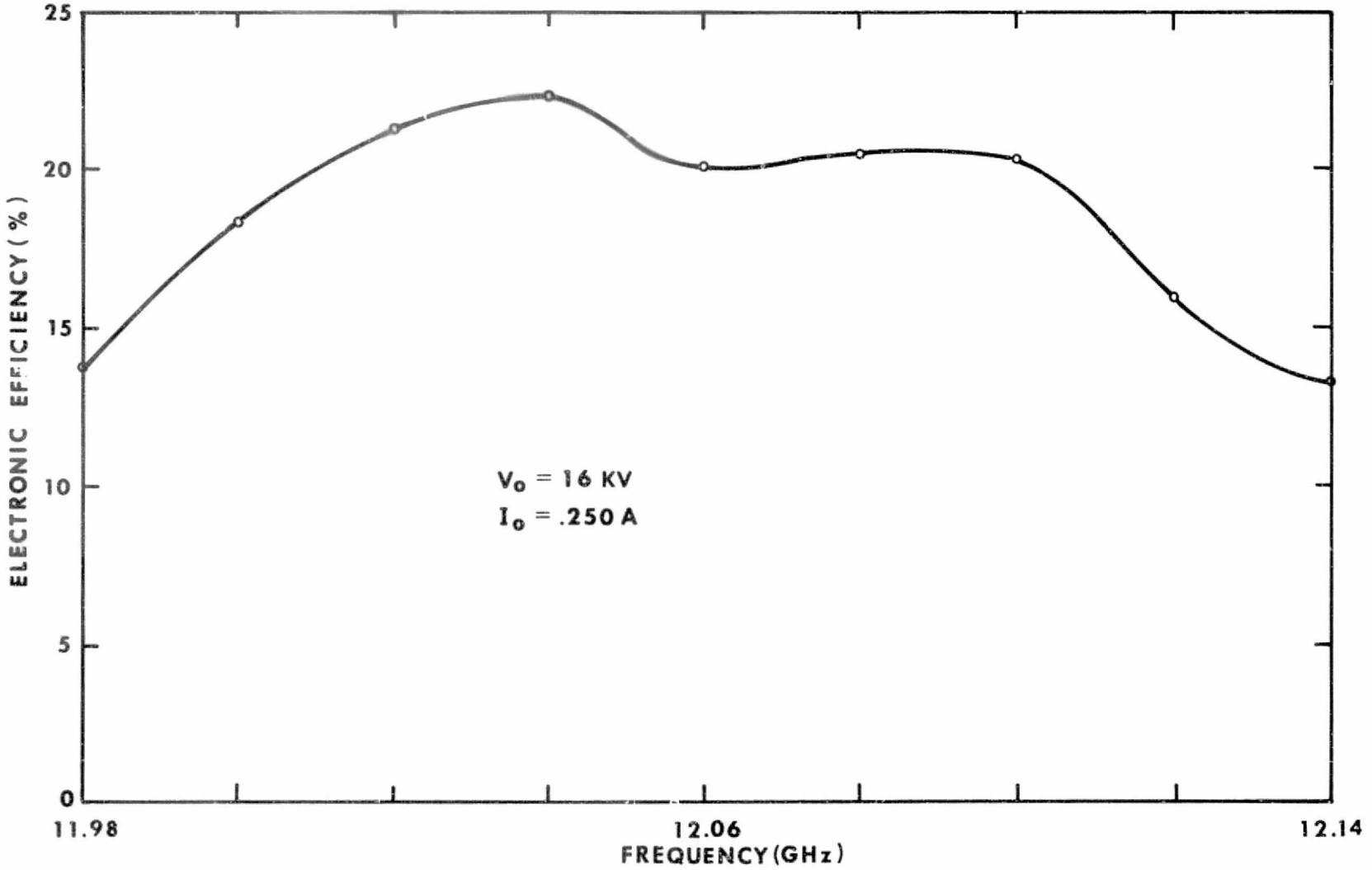

FIGURE 44 - ELECTRONIC EFFICIENCY OF DEVELOPMENT TUBE (MEASURED AT CW OPERATION)

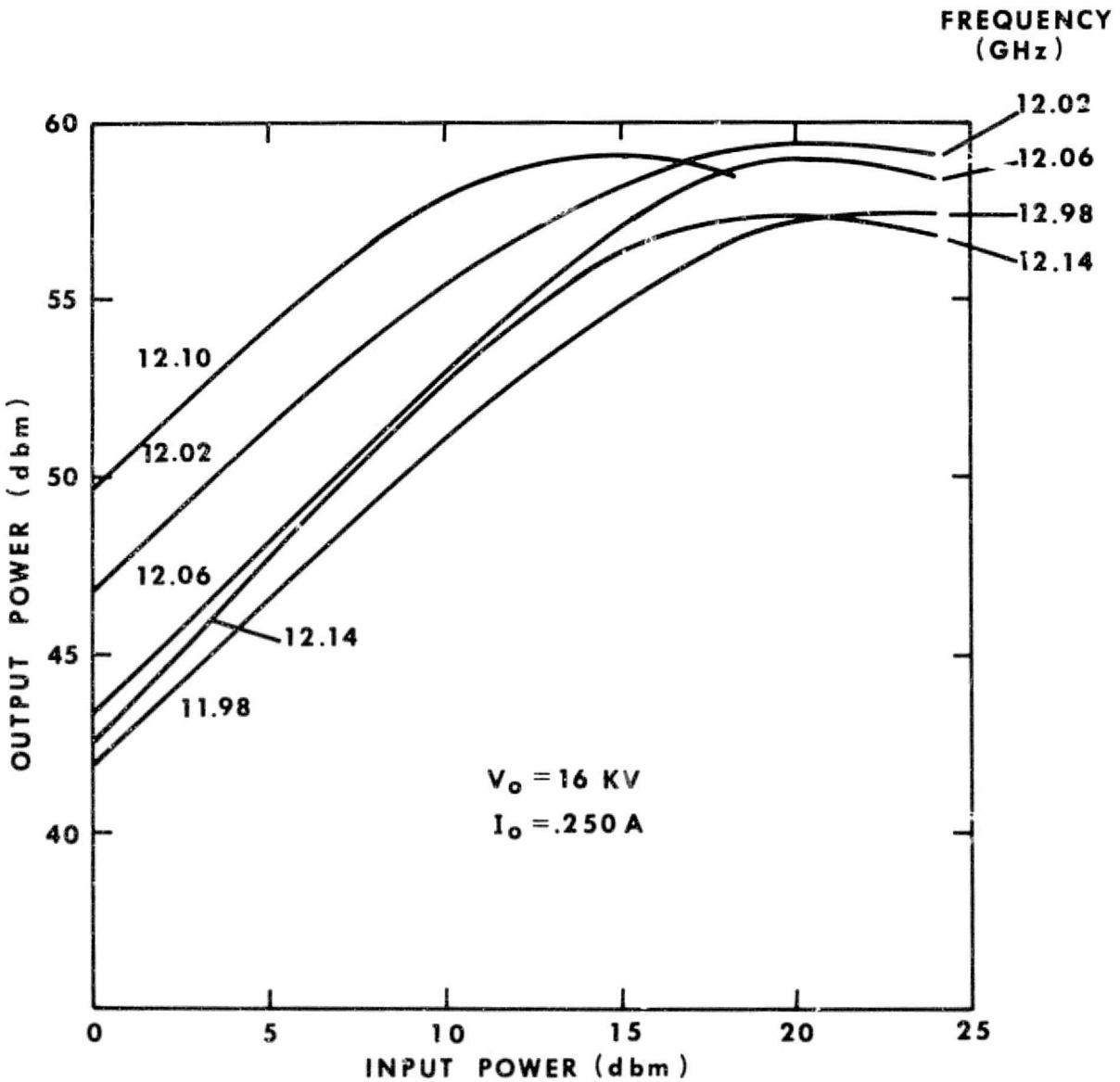

FIGURE 45 - DRIVE CHARACTERISTICS OF DEVELOPMENT TUBE
(MEASURED AT CW OPERATION)

9.0 CONCLUSIONS

The purpose of the program was to demonstrate the feasibility for the design of a 12 GHz high efficiency PPM-focused coupled cavity tube at the 1-2 kW CW power level. In addition the tube was to be designed such that it could be used as a test vehicle in a special vacuum chamber for advanced multistage collector experiments.

An experimental tube, a development tube, and associated hardware for multistage collector test experiments were delivered to NASA, Lewis Research Center, including 9 replacement cathodes, two conflat flanges and two collector baseplates with refocusing. Alternate refocusing designs with either solenoids or permanent magnets were also demonstrated. Construction of a second development tube was partially completed at the end of the program and it was also delivered to NASA, LeRC in this state.

During the design phase of the program unexpected problems were encountered with the circuit design. It was found that the coupled cavity slow wave structure exhibited excessively high losses when the cold bandwidth was chosen to fit the relatively small hot bandwidth requirement of 160 MHz. Such high losses would have been incompatible with high efficiency performance. An experimental tube was built with the original circuit design with high losses that did not include efficiency enhancement methods.

Construction of this tube served to evaluate a new thermal design and novel assembly techniques. Hot tests of this tube also provided information on the focusing and cooling design.

Extensive circuit studies were required to reduce the circuit losses to acceptable levels. This was achieved with a circuit of considerably larger cold bandwidth than the original one.

The reduced interaction impedance of this larger bandwidth design required that the hot bandwidth be shifted toward the lower range of the band (phase angle close to π) in order to provide better interaction impedance for efficiency enhancement.

A Development tube for the 1.25 kW CW power level was designed and constructed that was based on the new circuit. The tube design incorporated a velocity step taper for efficiency enhancement. The tube was tested initially at low duty and was proven to be capable of operating at the 1 kW CW level. The tube achieved the full specified bandwidth of 160 MHz with 35 dB to 45 dB saturation gain and was unconditionally stable in the operating range.

9.0 CONCLUSIONS (continued)

Peak power was 1000 watts with about 600 watts at the band edges. Beam transmission at full power was 90% corresponding to intercepted beam power of 400 Watts. This amount of beam interception is higher than was expected and improvements in the focusing design and performance appear feasible. The relatively high beam interception however demonstrates the excellent thermal capability of the circuit and tube. The critical focusing conditions become apparent with CW operation when an adjustment in the tube operation caused defocusing and consequent destruction of the tube.

Maximum electronic efficiency was 22.5% and lower than predicted. Subsequent analysis indicated that the velocity taper design is not yet optimized and higher efficiency can be achieved with design corrections. Further studies showed also that the new circuit design of the Development Tube is not yet optimized with respect to efficiency, bandwidth and loss. New studies indicate that a better circuit design can be achieved with a modified coupling slot configuration. Such a circuit has a smaller cold bandwidth, higher interaction impedance, lower circuit losses and larger phase angles in the operating range.

Tube designs based on such a circuit show promise of achieving the specified electronic efficiency of 35% at the 1.25 kW power level.

10.0 REFERENCES

1. Sauseng, O. Basiulis, A. Tammaru, I. "Analytical Study Program to Develop the Theoretical Design of Traveling Wave Tubes", NASA Contract No. NAS3-9719, Report No. CR-72450, October 1968.

2. Ayers, W. R. Harman, W. A. "Design, Construction and Evaluation of a 12.2 GHz, 4.0 kW-CW Coupled Cavity Traveling Wave Tube", NASA Contract No. NAS3-13728, Report No. CR-120920, March 1973.

3. Cohn, S. B. "Optimum Design of Stepped Transmission Line Transformers", IRE Transactions on Microwave Theory and Techniques, April 1955, Vol. MTT, No. 3 (p. 16-21).

4. Pierce, J. R. "Theory and Design of Electron Beams", D. Van Nostrand Co., New York, 1954.

5. Sterzer, F. Siekanowicz, W.W. "The Design of Periodic Permanent Magnets for Focusing of Electron Beams", RCA Review, Vol. 28 (No. 1), March 1957, (p. 34-59).